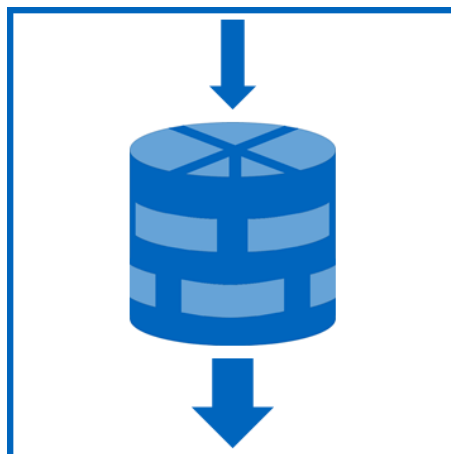


Using Packed Beds as a Strategy to Enhance Filtration Processes

Peter Michael Bandelt Riess



Using Packed Beds as a Strategy to Enhance Filtration Processes

Peter Michael Bandelt Riess

Vollständiger Abdruck der von der TUM School of Life Sciences der Technischen Universität München zur Erlangung eines Doktors der Ingenieurwissenschaften (Dr.-Ing.) genehmigten Dissertation.

Vorsitz: Prof. Dr.-Ing. habil. Mirjana Minceva

Prüfer der Dissertation: 1. Prof. Dr.-Ing. Heiko Briesen
2. Prof. Dr.-Ing. Harald Klein

Die Dissertation wurde am 25.01.2022 bei der Technischen Universität München eingereicht und durch die TUM School of Life Sciences am 01.06.2022 angenommen.

Abstract

Packed beds are conventionally used in absorption and rectification columns to maximize the contact surface between phases, allowing for efficient thermal separation processes. Furthermore, they can be favorable in the context of mechanical solid–liquid separations, providing additional wall support to a collapsible solid network. Innovative experimental and simulative procedures are applied in this work to systematically observe and clarify the effects of using packed beds in cake filtration processes on separation performance and assess the premise. Thus, a concept from one of the fundamental unit operations in chemical engineering is transferred to another one as a process strategy.

For the experimental section, model systems consisting of particles of different shapes, compressibilities, and sizes are selected and combined with packed ring beds exhibiting varying amounts of void space and wall support. The systems are separated through standardized dead-end filtration tests to evaluate changes in cake resistance and operation time. The packings cause remarkable permeability improvements under determined conditions, accelerating the filtration of compressible substances without compromising filtrate quality. Moreover, piston-driven compression tests are performed using a modified universal testing machine. The high-precision displacement and pressure measurements are conducted to monitor the response of the combinations to compressive stress. The additional structural support provided by the packing configurations significantly increases the cake resistance against compression; the greater the applied pressure and material compressibility, the more pronounced is the packing influence.

The numerical section is a case study that aims to elucidate the effects of the process strategy on filter cake porosity. Granular beds of spheres are simulated through discrete element method in cylinders with different geometric configurations of internal walls. Three main containing systems, namely concentric cylinders, angular walls, and a combination of both, are generated and compared. The added wall effects do cause a significant bulk porosity increase in the system that is proportional to the incorporated support, that is, the arrangement combining cylindrical and angular inserts displays the greatest effect. It is shown how the known near-wall sinusoidal porosity distribution is altered through the presented method. The obtained behaviors and profiles can be used to explore additional effects and further systems.

These results allow to generally understand the occurring phenomenological interplays of this strategy and provide a base to develop industrial applications in the future, which could lead to important process improvements.

Kurzfassung

Füllkörper werden herkömmlicherweise in Absorptions- und Rektifikationskolonnen verwendet, um die Kontaktfläche zwischen Phasen zu maximieren und effiziente thermische Trennprozesse zu ermöglichen. Darüber hinaus können sie im Kontext der mechanischen Fest-Flüssig-Trennungen vorteilhaft sein, indem sie einem komprimierbaren festen Netzwerk zusätzliche Wandstützung bieten. Zur Beurteilung dieser Prämisse werden in dieser Arbeit innovative experimentelle und simulative Verfahren angewendet, um die Auswirkungen der Füllkörperverwendung in Kuchenfiltrationsprozessen auf die Trennleistung systematisch zu beobachten und zu klären. Somit wird ein Konzept aus einer der Grundoperationen in der chemischen Technik als Prozessstrategie auf eine andere übertragen.

Für den experimentellen Teil werden Modellsysteme ausgewählt, die aus Partikeln unterschiedlicher Formen, Kompressibilitäten und Größen bestehen, und mit Füllkörperpackungen kombiniert, die unterschiedliche Mengen an Hohlraum und Wandstützung aufweisen. Durch standardisierte Dead-End-Filtrationstests werden die Systeme getrennt, um Kuchenwiderstands- und Betriebszeitänderungen auszuwerten. Die Packungen bewirken unter bestimmten Bedingungen bemerkenswerte Permeabilitätsverbesserungen und beschleunigen die Filtration komprimierbarer Substanzen, ohne die Filtratqualität zu beeinträchtigen. Außerdem werden kolbengetriebene Kompressionstests mit einer modifizierten Universalprüfmaschine durchgeführt. Die hochpräzisen Verschiebungs- und Druckmessungen werden genutzt, um das Verhalten der Kombinationen auf Druckspannung zu überwachen. Die zusätzliche strukturelle Unterstützung durch die Packungskonfigurationen erhöht die Kuchenfestigkeit gegen Kompression erheblich; je größer der ausgeübte Druck und die Materialkompressibilität sind, desto ausgeprägter ist der Packungseinfluss.

Der numerische Teil ist eine Fallstudie, die die Auswirkungen der Prozessstrategie auf die Filterkuchenporosität untersuchen soll. Granulare Kugelbetten werden durch Diskrete-Elemente-Methode in Zylindern mit unterschiedlichen geometrischen Innenwandkonfigurationen simuliert. Drei Systemhauptarten, nämlich konzentrische Zylinder, Radialwände und Kombinationen aus beiden, werden erzeugt und verglichen. Die hinzugefügten Wandeffekte bewirken eine signifikante Erhöhung der Bettporosität im System, die proportional zur eingebauten Stützung ist, d. h. die Kombination aus zylindrischen und radialen Einsätzen weist den größten Effekt auf. Es wird gezeigt, wie die bekannte sinusförmige Porositätsverteilung an den Wänden durch das vorgestellte Verfahren verändert wird. Die erhaltenen Verhalten und Profile können verwendet werden, um zusätzliche Effekte und weitere Systeme zu untersuchen.

Diese Ergebnisse ermöglichen es, die auftretenden phänomenologischen Wechselwirkungen dieser Strategie allgemein zu verstehen und eine Grundlage für die zukünftige Entwicklung industrieller Anwendungen zu schaffen, die zu wichtigen Prozessverbesserungen führen könnten.

Acknowledgements

So, this is it. I finished writing my dissertation about a year ago, and, after waiting for my last paper to be finally published, I have even officially submitted it by now. It is a moment you can only imagine over the years at the university, and it is not that easy to grasp once it comes. It is not a long dissertation, but I tried to make my writing my own, as you may have noticed. Nevertheless, the whole was without a doubt a joint effort, which is also made clear in many of its passages. Credit must be given where credit is due, so these acknowledgements are for you.

My doctoral supervisor, my “Doktorvater” (an expression the English language should contain, in my humble opinion), Prof. Dr.-Ing. Heiko Briesen, or just Heiko at the chair, made all this possible from the start. He interviewed me, believed in me, and then invited me to become a part of his team, which made me very happy. Afterwards, he became an inspiring boss who pushed the scientific creativity in all of us and with whom we could openly communicate. Heiko would always show us how to investigate and teach in direct and indirect ways. Of course, he is also the first evaluator of this thesis, for which I thank him as well. On this note, I am very grateful to Prof. Dr.-Ing. habil. Mirjana Minceva and Prof. Dr.-Ing. Harald Klein for immediately agreeing to complete my examination board. I hope that our discussion passes just as quickly.

Among the chair’s supervising staff, I would also like to thank my mentor, Prof. Dr.-Ing. Petra Först, who supported a considerable part of my work. She directed the funded investigation projects that I helped to finish, allowing me to guarantee my stay at the chair. Her guidance complemented Heiko’s in an amazing way, and you could additionally count on her to share a celebratory beer at the end of the week. Dr. techn. Daniel Schiochet Nasato not only helped me practice a little Portuguese but also assumed the role of corresponding author for my final paper. His ample knowledge of particle simulations was paramount in conceiving one of the goals of this dissertation. Dipl.-Ing. Jörg Engstle and Dr.-Ing. Michael Kuhn were my co-authors and unofficial mentors. They gave me some valuable orientation during my first months at the chair and paved the way for many investigations. Michael’s dissertation, being a foothold for this work, is especially referenced.

I certainly must thank the rest of the chair staff as well. As I wrote to them upon officially completing my time there, four years with them went by too quickly. It is not easy to write about so many positive experiences. The SVT was my second home; sometimes arguably the first one, as I would spend more time there than at my actual home. I learned so much from the mad scientists and the non-technical personnel. It is all incalculable, but, if anyone wants numbers, those years we watched over 14,000 min in presentations together! I am very happy that this was my first work in Germany, and that I decided to do a PhD with them. I accomplished many things in that time that I could not have imagined before. I only have you to thank for that, the highly qualified and helpful staff at SVT, who always ensured a pleasant, exciting, and fun atmosphere. SVTon even provided a musical reprieve from the science. Thanks to all of you (Alex, Alexandra, Ali, Annett, Bea, Carsten, Christoph K., Christoph M., Conny, Ekaterina, Esteban, Frederik, Friederike, Gabi, Hannes, Hans, Henri, Javier, Johannes, Karin, Marco, Mario, Martin, Mathias, Michaela, Mohd, Moritz, Petra D., Philip S., Sebastian,

Sepp, Simon, Solange, Steve, Thomas, Tiaan, Tijana, Verena, Vesna, Walter) for the nice cooperation, coffee breaks, rehearsals, celebrations; for everything.

My office, EG33, was undoubtedly the coolest from start to finish. Because of this, special acknowledgements go to my officemates. Bernhard and MGM received me with open arms and furthermore provided a dog and a coffee machine. Lakshmi substituted MGM for a short while, but his great sympathy left a permanent impression. My last officemates, Philip Pergam and Philipp Schweda, did not only make sure I would have fun working every single day but also gave me new true friends for life. I am certain I will never laugh as often in an office ever again. Thank you.

The SVT staff was not the only source of learning and conviviality during my stay. My students, as well some colleagues' students, taught me as much as I taught them (or more), and I am very grateful to them. Teaching was a very important experience for me at the university; both TM2 and supervising theses provided me with tools that I will always be able to apply. Regardless of whether your own work directly contributed to this dissertation or not, being your tutor certainly helped and amused me a lot. So, thank you very much, Constantin, David, Elena, Florian, Helge, Jan, Jendrik, Johann, Julian, Kilian, Lukas, Marcel, Maxi H., Maxi V., Nick, Tessi, Tobias, Torsten. I am also thankful for the time shared with staff of other chairs: Andi, Franzi, Jasmin, Martin, Raena, Simon, Simone.

Almost daily, I would spend a couple of hours training in the campus gym after working. This would keep me motivated on a good day and lift me up on a bad one. More than the training, the people whom I met there would soon start giving me a further familiar circle to rely on. Some of them, like my now good friend Friedrich, quickly went from being a training buddy to a significant part of my life. Luckily enough, I could also count on longtime friends and family members since I indefinitely came to Germany. Some even let me live with them for as long as I needed. Thank you so much, Alexa, Andreas, Erick, Marcel, Miguel, Pove. It is so nice to have a piece of home here.

Last and most important, I wholeheartedly thank my parents. I do not know how they managed it, but they were able to get me here without the least amount of pressure. They would always give me the best guidance but also enough free room to make my own decisions and lead my life however I saw fit. They live more than 8,000 km away, but I have always felt supported by them: something only a love like theirs could achieve. This also applies to the rest of my family, which would continuously ask "how the future doctor was doing". Literally nothing would have been possible without them. This is for you.

Peter Bandelt

Cham, February 21, 2022

Table of Contents

Abstract.....	i
Kurzfassung	ii
Acknowledgements	iii
List of Figures.....	vi
List of Symbols.....	vii
Chapter 1: Introduction.....	1
1.1 Motivation: Process Systems Engineering	1
1.2 Objectives.....	2
1.3 Study Outline: Hypotheses	2
Chapter 2: Theoretical Background	5
2.1 Filtration Explained	5
2.2 Cake Filtration	7
2.2.1 Relevance	7
2.2.2 The Role of Porosity	8
2.2.3 Cake Compression	9
2.3 Experimental Characterization of Filter Cakes	12
2.3.1 Classic Filtration Theory	12
2.3.2 Compressional Rheology.....	16
2.4 Counteracting Compression Issues	17
2.4.1 Classic Process Strategies	18
2.4.2 State of the Art.....	20
2.5 Packed Beds	24
2.5.1 Relevance	24
2.5.2 Establishing the Link to Filtration	25
Chapter 3: Methodology	27
Chapter 4: Published Results	29
4.1 Paper I: Decreasing Filter Cake Resistance by Using Packing Structures	29
4.2 Paper II: Investigating the Effect of Packed Structures on Filter Cake Compressibility	41
4.3 Paper III: Assessing the Wall Effects of Packed Concentric Cylinders and Angular Walls on Granular Bed Porosity	51
Chapter 5: General Conclusions and Future Work	63
References.....	67
List of Publications	75

List of Figures

Figure 1: Triangular representation of the study outline.....	3
Figure 2: Filtration processes according to the separation mechanism	5
Figure 3: Derivation of the research topic of cake filtration from chemical engineering.....	6
Figure 4: Evolution in time of cake filtration process variables differential pressure Δp , filtrate volume V , and flowrate dV/dt	7
Figure 5: Binarized image of a cross-sectional slice in the interior of a spent grain filter cake. The image was generated using computed X-ray microtomography and shows the cake solids in white and air in black.....	8
Figure 6: Spatial dependence of selected process variables inside an incompressible filter cake. Adapted from Alles and Anlauf (2003).....	10
Figure 7: Spatial dependence of selected process variables inside a compressible filter cake. Adapted from Alles and Anlauf (2003).....	10
Figure 8: Filter cake compression mechanisms. Adapted from Alles and Anlauf (2003).....	11
Figure 9: Filtrate volume over time and linearization of the filtration curve.....	14
Figure 10: Schematic illustration of a C-P cell. Adapted from Shirato et al. (1968).....	15
Figure 11: Compressive yield stress over solidosity determined using: VDI filter (● black), C-P cell (■ blue), C-P cell without permeation (◆ green), filtration rig (▲ orange). Adapted from Höfgen et al. (2019b).....	17
Figure 12: Schematic representation of the classic filtration process strategies: a) Screening, b) Pressure selection, c) Filter aids, d) Cake resuspension	20
Figure 13: Schematic representation of the modern process strategies: a) Gas bubble injection, b) Ultrasonic field, c) Magnetic field, d) Micromanipulation	23
Figure 14: Photographs (CC) of exemplary packed bed components. a) Raschig rings and b) super-rings for random packings (both from Raschig GmbH), c) Mellapak structured packing (Sulzer AG).....	25
Figure 15: Schematic overview of the thesis methodology	27

List of Symbols

A	[m ²]	Filtration area
b	[-]	Capillary form factor
D	[m ² s ⁻¹]	Solids diffusivity
d	[m]	Particle diameter
h	[m]	Cake height
K	[-]	Concentration constant, fitting parameter [m ⁻² Pa ^{-N}] if combined with α
k	[m ²]	Permeability
m	[kg]	Mass
N	[-]	Global compressibility
p	[Pa]	Pressure, compressive yield stress if combined with γ , fitting parameter if combined with α
R	[m ⁻¹]	Flow resistance, hindered settling function [Pa s m ⁻²] if combined with ϕ
r	[m]	Radius
t	[s]	Time
V	[m ³]	Volume

Greek Letters

α	[m ⁻²]	Relative flow resistance
Δ	[-]	Differential
ε	[-]	Porosity
η	[Pa s]	Viscosity
τ	[-]	Tortuosity, turbidity
ϕ	[-]	Solidosity

Subscripts

a	Turns p to a fitting parameter
b	Bulk
K	Filter cake
L	Liquid
M	Medium
P	Pores

S	Solid
y	Turns p to compressive yield stress
0	Initial, unstressed
α	Reference to relative flow resistance
ϕ	Reference to solidosity

Abbreviations

C-P	Compression-Permeability
DEM	Discrete Element Method
PSD	Particle Size Distribution
PVC	Polyvinyl Chloride
VDI	Verein Deutscher Ingenieure (Association of German Engineers)
3D	Three-dimensional

Chapter 1: Introduction

1.1 Motivation: Process Systems Engineering

What you are about to read, assuming you are willing to read the whole content from the start, is motivated by work developed over four years at the Technical University of Munich's Chair of Process Systems Engineering. At the risk of sounding a tad cheesy, I have always felt that the best way to start anything is with definitions (it is certainly a must when writing, for instance, computer code). As a matter of fact, "process systems engineering" is a term whose meaning has been a topic of discussion by many authors (Kuhn and Briesen 2019).

If the word "engineering" is searched for in the Merriam-Webster Dictionary (2020), the following definition will be found: the application of science and mathematics by which the properties of matter and the sources of energy in nature are made useful to people. This is a beautiful but very broad explanation, so the preceding "process systems" has not been inserted in vain. Put together, the expression has been more accurately defined by Grossmann and Westerberg (2000) as an area of chemical engineering which seeks to understand and develop systematic procedures for the design and operation of multi-scale chemical process systems.

This concept is very well suited for the following work since the investigations to be presented sought to apply innovative experimental procedures systematically to understand the occurring effects. Moreover, everything was done in the context of solid-liquid separation, filtration, which is indeed a fundamental unit operation studied in chemical engineering. Additionally, considering that the mentioned experimental procedures are based on the unconventional use of packed bed elements (normally found in absorption and distillation columns), further key unit operations are involved as well. Hence, this thesis explores an innovative process strategy, a combination of unit operations of sorts, to unravel, or rather unpack, its application potential and discover wherein the observed effects lie.

One of the ideas which deemed the topic worth investigating was published by Kuhn (2018) in his dissertation as a possible application for optimal control methods. Even though briefly mentioned, the possibility of using the diameter of a vessel as a control variable to optimize the fluid pressure drop is exposed in the context of flow through compressible porous media. By reducing the diameter where needed, more wall support should be provided in that region of the vessel, thus stabilizing compressible particles. Additionally, it is considered that the manipulation of wall support could also be achieved by somehow using random packing rings if changing the vessel diameter is not a possibility.

My predecessor accepted the challenge and performed preliminary experiments in the laboratory to find out if the theories could be turned into practice. An extremely compressible medium, the lautering filter cake (Engstle et al. 2015; Engstle et al. 2017), was chosen to do this since that would represent a potential industrial application. Promising observations were made as the cake was permeated in the presence of randomly packed rings. Nevertheless, a systematic approach was not undertaken then. That is where this thesis comes in.

As can happen with novelties, some of the findings raised more questions than they answered. Then again, that is how it should be because science and engineering are ever evolving. However, the findings did answer some questions, and the next chapters shall put them into perspective.

1.2 Objectives

As a logical consequence of the motivation, this thesis has the main goal of systematically observing the effects that packed beds produce when strategically used as part of cake filtration processes, correlating the key variables, and ultimately understanding why they occur and how they could eventually be applied. The goal is divided into three separate hypotheses and fulfilled following a triangular scheme (graphically represented below in Figure 1), where the higher step uses the previous one as a base.

1.3 Study Outline: Hypotheses

Hypothesis I: The first hypothesis is the foundation of the goal triangle and states that packed beds, the ones conventionally used for thermal separation processes, can also be beneficial for mechanical separation processes, such as cake filtration, and reduce flow resistance. Analogous to the abovementioned compressible medium application, the packed structures can provide additional wall support to the filtration vessel, which makes the filter cake more permeable and decreases pressure drop as well as needed operation time. To evaluate this hypothesis, different types of model suspended solids and packed beds are determined, and various combinations of them are made and analyzed in experimental dead-end filtrations. In short, it is an observational investigation, which is addressed with Paper I in Chapter 4.1, to identify the effects of the proposed strategy.

Hypothesis II: The second hypothesis takes advantage of the first experimental observations and states that the packings' structural support specifically counteracts solid network compression. It proposes that there are correlations between the key process parameters operating pressure, filter cake compression factor, and packing type. To test this hypothesis, the same previously determined combinations of suspended solids and packed beds are analyzed through purposefully designed filtration and compression experiments. This way, specific advantages of incorporating such packing configurations can be quantified. The results are exhibited with Paper II in Chapter 4.2.

Hypothesis III: The third hypothesis and peak of the goal triangle formulates that the porosity of a particle bed is heavily influenced by wall support in the container and that the latter can be manipulated in a way that greatly enhances said porosity. It is proposed that cases where additional structural support is incorporated through different wall arrangements in a cylindrical bed of spheres be studied through discrete element method simulations. This allows to consider several scenarios (facilitating the determination of optimal conditions) and continue understanding the phenomena at hand from a more mechanistic point of view. This last step in the triangle has a very specific focus but could foster many follow-up studies to achieve the optimization of real filtration processes through this strategy in the future. The hypothesis is addressed with Paper III in Chapter 4.3.

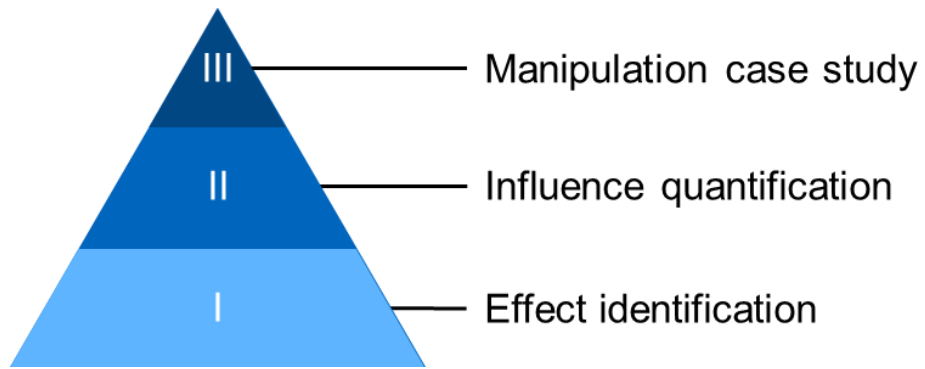


Figure 1: Triangular representation of the study outline

Chapter 2: Theoretical Background

After introducing the general terms, more key parameters and their validity range must be declared and defined for this work. Several keywords have already been mentioned and vaguely connected. To lay the groundwork for the evaluation of the hypotheses in the next chapters, it is necessary to start at one of the broader terms: filtration, one of the fundamental processes studied in chemical engineering.

2.1 Filtration Explained

To filter is to mechanically strip a fluid from dispersed matter using a porous medium. Considering this, further constraints should be introduced now: This work considers the fluid to be a liquid (with water as a reference) and the suspended matter to be solid particles. Thus, it is spoken of suspensions, slurries, or sludges. For this reason, the term mechanical solid–liquid separation process is frequently used. However, among such processes, filtrations are characterized by relying on a filter medium as physical barrier for separation and on differential pressure as driving force (Tiller and Hsyung 1993).

Due to the different variables involved in a filtration process, it is necessary to differentiate between kinds of filtrations (Ripperger et al. 2000). The most general and intuitive classification is probably according to what happens with the particles during the process in reference to the filter medium: the filtration mechanism. Figure 2 is a schematic representation of filtration mechanisms in different control volumes.

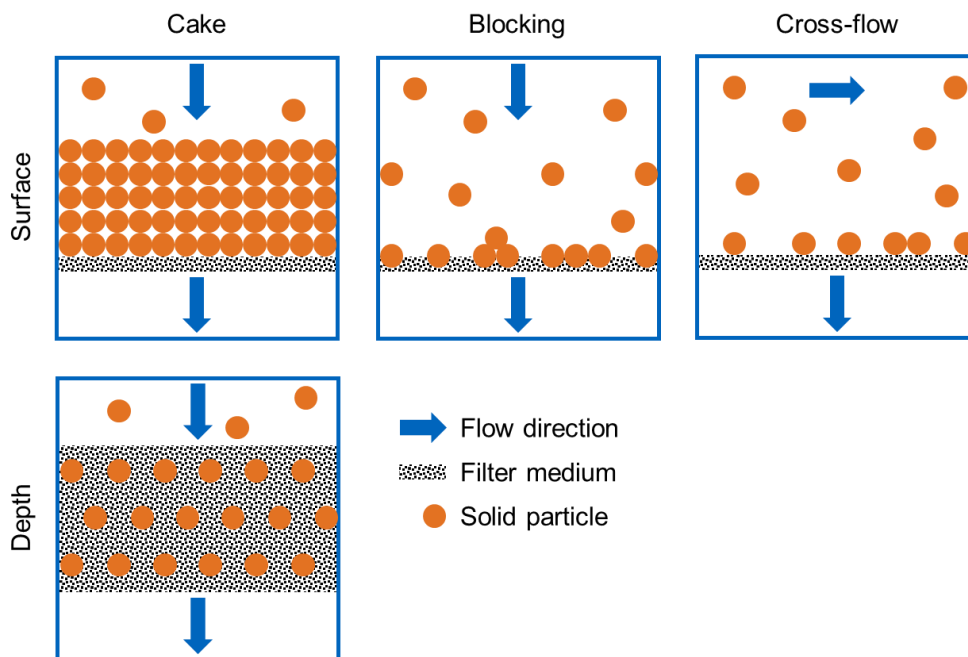


Figure 2: Filtration processes according to the separation mechanism

Two main mechanisms are shown in the rows of Figure 2. If the retained solids remain inside the filter medium because the particles are smaller than the pores at the medium inlet, it is a depth filtration process. Here, the solids can interact with the porous material, so they adhere to it at a deep filter bed layer. Phenomena like Brownian motion or van der Waals forces become relatively significant. In opposition, if the retained solids remain upstream outside the filter medium because the particles are bigger than the pores at the medium inlet, it is a surface filtration process. Here, the predominant separation mechanism is based on a more trivial screening effect (Ripperger et al. 2000). Surface filtration (the one of interest for this work) can, in turn, be broken down into the well-known processes in the first row of Figure 2: cake (the more specific one of interest for this work), blocking, and crossflow filtration (Anlauf 2020).

Blocking filtration can be roughly compared to sieving. It is an extreme case characterized by a complete obstruction of the medium's pores through solid particles, thereby increasing pressure drop exponentially at a constant flowrate (Hlavacek and Bouchet 1993). Cake filtration can be considered as a less extreme case than blocking filtration, and it therefore is a more widely applied model for hard, particulate solids. In the ideal case, all particles are retained by the filter medium and start to build a homogenous structure with constant properties; pressure drop increases linearly at a constant flow rate. The pores are not necessarily blocked since the particles can build bridges that do not restrict flow as much as in the previous case (Tichy 2007). In some applications, rather the cake itself acts as the filter medium after the first layers are formed; the main function of the original filter medium is to be a support layer. A very good example of this is the abovementioned lautering filter cake, whose coarse fraction is used to retain its fine fraction (Bandelt Riess et al. 2018b). These first two configurations of surface filtration are also referred to as dead-end filtration because the fluid flows directly towards the filter medium, where the particles are stopped.

Lastly, the configuration of crossflow filtration exhibits the particularity that the suspension flows tangentially to the filter medium in contrast to the other cases. Some filter cake formation and even blocking can occur over time, but this mode of operation takes advantage of the hydrodynamic forces to minimize solid contact and accumulation. After an equilibrium has been established, flowrate and pressure drop can be held constant for relatively long periods.

As mentioned, the specific kind of filtration pertinent to this thesis is cake filtration. However, the previous derivation (graphically represented below in Figure 3) exhibits the basic disciplines and principles which spawned the research topic and provides support for minor thematic overlaps in later discussions. From now on, more focus is put on cake filtration.

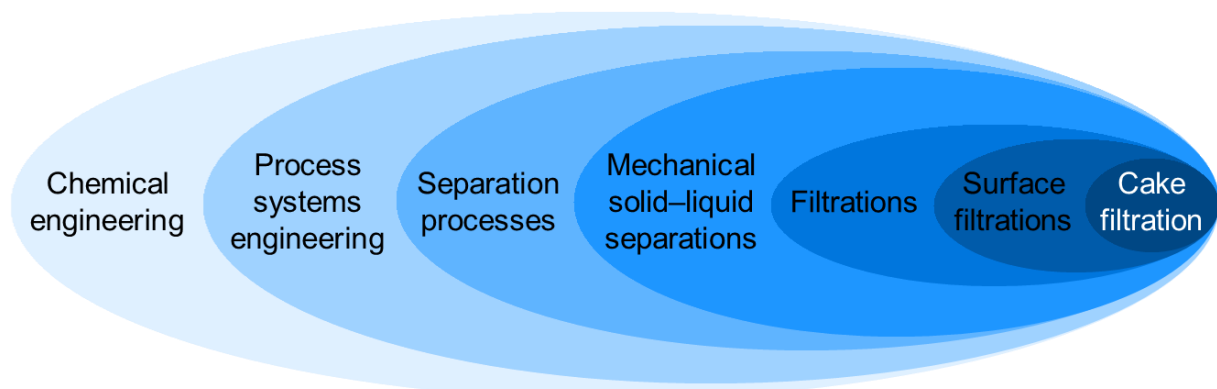


Figure 3: Derivation of the research topic of cake filtration from chemical engineering

2.2 Cake Filtration

2.2.1 Relevance

Also called wet cake filtration in the context of solid–liquid separations, it is a significant mode of operation because it offers many advantages, allowing for multiple applications whose ideal goal is either a dehydrated filter cake or a clear filtrate. Aside from the food and beverage industries, the process is found in water treatment as well as in the chemical and mineral industries, to name a few (Alles 2000). Sometimes used as a synonym for surface filtration, it is based on passing a suspension, normally with a solids concentration higher than 1%, through a relatively thin filter medium, on top of which the cake is formed layer by layer. The driving force behind the differential pressure can be generated by gravity, centrifugation, and hydraulic or vacuum pumps (Svarovsky 2001). Depending on the production process, the applied cake filtration can be operated either continuously (e.g., water purification) or in batches (e.g., lautering).

Cake filtration processes are especially applied where a direct post-treatment of the collected solids is desirable, such as washing, deliquoring, and drying. During the operation, the porous, permeable layers formed by these solid particles have thicknesses that can go from millimeters up to decimeters, depending on the system. Because of this, the filtration process must be adapted or designed, resulting in a myriad of different apparatuses: rotary filters, filter presses, centrifuges, among others (Anlauf 2020).

Moreover, cake filtration studies performed at laboratory scale allow gathering relevant data about a suspension at hand, which are then used to determine the large-scale optimal process operation or even design new apparatuses for specific applications. Thus, several variables and correlations should be considered. At the operational level, the relation between pressure and flowrate is paramount. This thesis considers the operation at constant differential pressure. If that is the case, flowrate will decrease (slowing the filtrate volume accumulation) with filtration time, as shown in Figure 4, due to the ongoing increase in filter cake height and the added flow resistance.

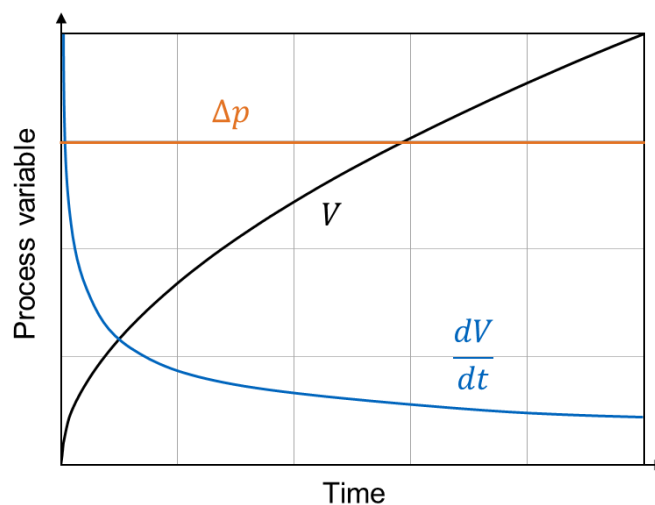


Figure 4: Evolution in time of cake filtration process variables differential pressure Δp , filtrate volume V , and flowrate dV/dt

As mentioned, the forming filter cake itself is a porous medium, meaning it is a defined volume that is only partly occupied by solid particles. The other part can be occupied by one or more fluid phases; it is heterogeneous in essence, as shown in Figure 5 with an actual filter cake. In filtration applications, however, the continuum and space-averaging approaches are taken to describe the filter cake's relevant properties. That is, it is assumed that said properties can be used to describe each point of the solid network and, additionally, that a determined property value can be assigned to all points in the control volume at a macroscopic scale (Bear 2018). The medium is thus somehow homogenized for calculations. Looking at the filter cake slice in Figure 5, it becomes clear that a detailed structural description of the entire network would otherwise not be an easy task. Among these relevant filter cake properties, porosity is one that has a key role in filtration.



Figure 5: Binarized image of a cross-sectional slice in the interior of a spent grain filter cake. The image was generated using computed X-ray microtomography and shows the cake solids in white and air in black

2.2.2 The Role of Porosity

Porosity ε is an intensive property used to express the volume fraction of void spaces or pores, the ones occupiable by the fluid phases, in a medium. The complementary property is the medium solidosity ϕ , the volume fraction occupied by the solid particles. Both quantities are defined in Equation (1) in the specific case of a filter cake:

$$\varepsilon = \frac{V_P}{V_K} = \frac{V_K - V_S}{V_K} = 1 - \frac{V_S}{V_K} = 1 - \phi, \quad (1)$$

where V_P , V_K , and V_S are the pore, filter cake, and solid volumes, respectively. Normally, it is assumed that this porosity value is also the effective value, the volume fraction where the fluid can flow, even though the medium might exhibit closed, isolated pores. The inner porosity of solid particles is commonly neglected as well (Luckert 2004).

One important aspect of porosity is that it is an elementary quantity that can be used to estimate further relevant cake properties and vice versa, such as Darcy's permeability k (Darcy 1856), a proportionality coefficient that describes how easily the fluid flows through the cake (Equation (2)):

$$\frac{dV}{dt} = \frac{k \cdot A \cdot \Delta p}{h \cdot \eta}, \quad (2)$$

where t is filtration time, V is liquid volume, η is liquid viscosity, A is filter area, and h is cake height. The most widely used equation to obtain k through ε is probably the one of Kozeny and Carman (Equation (3)):

$$k = \frac{4 \cdot d^2}{9 \cdot b \cdot \tau} \cdot \frac{\varepsilon^3}{(1 - \varepsilon)^2} \quad (3)$$

This is a simplified approach derived from the Hagen–Poiseuille law for laminar capillary flow through a bed of monodisperse, spherical particles, where d is the particle diameter, b is the capillary form factor, and τ is the tortuosity (Epstein 1989). There is a direct proportionality to particle size and porosity, as they increase the equivalent capillary diameter. The capillary form factor and tortuosity are related to its surface, which can brake the fluid, and its intricacy throughout the medium. Using permeability, it is possible to further characterize the solid network and compare different porous media (Bear 2018).

It becomes clear how crucial porosity is as a filtration process variable. Consequently, it has been thoroughly described by Tiller et al. in their notable works: The role of porosity in filtration. It has become an extended series of research articles, which started with the description of standard filtration operation modi, also based on Kozeny’s law, in the first part (Tiller 1953) and has reached its thirteenth part since then (Tiller and Kwon 1998). Up until the third part of the series (Tiller 1958), filter cakes are considered to behave ideally, as they have also been in this thesis so far: They are isotropic networks since the solid particles are monodisperse, firm spheres that remain static after becoming part of the cake. However, in reality, the suspensions to be separated are very rarely ideal, a flaw Tiller recognized and started to address in the fourth part (Tiller and Cooper 1960). It is therefore distinguished between incompressible and compressible filter cakes.

2.2.3 Cake Compression

For the ideal case of an incompressible filter cake, intensive properties, such as porosity, do not change along its height. If the process is represented as simplified as in Figure 2, then the relevant variables along cake height behave as depicted in Figure 6.

The cake is a stable, uniform structure, rendering constant porosity and permeability values over space and time. In turn, this causes pressure on the liquid side p_L to depend mainly on filter cake height and drop linearly in direction of the filter medium. The dissipated energy is transferred as p_S to the solid particles, which have sufficient mechanical stability and are not deformed by it. However, for the real case of a compressible filter cake, the process cannot be represented as simplified, and the relevant variables do change along cake height, as depicted in Figure 7.

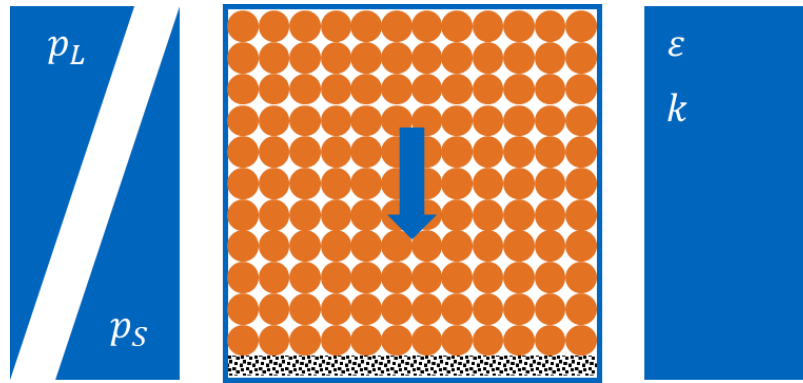


Figure 6: Spatial dependence of selected process variables inside an incompressible filter cake. Adapted from Alles and Anlauf (2003)

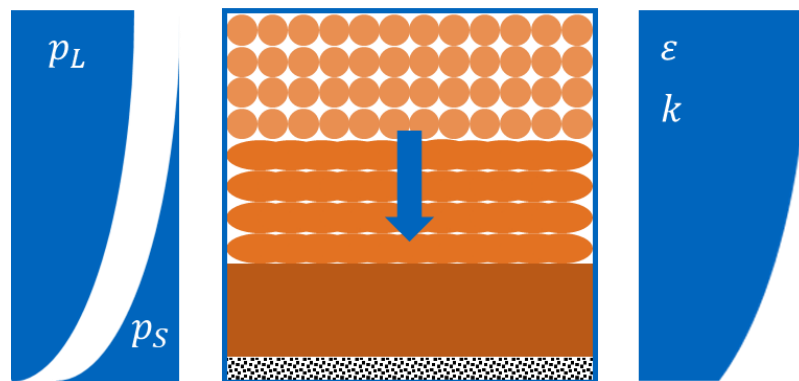


Figure 7: Spatial dependence of selected process variables inside a compressible filter cake. Adapted from Alles and Anlauf (2003)

Here, the cake is an unstable, heterogeneous structure where additional forces, such as adhesion, come into play, generating property gradients over space and time. For compressible solid particles, as represented in Figure 7, filter cake porosity and permeability are reduced in the direction of the filter medium, where the weight of the whole network is supported, and hydrodynamics are most affected. The upper layers are rather loose whereas the lower ones become very densely packed. This phenomenon has been baptized as “the skin effect” (Tiller and Green 1973) and causes p_L and p_S to stop behaving linearly inside the filter cake, which can lead to drag and further cake compression. Therefore, in addition to filter medium clogging, complications may arise during equipment operation.

Taking a closer look at the discretized porosity profile in Figure 7, the thesis formulated in Kuhn’s (2018) dissertation becomes clearer (see Chapter 1.1). In contrast to the incompressible filter cake in Figure 6, where changing the vessel somehow would not influence the solid network, adjusting wall support gradually to match each layer’s needs would certainly have an effect here. However, to adequately describe the behavior of the filter cake and meet the process requirements, the system must be studied in detail, considering the specific mechanical properties of the solid particles along with their shape and size distributions (Bourcier et al. 2016). Only then can the resulting compression mechanisms be understood and effectively counteracted.

Suspensions which form compressible filter cakes frequently have a biological origin. They can show slight to extremely high degrees of compressibility. Among the various highly compressible materials, branched glucan gels (Hwang et al. 2006), alginate beads, bacteria and yeasts (Hwang et al. 2016), activated wastewater sludge (Lee and Wang 2000; Skinner et al. 2015), microcrystalline cellulose (Mattsson et al. 2012), and chromatography gels (Kong et al. 2018) deserve to be mentioned. Such systems tend to exhibit a pronounced skin effect, forming a nearly impenetrable layer at the filter medium and stopping the process (Tiller and Green 1973).

Even though all the mentioned materials are highly compressible, they are different in nature and therefore react to compression differently as well. There are several known compression mechanisms which depend on the composition of the solid, and each one will affect the filter cake structure in its way. The most representative compression mechanisms are shown in Figure 8.

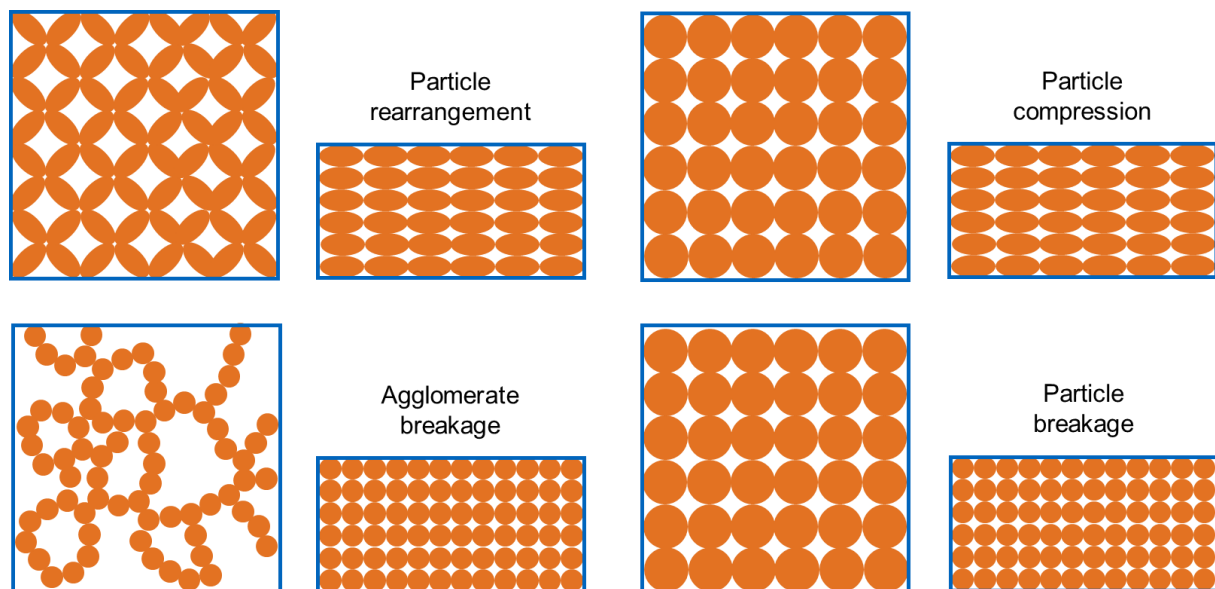


Figure 8: Filter cake compression mechanisms. Adapted from Alles and Anlauf (2003)

Particle rearrangement can apply even to incompressible solids. When they come into contact with the filter cake, the first assumed position is random and may not be the most stable one. As more cake layers are formed or more pressure is applied, particles can budge and find a more stable arrangement, becoming a denser network. This mechanism particularly affects solids with platelet shape, as roughly represented in Figure 8. The filter cake may exhibit a house-of-cards structure, which can be significantly compressed. A good example for this case is a suspension of ground leaves, such as the ones of hops flowers (Bandelt Riess et al. 2018a).

Filter cakes can also be compressed because each particle is a compressible solid itself. If the forces at a cake layer overcome the compressive strength of the particles, they will be deformed, and the whole structure will be condensed. Good examples for this case, which are compacted even at low pressures, are gelatinous and fibrous particles, such as living cells and cellulose-based products. However, if the forces at a cake layer overcome the compressive strength limit of the particles, they will fracture in some way. In the case of a destabilized suspension, particles form agglomerates that constitute relatively porous structures, which are

then reduced to their building blocks and compressed. It is, of course, imaginable that more than one mechanism occurs simultaneously during the filtration. Applications very rarely treat ideal systems, and each case exhibits peculiarities.

In summary, filter cake compression is one of the fundamental phenomena and therefore an intensively studied subject in solid–liquid separation research. It has been described numerically by, for example, Vorobiev (2006) and via extensive experimentation by Alles (2000). Furthermore, in more specialized works, Selomulya et al. (2005) utilized visualization techniques to monitor floc permeability, which can help to explain and predict how the aggregates are compressed. Park et al. (2006) investigated the correlation between porosity and flow resistance while incorporating the cake-collapse effects from a theoretical perspective. The list of studied influencing factors goes on, e.g., solid–liquid interactions and suspension stability in time (Wakeman 2007), filtration mode of operation (Mahdi and Holdich 2013), and, of course, differential pressure (Iritani et al. 2012).

However, it is always possible to further optimize the approaches to handle specific materials in separation processes, as this thesis intends to. Since the applied methodology is mainly experimental, the following question arises: How can filter cake compression be measured and evaluated?

2.3 Experimental Characterization of Filter Cakes

Comparisons between two frameworks describing the dewatering of compressible suspensions have been made in recent investigations (Höfgen et al. 2019b). They are known as conventional filtration theory, attributed to Ruth, Tiller, and Shirato (Tiller et al. 1987), and compressional rheology, developed by Buscall, White, and Landman (Buscall and White 1987). While the former mostly uses space-averaging approaches to quantify separation descriptors empirically, the latter yields local information from a phenomenological point of view. Nevertheless, the two theories have been proven to be interchangeable and are able to complement each other (Landman et al. 1995; Stickland 2015; Höfgen et al. 2019b). Hence, this study benefits from both frameworks to evaluate process strategies based on dealing with filter cake compressibility.

2.3.1 Classic Filtration Theory

For the relatively trivial case of incompressible cake formation, standardized procedures for the experimental determination of the flow resistance of the filter medium R_M and relative filter cake resistance α_K have been described in detail for decades (Anlauf 1994). The current guidelines are compiled in the well-known directive VDI-Norm 2762 Part 2 (updated in 2010), which represents the theoretical basis for the methodology applied in the first research article (see Chapter 4.1). Logically, these works are based on Darcy’s law (Darcy 1856), which, solved for differential pressure Δp , looks like:

$$\Delta p = \frac{\eta \cdot R}{A} \cdot \frac{dV}{dt}, \quad (4)$$

where h/k has been replaced with R , the total flow resistance of the porous medium. Considering that the total pressure drop across a filter is composed of the pressure drop across

the filter cake Δp_K and the pressure drop across the filter medium Δp_M , then it is possible to describe each pressure drop contribution using Equation (4).

$$\Delta p = \Delta p_K + \Delta p_M = \frac{\eta \cdot R_K}{A} \cdot \frac{dV}{dt} + \frac{\eta \cdot R_M}{A} \cdot \frac{dV}{dt} \quad (5)$$

At this point, it makes sense to introduce the definitions of concentration constant K and relative filter cake resistance α_K (the reciprocal of the permeability k), since filter cake height h and therefore total cake resistance R_K are time-dependent variables and substitute them into Equation (5).

$$\alpha_K = \frac{R_K}{h} \quad (6)$$

$$K = \frac{h \cdot A}{V} \quad (7)$$

$$\Delta p = \frac{K \cdot \eta \cdot \alpha_K}{A^2} \cdot V \frac{dV}{dt} + \frac{\eta \cdot R_M}{A} \cdot \frac{dV}{dt} \quad (8)$$

If Δp is maintained constant during the experiments (see Figure 4), it is valid to solve Equation (8) for time by separating variables for $V = 0$ at $t = 0$, yielding thusly the linear V function on which the VDI-Norm 2762 Part 2 is based:

$$\int_0^t dt' = \int_0^V \left(\frac{K \cdot \eta \cdot \alpha_K}{A^2 \cdot \Delta p} \cdot V' + \frac{\eta \cdot R_M}{A \cdot \Delta p} \right) dV' \quad (9)$$

$$t = \frac{K \cdot \eta \cdot \alpha_K}{2 \cdot A^2 \cdot \Delta p} \cdot V^2 + \frac{\eta \cdot R_M}{A \cdot \Delta p} \cdot V \quad (10)$$

$$\frac{t}{V} = \frac{K \cdot \eta \cdot \alpha_K}{2 \cdot A^2 \cdot \Delta p} \cdot V + \frac{\eta \cdot R_M}{A \cdot \Delta p} \quad (11)$$

Hence, if the experimental filtration data (accumulated filtrate volume over time) are plotted according to Equation (11) (in the form of time/accumulated filtrate volume over the same volume), R_M and α_K can be respectively solved from the intercept and the slope taken from the linear portion of the plot. However, selecting the relevant data for the linear fitting can become somewhat arbitrary.

Considering this, recent research conducted by Kuhn et al. (2020) has effectively shown that fitting the filtration data nonlinearly to a root function is more precise both in terms of execution and results (the filtration data is not cropped anymore). It is proposed to take a step back and rather solve Equation (10) to describe filtrate volume over time.

$$V = \sqrt{\frac{2 \cdot A^2 \cdot \Delta p}{K \cdot \eta \cdot \alpha_K} \cdot t + \left(\frac{R_M \cdot A}{\alpha_K \cdot K}\right)^2} - \frac{R_M \cdot A}{\alpha_K \cdot K} \quad (12)$$

The sought resistances can again be estimated by finding the deviation minimum with a usual least-squares method. Thus, choosing this fitting strategy allows for an analysis of all gathered data, rendering more exact values (Kuhn et al. 2020). An example of raw and linearized representations of real filtration data is shown in Figure 9. The linear portion of the plot does not start at 0 but at around 200 mL.

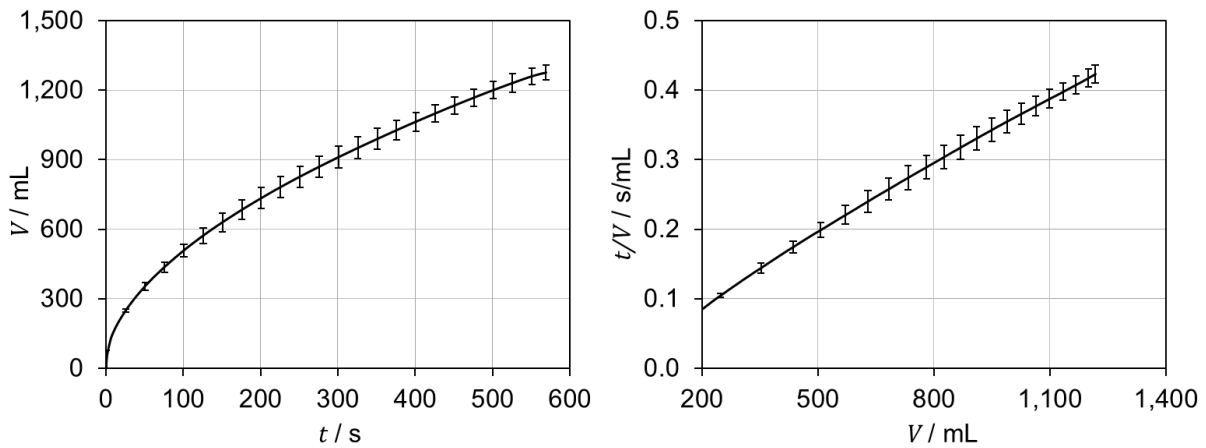


Figure 9: Filtrate volume over time and linearization of the filtration curve

It was previously mentioned that these guidelines apply in the case of incompressible cake formation (Equation (7) assumes the h/V proportionality remains constant) or, at least, in the case that process parameters allow for not very differentiable compression zones. Under these conditions, space-averaged but definite α_K values can be obtained for different Δp . Furthermore, multiplying Equation (11) by Δp yields a function where neither the slope nor the intercept is pressure dependent. This means that plotting $\Delta p \cdot t/V$ over V at different Δp values will yield markedly different functions if the solid network is compressible, and α_K is indeed pressure dependent. This is demonstrated in the second research article (see Chapter 4.2).

It is possible to draw conclusions about a solid network's compressibility if α_K is described as a function of Δp , for which several empirical approaches have been used. Filter cake compressibility is often determined by fitting power functions, such as Equation (13) (Tiller and Horng 1983; Alles 2000; Chen 2006; Kovalsky et al. 2007), to the observed changes in flow resistance due to increases in differential pressure:

$$\alpha_K = K_\alpha \cdot \Delta p^{N_\alpha} \quad (13)$$

Here, N_α represents global compressibility, and its value can be used as a point of reference for comparison between compressible network behaviors. Perfectly incompressible networks will exhibit a N_α value of 0, making α_K invariable, whereas highly compressible ones will exhibit a N_α value of approximately 1 (Anlauf 2020). The coefficient K_α does not necessarily have a physical meaning, but it is often associated with filter cake resistance at a low differential

pressure. Another (probably more cited) approach is the following one, attributed to Tiller et al. (1987):

$$\alpha_K = \alpha_{K,0} \left(1 + \frac{\Delta p}{p_a}\right)^{N_\alpha} \quad (14)$$

The compressibility number N_α is present again as well as one further fitting parameter p_a and the relative filter cake resistance for an unstressed porous network $\alpha_{K,0}$. For highly compressible systems, however, it is not recommended to determine the empirical parameters in Equation (14) in the laboratory following the equipment guidelines and experimental procedures in the VDI-Norm 2762 Part 2 as the application of pressure variations is not possible. Piston-driven experiments are needed to achieve this, which brought about the introduction of the Compression-Permeability (C-P) cell, illustrated in Figure 10, as equipment for filterability measurements (Ruth 1946).

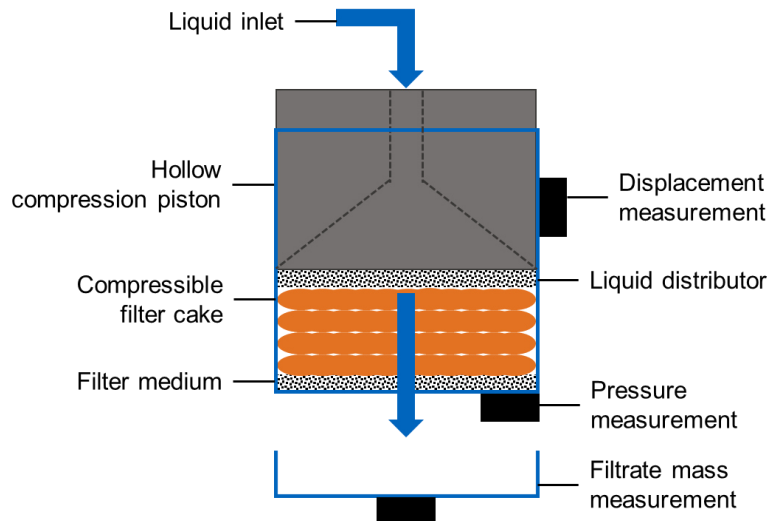


Figure 10: Schematic illustration of a C-P cell. Adapted from Shirato et al. (1968)

A piston is used to compress a filter cake to a given degree while the load supported by the network and the resulting cake height are measured. Since the piston is hollow, liquid can be pumped through it and the distributor to permeate the cake and determine filtrate accumulation rate under the given state of compression. This is repeated for variable conditions to express the cake properties as a function of pressure and fit the characteristic parameters of Equation (14).

Nonetheless, these conventional theory approaches have a rather empirical basis, as mentioned, and therefore merely relate pressure with flow resistance (or porosity) in an indirect manner. On the contrary, solid network compression is studied in compressional rheology as a material property and is thus explicitly described using these parameters (Höfgen et al. 2019b). Since both frameworks have advantages and are interchangeable and linked through Darcy's permeability (Landman et al. 1995; David Suits et al. 2005; Stickland 2015), solid-liquid separation research should profit from both.

2.3.2 Compressional Rheology

Compressional rheology's fundamental variables, aside from the ones presented already, are all expressed as functions of the solid volume fraction ϕ in the suspension. They are known as compressive strength or compressive yield stress p_y , hindered settling function R_ϕ , and solids diffusivity D_ϕ (Stickland 2015). This thesis is mainly focused on p_y since it represents interparticle attraction and repulsion strength in the forming network and can be directly measured during compression experiments: If a filter cake is compressed to a specified degree, mechanical equilibrium is reached, and there is a significant drainage rate (filtration), then the solid pressure p_s can be equated to p_y (Buscall and White 1987).

Taking a closer look at the formal definitions of the ϕ functions, the abovementioned link between classic filtration theory and compressional rheology is revealed. The hindered settling function R_ϕ is in fact inversely proportional to Darcy's permeability and describes the solid-liquid interphase drag and, therefore, the rate of dewatering. D_ϕ establishes a proportionality between p_y and R_ϕ and is used to describe the densification propagation speed throughout the network (Stickland 2015). The formal definitions are presented in Equations (15) and (16).

$$R_\phi = \frac{\eta}{k} \cdot \frac{(1 - \phi)^2}{\phi} \quad (15)$$

$$D_\phi = \frac{dp_y}{d\phi} \cdot \frac{(1 - \phi)^2}{R_\phi} \quad (16)$$

With the fundamental variables, suspensions are described as interconnected particles which are collapsed and dewatered when a sufficiently strong load is applied. The compressibility of this particulate network has a key role in separation processes as it is related to solid pressure, concentration, and therefore permeability. In consequence, contrastingly to the classical filtration theory, compressibility is always accounted for as a material property through the compressive strength p_y in the phenomenological descriptions of compressive rheology. Hence, both theoretical frameworks require to determine key parameters and have spawned analogous experimental techniques to this end.

The works by Höfgen et al. (2019b) are very representative in this regard because they have made detailed comparisons between the classical and compressional methods from both theoretical and practical points of view. Moreover, their evaluations of laboratory filtration equipment allow to conclude about best practices when characterizing filter cakes. Agglomerated calcium carbonate suspensions were separated under increasing pressure steps in three typical filtration devices: a VDI-standardized filtration chamber (also known as Nutsche filter), a C-P cell, and a piston-driven filtration rig (like the one in Figure 10 but lacking the liquid inlet). The contrast between the experimental results obtained through the different methods can be seen in Figure 11.

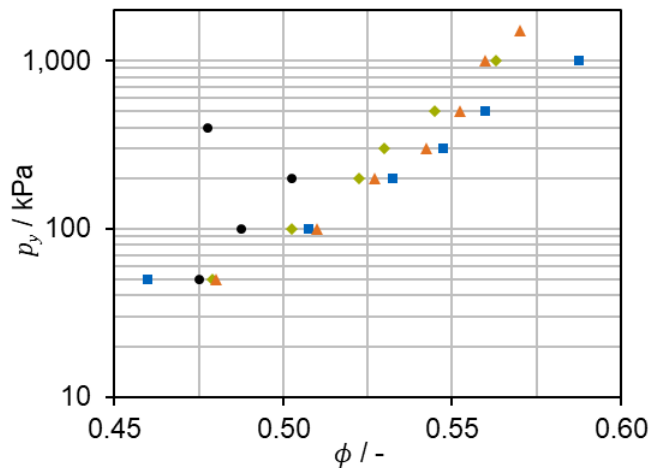


Figure 11: Compressive yield stress over solidosity determined using: VDI filter (● black), C-P cell (■ blue), C-P cell without permeation (◆ green), filtration rig (▲ orange). Adapted from Höfgen et al. (2019b)

The data gathered using the Nutsche filter does not yield a clear compressibility trend and is limited to 400 kPa. The compression runs performed with the C-P cell and filtration rig show agreement at low solid fractions but start to diverge at higher values. However, repeating the compression in the C-P cell without starting the usual liquid permeation yields a more similar curve to that obtained through the filtration rig, proving that the liquid drag in the cell contributes to further cake consolidation. This result comparison clearly justifies the recommendation that piston-driven equipment should be used for filterability experiments if the cake exhibits a certain degree of compressibility. Additionally, the comparison also motivated the development of the experimental method applied in Chapter 4.2, where a modified universal testing machine is used as a filtration rig to compress filter cakes instead of a standard C-P cell, avoiding liquid drag.

Thus far, it has been established that filter cakes can exhibit significant compressibilities and that various collapse mechanisms can be the cause. Hence, different theoretical and experimental approaches are taken to quantify and evaluate filtration-related phenomena. With these proper tools, it becomes possible to detect and describe improvements in the process, consequence of performing parameter variations aimed at counteracting filter cake compression and enabling more efficient separations.

2.4 Counteracting Compression Issues

Considering the economic relevance of cake filtration processes and the fact that filter cake compression is a generalized issue, process strategies must be designed and applied to prevent and deal with potential production inefficiencies. As exposed, a differential pressure is both the driving force behind filtration and the cause of cake collapse. In the sight of this paradox, the need for a compromise, or rather for optimization, arises along with very specific engineering tasks. As a result, various methods have been and are continuously being developed to counteract the compression and clogging of filter cakes. This chapter aims to provide an overview of well-established process strategies as well as an introduction to relatively new technological advancements.

2.4.1 Classic Process Strategies

Suspension Pretreatment

Some of the causes for filtration process difficulties are noticeably worsened if the suspended particles are too small, heterogeneous, or diluted (Anlauf 2020). Therefore, operational problems can be nipped in the bud by treating the suspension before it reaches the separation stage.

Fine particles can be enlarged through agglomeration, which should increase filter cake permeability according to the proportionalities in Equation (3), assuming the agglomerates are mechanically stable for the operational pressure. In this regard, the effect of agglomerate breakage represented in Figure 8 would occur in reverse. Agglomeration is achieved using clarifying agents which bind the fines and build flocs of larger size and mass. Consequently, the solids become easier to retain and the clarifying process is accelerated (Jiao et al. 2017). Moreover, if the suspension exhibits a broad particle size distribution, agglomeration can be specifically applied to the fine particle fraction to homogenize the solids' properties and make the separation process more efficient (Bandelt Riess et al. 2018b).

Heterogeneity is characteristic of non-ideal systems. If a particulate collective is perfectly bidisperse, the porosity and permeability of the resulting filter cake will be significantly smaller than those of an ideal, monodisperse system. The worst-case scenario in this regard is that where the smaller particles can perfectly fit into the pores between the bigger ones and block them (Hudson 1949). As an alternative to agglomeration, the polydisperse systems can be subdivided into two (or more) rather monodisperse ones through screening or classification, rendering more permeable cakes. This is often the aim of hydrocyclones, centrifuges, decanters, and basins (Svarovsky 2001).

As mentioned in preceding chapters, some filtration processes require a solid fraction minimum to operate. One of the dangers of very low concentrations is spontaneous particle classification, which can again yield heterogeneous filter cake structures and cause a blockage. In this case, the solid fraction should be increased to promote particle-particle interactions and swarm behavior (Richardson and Zaki 1954). Apparatuses for suspension thickening take advantage of this and allow for homogenous sedimentation. Further treatments of chemical and thermal nature are thinkable, depending on the process.

Operational Pressure Selection

Once the suspension reaches the separation stage, strategically selected operational parameters shall guarantee efficient filtration times. Differential pressure is critical in the case of compressible filter cakes. Several investigators, such as Alles (2000), have analyzed filter cake compression in detail and derived general guidelines to properly match different kinds of suspensions with operational pressure. Through an incompressible cake, more pressure is simply translated to a directly proportional throughput. However, proportions change with the degree of compressibility, and the pressure effects become less significant as it increases (Alles and Anlauf 2003). The worst-case scenario in this regard is that where the filter cake is so compressible that it collapses with a relatively low differential pressure, making filtrate flow impossible. In most real cases, however, a pressure limit can be established for the system to maximize flow without wasting energy through stagnation (Tiller et al. 2001).

The preceding considerations are especially valid in the trivial case of a single and constant operational pressure. Nonetheless, the practical method is rather based on a pressure profile,

which prevents premature filter cake consolidation through gradual increases (Alles 2000). Logically, lower pressures and flow rates slow down cake accumulation and flow resistance increase. Besides, avoiding high pressures during cake formation helps guarantee particle bridge integrity at the filter medium, avoiding filtrate contamination (Alles and Anlauf 2003). Operational parameter variations are, of course, strongly dependent on material properties, generating further optimization tasks.

Filter Aids

An extensively applied strategy for compressible systems is the use of filter aids, which allows to increase cake porosity and operating time. In the special case of fermentation products, the removal of cells, subcellular matter, and precipitated components for liquid clarification is necessary (Hunt 2002). The use of filter aids or powdered media is also known as body feed because, in opposition to the abovementioned strategy of particle classification, material is dynamically added to the process, becoming part of the suspension and the filter cake. Common filter aids are solid particles (e.g., diatomite, perlite, cellulose) that help mechanically stabilize the suspended impurities; they minimize contact between compressible fines, counteracting cake compression and improving overall permeability.

The strategy of filter aid filtration has been mechanistically described by Kuhn and Briesen (2016) at the Chair of Process Systems Engineering to find optimal operational parameter profiles, although only for incompressible filter cakes so far. Thus, it was proven that a constant filter aid dosage is generally the optimal path. However, depending on the separation mechanism, a dosage variable in time could lead to slight energy minimizations. Due to the mechanical support filter aids provide in a cake, packed bed elements (see Chapter 2.5) have been referred to as macroscopic filter aids (Kuhn 2018).

Apparatus Selection

Both apparatus and filter medium selection are crucial for an efficient separation process operation. As discussed earlier, multiple applications have been made possible because of permutations of different factors: solids size and concentration, cake thickness, material compressibility, throughput, driving force, continuity, among others (Hess and Thier 1991). Most of all, the separation step and the corresponding apparatus must be compatible with the process goal and product specifications, e.g., dry solids or clarified liquids. In this regard, the separation as well as the post-treatment processes, dedicated to polish and improve the quality of the desired suspension components, often deal with deliquoring, washing, pressing, or drying of the filter cake (Wakeman and Tarleton 1999).

The special case of considerably compressible filter cakes has spawned filtration equipment which partly fuses separation and post-treatment and allows for an additional apparatus classification with and without pressing capabilities (Alles 2000). Considering the highly porous upper layer of a collapsed filter cake, the need for compaction during or after the process is a given. Thus, the potential weakness of the filter becomes the strength of the press, ultimately yielding the sought results when combined. Nevertheless, choosing whether the operation units are to be performed separately or together is primarily dependent on the specific process economy.

Cake Resuspension

A very intuitive process strategy is the resuspension of the filter cake, also known as intermittent cake filtration (Alles and Anlauf 2003). This mode of operation is based on the

logical principle that flow resistance is temporarily minimized if the growing filter cake is reincorporated into the suspension, practically resetting its formation with a certain frequency during the filtration. Due to the liquid loss before each resuspension step, such an apparatus also acts as a thickener, additionally bringing about the advantages mentioned above. This strategy can be considered as a middle ground between a standard cake filtration, where the resuspension frequency is zero, and crossflow filtration, where resuspension happens continuously, and a filter cake is not desired (see Chapter 2.1).

Cake resuspension is a filtration method that has inspired alternative separation technology, such as harnessing shear forces between plates in a dyno-filter (Michel and Gruber 1971) or using scraping tubes in a pressure filter with rotating disks at variable speeds (Koch et al. 1999). However, being as intuitive as it is, this concept has been present in very traditional fabrication methods for many decades, such as beer mash filtration in a lauter tun with raking knives (Narziß and Back 2009). Here, an arrangement of blades is lowered into the filter cake to loosen it when the throughput has become too low. Relatively low speeds and controlled invasiveness lower cake resistance while minimizing the effect on filtrate turbidity (Engstle et al. 2015). This and a selection of the aforementioned classic process strategies to counteract cake compression problems have been schematically represented in Figure 12.

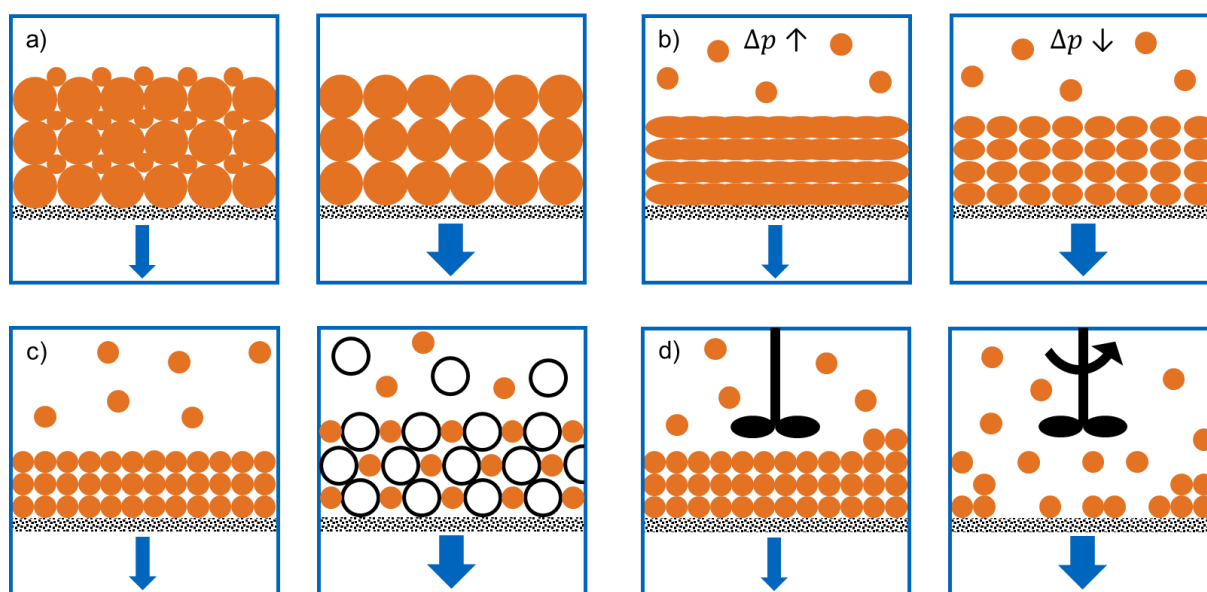


Figure 12: Schematic representation of the classic filtration process strategies:
a) Screening, b) Pressure selection, c) Filter aids, d) Cake resuspension

2.4.2 State of the Art

There is never a one-size-fits-all solution. Consumer needs have evolved rapidly, and industries have had to adjust accordingly to deliver the expected goods and conditions, producing even paradigm shifts (Xu et al. 2018). At process level, numerous innovative separation strategies have been published to date to improve various production methods one way or another. The spectrum of complexity has become very broad since the strategy must always be tailored to the application at hand. Depending on the industry, measures based on, e.g., suspension pretreatment will have different kinds of effects and not necessarily make the separation more efficient (Eshed et al. 2008). Hence, the approach angle varies as well and is

to be carefully determined, multiplying the available strategies. Some of them are briefly presented in the following.

Gas Bubble Injection

On the current note of lauter tun technology in the beer industry, it is also an example where innovative techniques have been put to the test. Through the installation of a nitrogen bubble distribution system at the bottom of the lauter tun, Tippmann et al. (2010) observed two positive effects for the process: filtrate flow rate was greatly increased, and the gas also removed part of the unwanted aroma compounds in the suspension. Analogous to the traditional raking knives, the fine bubbles loosened the compressible filter cake, preventing blockage and lowering its flow resistance. This approach for a very specific filtration process thusly achieved considerable time and energy savings. In the case of crossflow applications, this strategy helps to remove membrane scaling, preventing operation problems (Drews et al. 2010).

Mechanical Oscillations

Filter cake loosening to increase flow rate can also be observed by using mechanical oscillations during the process. Continuous low-frequency vibrations (up to 500 Hz) of the filter medium support altered the structure of a PVC filter cake and considerably enhanced its permeability (Wakeman and Wu 2002). Depending on the system, a specific combination of vibration frequency and acceleration can be found, which prevents the filter cake to form as such and allows the filtrate to permeate much more freely. This was also evaluated in the case of a more complex system: blood (Kim et al. 2018). A portable vibration-assisted filtration device succeeded in separating the desired leukocytes from the sample and increasing the application throughput.

The advantages of mechanical oscillations during filtration processes have also been evaluated by using pulsating overpressure (Shevchenko and Tynyna 2017) and ultrasound (Bosma et al. 2003; Trujillo et al. 2014). Like gas bubble injection, the latter strategy is usually applied in crossflow filtration to avoid and remove membrane fouling (Kyllönen et al. 2005; Borea et al. 2018). However, the manipulation of ultrasound standing waves is very useful when separating organic microparticles also because they are agglomerated in the nodes of the ultrasonic field, making them easier to separate.

Mechanical oscillations can be applied during filter cake post-treatment as well. Illies et al. (2017) used a vibrating plate on top of a formed filter cake to tackle cracking problems and improve the air-drying process. The shear caused by the oscillations compacted the cake enough to significantly reduce cracking.

Magnetic Force Field

Alternatively to an ultrasonic field, a magnetic force field can also render more permeable filter cakes. Eichholz et al. (2007) successfully built a filter press which allowed for a superposition of cake filtration and magnetic separation in an inhomogeneous external field. Two different effects are observed when using this strategy, which make cake filtration processes more efficient. While the solids are still suspended, the magnetic field alters their movement in relation to the liquid and slows down cake formation. This phenomenon is analog to the ones occurring during thickening and pressure control. Once the solids become part of the cake, the magnetic force maintains their induced polarity and causes them to link with each other and align with the field. This behavior modifies the whole cake structure, making it much

more permeable than one in absence of magnets. The addition of these phenomena greatly contributes to a cake resistance reduction (Stolarski et al. 2006).

The abovementioned effects are valid for the trivial case where para- and ferromagnetic solids are present in the suspension. However, in the opposed case of purely diamagnetic materials, the strategy can still be applied if functionalized magnetic adsorbents are purposefully added to the mixture (Eichholz et al. 2008). This way, key components can be selectively separated from complex broths and post-treated.

Treatment Superposition

‘Less is more’ is a notion that often leads to good design. Nevertheless, sometimes ‘more is more’, meaning that greater effects can be achieved by applying more than one kind of treatment simultaneously. The classic filtration strategies are known to be combined and permuted in industry (Svarovsky 2001), but this is also true for more current ones, exponentially increasing the number of possibilities. For instance:

The classic method of coagulation of raw water contaminants (microorganisms and organic acids) can be combined with further chemical processing, such as ozone oxidation, to significantly reduce membrane fouling (Yu et al. 2016). Coagulation is a standard pretreatment method to destabilize suspensions and allow solid particles to come into contact and agglomerate (Bellmann 2003). However, if an oxidation stage is added downstream as part of the pretreatment process, irreversible membrane fouling can be minimized. The combined effects reduce bacteria and the production of blocking extracellular polymers, limiting filter cake formation. Additionally, the organic acids are oxidized, thereby increasing the overall suspended solids but also their filterability.

In the case of sludge dewatering, the superposition of compression and shear forces to increase process efficiency is an ongoing subject of investigation (Höfgen et al. 2019a). To this end, the drum filter was redesigned to study the simultaneous effect of both forces. The dewatering equipment consists of two adjacent high-pressure rollers, and the suspension is fed through the gap between them to be compressed. Additionally, shear is generated within the gap by rotating the rollers at different speeds, which greatly enhances the process efficiency. These investigations have also helped to develop laboratory equipment and methods, which allow to quantify the superposed effects during the same experiment, by installing a rotating vane in a piston-driven filtration device (Höfgen et al. 2020).

Cake filtration and post-treatment (both washing and drying) can also be cleverly superposed in the same apparatus. When producing gypsum for construction, the final briquettes need to have low moisture and chloride contents. For such an application, filtration equipment that uses steam pressure as driving force offers the potential to make production more efficient (Peuker and Stahl 2000). The combined unit operations allow for filter cake build-up on the medium which is constantly penetrated by condensing steam. The condensate forms a homogenous front that mechanically displaces the suspension liquid while heating the solids. Once the pores have been emptied, the steam is used further to reduce the moisture of the filter cake (Peuker and Stahl 2001).

System Micromanipulation

All classic process strategies as well as most of the aforementioned, more current ones consider filtration processes from a rather macroscopic point of view and were developed within that context. As discussed earlier, the industry has had to undergo paradigm shifts, and this is

also true for the field of solid–liquid separation. The continuum and space-averaging approaches were justified in previous chapters as macro-theoretical analysis methods to study filtration. However, micro-theoretical ones have also become well known to the point of producing the latest paradigm, a framework that has been referred to as micro-manipulation (Kuhn et al. 2017). As a result, this last part of the ‘State of the Art’ chapter makes some honorable mentions regarding the introduction of parameter variations, this time on the microscopic scale.

Within this technological paradigm, elements of the filtration equipment are functionalized and tailored to the suspended particles themselves. The membrane properties can be chemically or physically changed to display selective or anti-fouling behavior without altering the process. Liu et al. (2016) reviewed the available technology to modify traditional membranes and make them smart gating according to specific stimuli (e.g., temperature, pH, charge, light). Low et al. (2018), for instance, could fabricate mixed-matrix membranes for wastewater treatment with boron nitride nanosheets, which changed the membrane surface roughness and charge as well as overall structure, resulting in both high water permeance and fouling resistance. Al-Shimmery et al. (2019) modified the membrane support to give it a wavy (double-sinusoidal) construction. This simple physical change significantly increased filtration area and positively altered the local hydrodynamics, thusly achieving greater water permeance and filtration capacity recovery after cleaning. These examples prove that micromanipulation is indeed an ongoing investigation subject that yields potentially applicable results.

Furthermore, due to recent advancements in additive manufacturing (3D printing) and membrane technology, it is now possible not only to modify the filter medium but also to completely generate it according to predetermined structures, which are previously designed to fulfill specific objectives, and subsequently functionalize them. Techniques have already been developed that allow to make various patterned modifications to the surface of membranes. For example, increased roughness of the membrane at the nanoscale delays protein deposition and prolongs operation time (Low et al. 2017). This and other selected process strategies have been schematically represented in Figure 13.

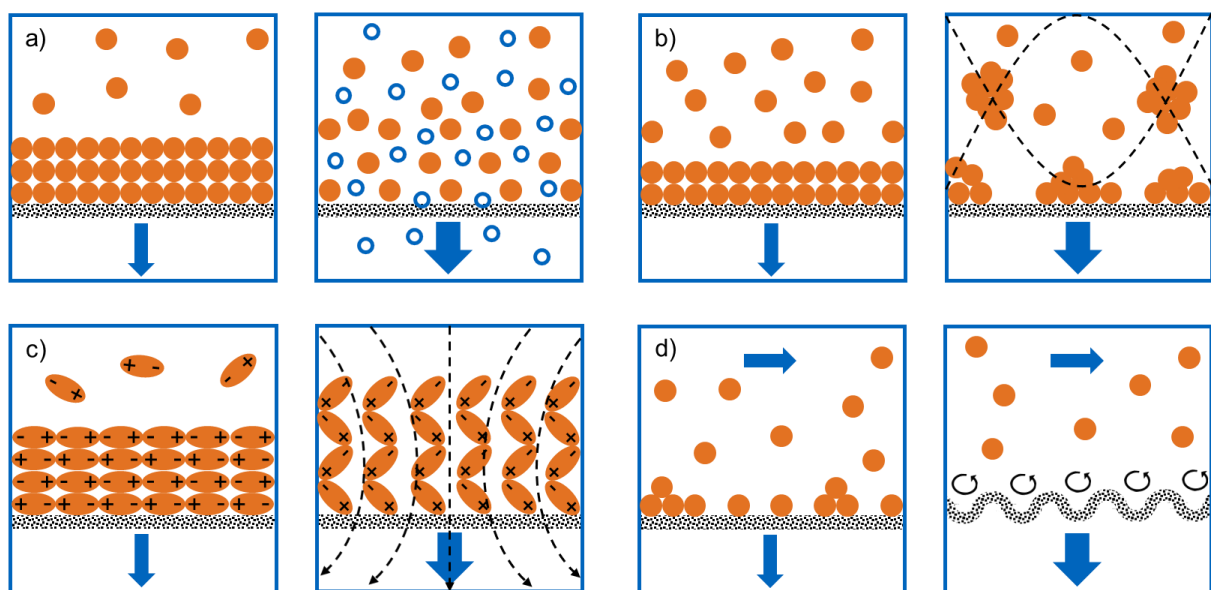


Figure 13: Schematic representation of the modern process strategies:
a) Gas bubble injection, b) Ultrasonic field, c) Magnetic field, d) Micromanipulation

Aside from separation membranes, 3D printing can benefit the fabrication of porous media in general. Fee et al. (2014) and Nawada et al. (2017) proved that it is a valid method to create packed monolithic structures using computer-aided design. Reproducible microscopic geometries and arrangements of different kinds (e.g., spheres, tetrahedra, octahedra) were printed, which showed high fidelity towards previous calculations and model predictions. Since this technology has made it possible to manipulate the shape, position, and orientation of particles in a microstructure, it could also help to support and control cake formation in filtration applications.

The possible connection between these two investigation topics would be one based on medium porosity and its influence on permeability and fluid pressure drop. It is well known that particulate beds packed inside a containment column can exhibit behaviors such as channeling and preferential flow caused by wall effects, frustrating complete reproducibility in their design (Fee et al. 2014). However, this could be harnessed and applied to filtration processes to purposefully incorporate wall support and counteract cake compression. This way, friction at the added filter walls would consume part of the increasing solid pressure.

Thus, the conjectures that link packing wall support with cake filtration optimization become more evident (see Chapter 1.1). However, the potential correlations have not been analyzed in the literature yet, not even on the macroscale. This makes experimentation with conventional, macroscopic packed bed components already available in industry a good starting point to discover said interplays. Such packed beds already have a fundamental role in the field of thermal separation processes in other unit operations, such as absorption, extraction, and rectification. For this reason, the next chapter provides a brief theoretical introduction about them before experimentally fusing the two concepts.

2.5 Packed Beds

2.5.1 Relevance

Packed beds are extensively used in industrial thermal separation processes due to their capability to increase the contact surface between phases, which is of paramount importance. At the same time, they pose the highly demanded benefit of maintaining relatively low hydraulic pressure drops through the apparatus (Maćkowiak 2003). Hence, the heat and mass transfers from one phase to another are accelerated, allowing for more compact and efficient separation columns. Packed bed manufacturing technology, be it for random or structural arrangements, has seen considerable advancements in the last century: from the original Raschig rings made of ceramic tube pieces to the latest generation of Raschig super-rings made of intricately folded metal one hundred years later (Schultes 2003). The packed bed type suitable for an application depends on factors like size, shape, heat and corrosion resistance, and costs. Figure 14 shows some representative packed bed components.

Due to their versatility and wide applicability, packings are still a current investigation topic that has been studied from all kinds of perspectives. The most ambitious goals are, of course, to achieve larger surfaces and void volumes to reduce pressure drops even further and to make accurate predictions thereof (Allen et al. 2013; Erdim et al. 2015). To do so, some of the packing's properties and effects that have been evaluated in detail are porosity distribution (Wang et al. 2001), mass transport phenomena (Wang et al. 2005), operation conditions (Qian et al. 2011), liquid retention (Fourati et al. 2012), and tortuosity (Pardo-Alonso et al. 2014). Once these properties are well known, optimization potential can be found.

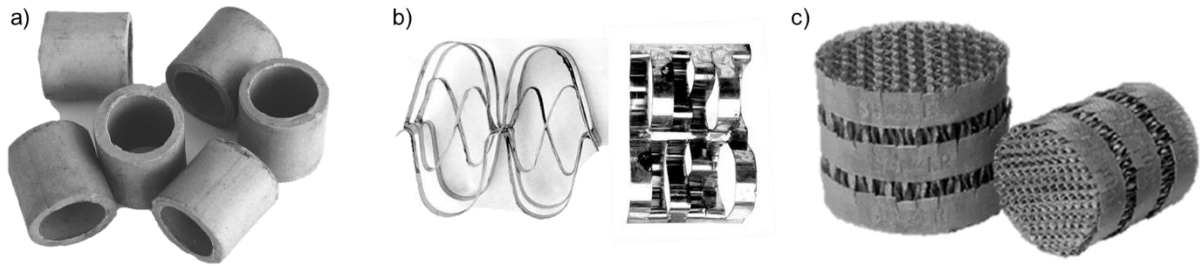


Figure 14: Photographs (CC) of exemplary packed bed components.
 a) Raschig rings and b) super-rings for random packings (both from Raschig GmbH),
 c) Mellapak structured packing (Sulzer AG)

Additionally, algorithms to generate simulated random packings using numerical methods have been successfully validated, allowing to perform different case studies without the need for expensive and complex experimentation (Mueller 2005; Niegodajew and Marek 2016). On the liquid side, simulations via computational fluid dynamics for both structured and random packings have been used to determine flow velocity and distribution (Zhang et al. 2013; Niegodajew et al. 2014). Nevertheless, recent studies have developed experimental methods to even determine ring orientation within random packings (Marek and Niegodajew 2020).

Packed beds for separation columns have not escaped the additive manufacturing trend either. The structured designs of Neukäuffer et al. (2019) based on crystal lattices show that very specific modifications are possible and that they could be adapted to numerous applications. Therefore, a modification of this method to functionalize and improve filtration equipment is conceivable.

2.5.2 Establishing the Link to Filtration

When modeling disperse particulate systems, a supposition that is made often to accelerate calculations is that the dimensions of the container are endless. For actual applications confined to finite spaces, however, physical boundaries must be established and considered, frequently in the form of receptacle walls, because of their influence on the system. The authors of copious experimental and numerical studies address the effects of the column wall on packed bed porosity in some way (Cohen and Metzner 1981; Bey and Eigenberger 1997; Wang et al. 2001; Di Felice and Gibilaro 2004; Allen et al. 2013). Since filter cakes consist of solid particle networks confined in a vessel as well, the first parallel between the two unit operations can be drawn here.

Even for the relatively trivial case of randomly packed, uniform spheres, local porosity changes dramatically with the radial coordinate in a cylindrical bed. This has been investigated for decades, and well-known works, such as the ones by Sonntag (1960) and Jeschar (1964), have gathered considerable amounts of data and bulk porosity correlations, which also allows for pressure drop predictions. More recently, Mueller (2019) compiled the abovementioned and several other works as a basis to improve the existing models for predicting near- and far-wall radial porosities in a cylindrical bed. All these models indicate that the highest porosity value is located at the column wall. However, using packed beds as a strategy to incorporate more wall support into a forming particulate network is an approach that has not yet been discussed in the literature.

Wall effects are thus known to cause channeling, which promotes preferential flow and less residence time for the liquid during absorption or rectification. This is a clear disadvantage for thermal separation processes, but, for mechanical ones, it could mean the contrary. There is already evidence that high-performance liquid chromatography benefits from additional walls found in Lan et al. (2012) and Lan (2013). They investigated the effects of using different configurations of cylindrical inserts inside a chromatography column packed with compressible resins. It was shown that, when these inserts were put at the bottom of the column, the resin beads could endure a significantly higher throughput velocity at the onset compression by losing only a small amount of accuracy. The results were not only a function of the position of the inserts but also of other factors, such as insert number and dimensions, mechanical properties of the resins, and wall roughness. Their conclusions speak for applying the strategy to cake filtration as well.

Hence, it has been shown not only that packings can be innovatively designed and manufactured accordingly but also that the manipulated properties can fulfill their intended function. It would be very beneficial for cake filtration processes if these advantages could be transferred somehow. To do so, the new interactions and correlations must be well understood first. The hypotheses presented in Chapter 1.3 and the following methodology were formulated to lay the groundwork for the use of this potential process strategy, which introduces the macroscopic manipulations of a packed bed to produce favorable microscopic effects in cake filtration.

Chapter 3: Methodology

To avoid repetitiveness, this chapter consists of one schematic representation in Figure 15, which gives an overview of the methods used and measurements made throughout the studies that compose this thesis. The details of each procedure are given in Chapters 4.1 through 4.3.

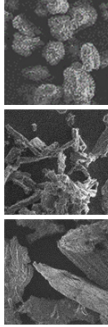
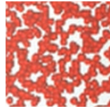

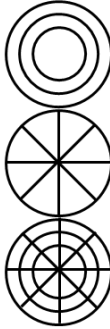
Paper Investigation Type	I & II Experimental	III Numerical
Model Systems	 <p>Polymer Beads</p> <p>Cellulose Fibers</p> <p>Ground Hops</p>	 <p>Glass Spheres</p>
Packed Ring Beds	 <p>Raschig (random)</p> <p>Ralu (random)</p> <p>Raflux, adjacent (structured)</p> <p>Raflux, concentric (structured)</p>	 <p>Concentric Cylinders</p> <p>Angular Walls</p> <p>Combinations</p>
Main Tools	Filtration and compression equipment	Discrete element method simulations
Measured Variables	Particle size distribution PSD Filtrate accumulation $m(t)$ Filtrate turbidity τ Filter cake height h Compressive yield stress p_y	N/A
Calculated Properties	Relative cake resistance α_K Filter medium resistance R_M Global compressibility N_α Cake compression ΔV_K	Bulk porosity ε_b Radial porosity $\varepsilon(r)$

Figure 15: Schematic overview of the thesis methodology

Papers I and II were based on purely experimental approaches and designed to gather data sets that would complement each other in the end. Hence, the selected model systems and packed ring beds remained constant. To analyze filter cakes made of particles of different shapes, compressibilities, and sizes, incompressible polymer beads, mildly compressible cellulose fibers, and highly compressible ground hops were selected. All solids were eventually combined with packings consisting of random Raschig or Ralu rings and structured Raflux rings (adjacent or concentric, depending on the equipment size). The varying rings provided different amounts of void space and wall support.

The key parameters of Paper I were α_K and R_M , so the methodology was based on standardized dead-end filtration tests to form filter cakes and detect changes in their permeability occasioned by the packings. This was achieved by automatically recording filtrate mass over time $m(t)$ and applying Equation (11). Moreover, a laser diffraction setup was used to characterize the model systems through their particle size distributions (PSD), and the turbidity τ of filtrate samples was measured to detect eventual quality changes. More details are given in Chapter 4.1.

Paper II was focused on filter cake compressibility N_α and compression ΔV_K . To this end, the methodology was divided into two procedures. The first one was analogous to the previous filtration tests but incorporated a variable Δp to induce α_K gradients (calculated with Equation (12)) through liquid flow. This way, N_α was found by using Equation (13). The second procedure consisted of piston-driven compression tests which were performed with a modified universal testing machine. The equipment allowed accurate cake height h and compressive stress determinations p_y . Chapter 4.2 specifies the procedures.

In contrast to the first two, Paper III took a purely numerical approach. It was identified that programming DEM simulations with LIGGGHTS software and analyzing them with Monte Carlo integrations would be advantageous for performing case studies with different packed structures. The selected model system consisted of monodisperse glass spheres, and the packings were permutations of glass concentric cylinders and angular walls. This way, the effect of the Raflux packings in the preceding cases could be broken down. To compare the different scenarios, the variables bulk porosity ε_b and radial porosity distribution $\varepsilon(r)$ were evaluated. More information can be found in Chapter 4.3.

Chapter 4: Published Results

The results of this thesis are presented cumulatively as a series of three original research papers which explore the potential of applying packed beds to improve filtration processes. Each article lays the groundwork for the next one to continue the investigation. Every paper is introduced by a one-page summary as follows.

4.1 Paper I: Decreasing Filter Cake Resistance by Using Packing Structures

The first paper is an observational investigation and represents the foundation for the succeeding works. This systematic approach was conceptualized collectively. The methodology design, formal data analysis, and result visualization were also a joint effort. The experiment validation, background investigation, and writing lie with the first author.

The background of this paper is set in the context of cake filtration as a significant solid–liquid separation process. Considering challenges which arise during the filtration of compressible suspensions, investigation methods and ways to counteract compression are mentioned. After listing state-of-the-art strategies, the application of a simple alternative is proposed: This work’s hypothesis states that packed beds, which are conventionally used for thermal separation processes, e.g., in absorption columns, can also be beneficial for cake-forming solid–liquid separations. Relevant properties for both techniques, such as tortuosity and wall effects, are cited. It is proposed that packed structures can provide additional wall support, which loosens the cake and reduces pressure drop as well as operation time.

To evaluate the hypothesis, three model systems of different particle shapes and compressibilities were selected and combined with three different types of packings. The solids suspended in water were the polymeric extrudate Crosspure XF (relatively spherical and incompressible), the cellulose fibers Arbocel UFC 100 (mildly elongated and compressible), and the pelletized hop Cascade (very polydisperse and compressible). All solids were analyzed using scanning electron microscopy and laser diffraction (particle size distribution). As a reference, the systems were dispersed and separated in a dead-end filtration chamber according to an official VDI methodology without packing structures. The suspensions were then combined with two random packings consisting of Raschig and Ralu rings and one structured packing made of Raflux rings. For each case, the filtrate mass over time and filtrate turbidity were evaluated to quantify filter cake resistance and filtrate quality.

The discussion first focuses on the particle size distributions, and then the filtration runs without and with packed beds are compared for each suspension. The experiments show a high degree of reproducibility, and it is concluded that the use of packings for the separation of both approximately incompressible solids is not beneficial. The three variations increase the flow resistance through the filter cake and prolong the whole process noticeably. This is attributed to increased cake height and clogging. The effect on filtrate quality when comparing the resulting turbidities is not positive either.

On the contrary, all packed beds considerably decrease the flow resistance of the compressible hop filter cake and accelerate the separation. A possible direct correlation between packing void volume and filtration speed is discussed. The supporting structures enhance cake porosity and counteract network collapse as the solids accumulate on the filter medium. Additionally, it is possible to achieve much higher flow rates without compromising filtrate quality, according to the obtained turbidities. In this regard, the structured packing is the most promising one for applications where complex biogenic substances are to be separated.

Because this simple strategy has shown a considerable potential to increase the efficiency of the separation of complex organic substances, further exploration is recommended. Factors, such as network compressibility and interactions between materials, are also worth looking into. Hence, having observed the existence of the effect of packings on cake filtration, continuation experimental works are planned to investigate the reach of the strategy's benefits.

Peter M. Bandelt Riess
Jörg Engstle
Michael Kuhn
Heiko Briesen
Petra Först*

Decreasing Filter Cake Resistance by Using Packing Structures

Packed beds used in absorption columns are evaluated to determine whether they can also be beneficial for cake-forming filtrations. To assess this, model systems are characterized and separated by using a dead-end filter cell. Filtrations are conducted with different packings; the filtrate amount over time and resulting turbidity are evaluated. Packings increase the filter cake resistance and the separation time of the cakes formed with approximately incompressible solids. However, they exhibit a positive effect on the filtration of a more complex, compressible substance; the process is not only accelerated, but also the quality of the obtained filtrate is not compromised. These results demonstrate potential in the use of packed beds for the filtration of complex biogenic suspensions.

Keywords: Biogenic suspension, Cake filtration, Filter cake resistance, Packed bed, Process strategy

Received: May 24, 2018; *revised:* July 23, 2018; *accepted:* July 27, 2018

DOI: 10.1002/ceat.201800254

1 Introduction

Cake filtration is a significant solid-liquid separation process. It is often necessary to deal with suspensions, which form compressible filter cakes. These mixtures frequently have a biological origin; various materials, such as biopolysaccharides [1], bacteria and yeast [2], activated sludge [3], and microcrystalline cellulose [4], have been studied. Therefore, it is important to consider the mechanical properties of specific solid particles, along with their shape and size distributions, to adequately describe the behavior of the respective cake and the separation characteristics. Several authors have investigated the influence of these parameters [5] and other factors on cake filtration, e.g., solid-liquid interactions and suspension stability over time [6], filter testing method [7], and operating pressure [8].

There are several known compression mechanisms, which depend on the composition of the solid. More than one mechanism may simultaneously occur during the process, and each one will affect the filter cake differently. They have been described numerically by, e.g., Vorobiev [9] and through extensive experimentation by Alles [10]. Additionally, Selomulya et al. [11] utilized visualization techniques to monitor floc permeability, which could help to explain and predict the manner in which aggregates were compressed. Park et al. [12] investigated the correlation between porosity and flow resistance, while incorporating the cake-collapse effects from a theoretical perspective. However, it is possible to further optimize the approaches to handle specific materials during separation processes.

Various methods are continuously being developed to counteract the compression and clogging of filter cakes. An extensively applied strategy is the use of filter aids, which allow an increase in the cake porosity and operating time during, e.g.,

clarification in biopharmaceutical processing [13]. This approach has been mechanistically described by Kuhn and Briesen [14]. Other strategies proposed by Alles [10] are the selection of an optimal filtration pressure profile or the performance of intermittent cake filtrations. Additionally, Eshed et al. [15] reported that the membrane cross-flow separation, a widespread operation method, must be adjusted according to the process.

As a result of recent advances in 3D printing and membrane technology, scientists have been able to generate predetermined structures that can be tailored to counteract compression or clogging, which is a framework referred to as micromanipulation by Kuhn et al. [16]. Fee et al. [17] and Nawada and Dimartino [18] proved that 3D printing was a valid method to create packed structures by using computer-aided design, whereas Low et al. [19] presented a discussion on the potential of this technology for printing separation membranes. Additionally, Liu et al. [20] reviewed available technology to modify already existing membranes and to make them responsive to various stimuli. All of these strategies, however, still represent rather complicated, expensive, and time-consuming alternatives to control the separation processes. Although self-generated media would be beneficial, the usage of conventional, industrially available, packed beds could be a much simpler alternative.

Packed beds are extensively used in industry due to their ability to increase the contact surface. They accelerate heat and

Peter M. Bandelt Riess, Jörg Engstle, Dr.-Ing. Michael Kuhn, Prof. Dr.-Ing. Heiko Briesen, Prof. Dr.-Ing. Petra Först
petra.foerst@tum.de

Technical University of Munich, School of Life Sciences Weihenstephan, Chair of Process Systems Engineering, Gregor-Mendel-Strasse 4, 85354 Freising, Germany.

mass transfer between the phases and allow for more compact or efficient absorption and distillation columns. The bed can be randomly or structurally packed; its selection depends on factors such as shape, heat and corrosion resistance, and costs. Due to their wide applicability, they have been investigated from different perspectives, e.g., liquid flow [21], porosity [22], applicability of mass transfer correlations [23], and industrial uses [24].

Large surfaces and void volumes have been achieved in packed beds, resulting in small pressure drops during the process, which is an extensively analyzed topic [25, 26]. Some case studies have been performed through computational fluid dynamics [27, 28] that aimed to study or generate a structure [29, 30], or to predict the flow behavior inside a packing and its consequences for a certain process [31]. Other studies have focused on analyzing the tortuosity [32] and wall support effects [33] in the packed bed. These properties are also relevant if performing cake filtration; it is, therefore, plausible to develop a connection between the two-unit operations.

Herein, packed beds were used unconventionally to perform dead-end filtrations. It is proposed that they may positively influence not only thermal processes, but also the cake-forming filtration of compressible substances such as biological mixtures. Moreover, the packed-bed structures may provide additional wall support and distribute dispersed solids, so that the filter cake loosens and the operation time is reduced. To evaluate this hypothesis, various combinations of suspended solids and packed beds were analyzed.

2 Materials and Methods

2.1 Model Systems

The first suspended solid was the virtually incompressible Crosspure[®] XF (CP; BASF SE). CP was a mixed extrudate comprising 70 % polystyrene and 30 % polyvinylpyrrolidone used in beer filtration as a filter aid. It was selected because of its simplicity; in addition to its incompressibility, the particles exhibited a rather spherical form.

The second substance, Arbocel[®] UFC 100 (AC), contained 99.5 % cellulose fibers (J. Rettenmaier & Söhne GmbH & Co. KG). The average particle size was between 6 and 12 μm . Because the particle structure had more degrees of freedom than those in CP, particles could be reorganized during filtra-

tion; thus, the material was slightly more compressible. Given that the fibers were finely cut, this material, however, did not exhibit a high compressibility.

Hop pellets (HO) are a good example of a complex biogenic solid. They comprised dried and ground hops. Once the pellets were dispersed, the system became noticeably polydisperse. The pellets used were obtained from Cascade hops (Simon H. Steiner, Hopfen, GmbH). This variety contained 16.5 % resin, which contributed to its compressibility. The filter cakes formed from it were porous structures, which could be easily compacted. Fig. 1 depicts images of the materials.

2.2 Packed Beds

The first random packing used was of Raschig rings (1400/6, Glaswarenfabrik Karl Hecht GmbH & Co. KG). Ralu rings (Raschig GmbH) were used in another experiment series as second random packing. These rings had to be weighted down due to their low density. Finally, a structured packing was fabricated by using Raflux rings 25-4 (RVT process equipment GmbH). Their structure was expanded to fit the diameter of the filtration equipment. The packings are exhibited in Fig. 2, and their properties are presented in Tab. 1.

Table 1. Properties of the packings.

Ring type	Raflux	Raschig	Ralu
Material	Steel	Glass	Plastic
Diameter [mm]	80	6	15
Length [mm]	25	6	15
Thickness [mm]	0.5	1	1
Surface [$\text{m}^2 \text{m}^{-3}$]	215	940	320
Void volume [%]	95	58	94
Quantity [-]	1	438 (CP, AC); 730 (HO)	32

The number of rings introduced into the filter was determined by ensuring that the packed-bed height was at least as tall as the resulting filter cake.

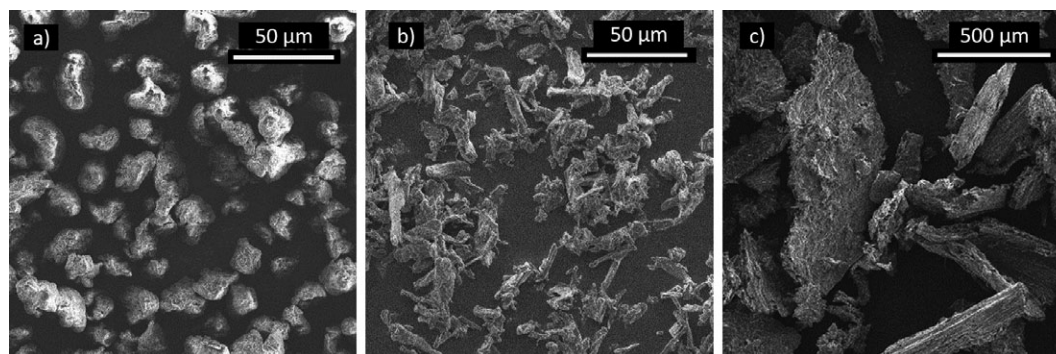


Figure 1. SEM images of (a) CP, (b) AC, and (c) HO.

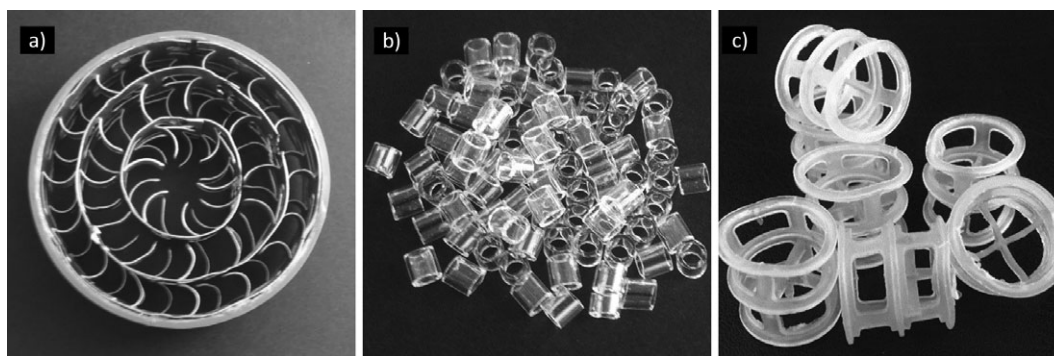


Figure 2. Photographs of (a) Raflux, (b) Raschig, (c) Ralu rings.

2.3 Particle Size Distribution (PSD) Analysis

The PSDs of the model systems were analyzed by using a laser diffraction setup (HELOS/KR; Sympatec GmbH). The samples were suspended in water and uniformly dispersed in the setup by using the dispersion unit QUIXEL.

2.4 Filtration Equipment

The experiments were conducted by using a filtration stand designed and built by Banke Process Solutions GmbH & Co. KG following the standards of the Association of German Engineers (Verein Deutscher Ingenieure (VDI)) [34]. The equipment comprised two separate glass housings to disperse and filter the suspensions under pressure. The first housing was equipped with a stirrer and had an internal diameter of 130 mm and a volume capacity of 2 L, whereas the second housing had an internal diameter of 80 mm, which was equivalent to a filtering area of 50.27 cm², and was maintained at 20 °C with a Julabo GmbH F30 VC/3 thermostat. Filter paper DP 1575 090 (Hahnemühle FineArt GmbH), with a retention capacity of 2 μm, was used for CP and AC, and a steel sieve with a retention capacity of 55 μm was used as the filter medium for HO. The filtrate mass was automatically measured by using a Kern & Sohn GmbH KB 10000-1N precision scale. The data was processed by using a MATLAB (The MathWorks, Inc.) code. A schematic of the equipment is illustrated in Fig. 3.

2.5 Transmission Analysis

To characterize the accumulated filtrate, infrared light ($\lambda = 850$ nm) transmission analyses were performed after each experiment by using a Turbiscan MA 2000 (Formulation) instrument and the software Turbisoft (version 1.2.1).

2.6 Experimental Procedure

A series of experiments without packings was performed for reference. The standard filtration curves were thus obtained for each system. The CP and AC systems were separated under 1.5 bar, whereas the HO system was separated under 0.2 bar; strong cake compression during filtration was avoided by using

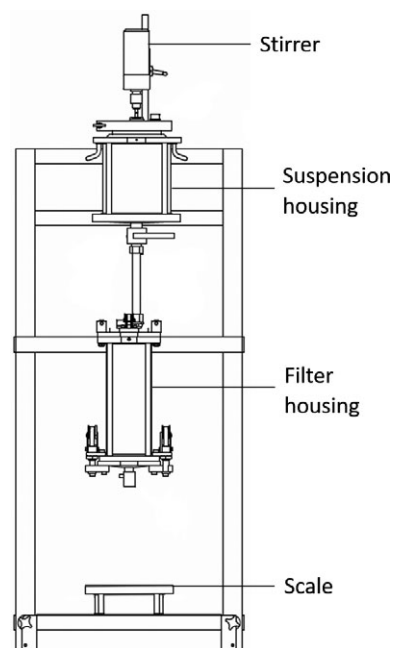


Figure 3. Schematic illustration of the experimental filtration equipment.

these pressures. Furthermore, three series of experiments with different packings were conducted to detect variations in the separation behavior of the systems. All experiments were performed three times, and the results were represented as the arithmetic mean value. Error bars indicated confidence intervals of 95 %.

The dead-end filtrations were conducted by following a standard procedure [34]. Each suspension was prepared by using distilled water at a final volume of 1.5 L. Subsequently, the filter was filled with a predetermined quantity of packed elements.

The CP and AC samples were weighed and presuspended in distilled water before homogenization in an ultrasonic tub. HO should be dissolved first; therefore, the pellets were submerged in water overnight before suspension. The sample quantity was determined based on a cake height of 1.2 cm for CP and AC (30 and 20 g, respectively) and 2.7 cm for HO (20 g). The latter was set to be higher to achieve filtration times that were similar to those of the first two cases.

The sample was transferred to the suspension housing after configuring its stirrer to maintain homogeneity. Subsequently, the valve to the filter housing was opened, the system was pressurized, and filtration and data recording were initiated.

The filtration data (accumulated filtrate mass over time) were linearized in the form of time/accumulated filtrate volume over the same volume to obtain the flow resistance of the filter medium, $R_M^{(1)}$, and the relative filter cake resistance, α_K , according to Eq. (1):

$$\frac{t}{V} = \frac{k\eta\alpha_K}{2A^2\Delta p} V + \frac{R_M\eta}{A\Delta p} \quad (1)$$

in which t is the filtration time, V is the filtrate volume, k is a concentration constant calculated from the cake thickness, η is the fluid viscosity, A is the filter area, and Δp is the pressure difference. The cake thickness was measured and the transmission of the whole filtrate volume was analyzed to detect quality changes.

3 Results and Discussion

3.1 Particle Size Distribution (PSD)

The results of the volumetric PSD analyses are presented to compare the different model systems. The PSDs are presented in Fig. 4 in a normalized differential (q_3) and accumulated form (Q_3).

CP shows a marked modal value, which coincides with its $x_{50,3}$ value. Its relative PSD span, S , was estimated from Eq. (2).

$$S = \frac{x_{90,3} - x_{10,3}}{x_{50,3}} \quad (2)$$

AC has two modal values and its PSD is broader than that of CP. Regardless, only approximately 10% of the particles are larger than $40\ \mu\text{m}$, and the $x_{50,3}$ value is of the same order of magnitude as that of CP. AC was used because of its different material properties.

HO particles are more complex than those of CP and AC because they consist of various substances, thereby making their behavior more difficult to predict. The estimated S value is comparable to that of AC. The $x_{50,3}$ and the modal values are considerably larger than those of the other systems; therefore, the filter medium was changed from $2\ \mu\text{m}$ filter paper to a $55\ \mu\text{m}$ steel sieve. The operating pressure was also adjusted to 0.2 bar. These optimizations ensured the reproducibility of this series and also maintained a timescale that was comparable to that of CP and AC. The PSD properties of the three systems are summarized in Tab. 2.

3.2 Relative Flow Resistance

The filtrate mass as a function of time displayed a standard behavior with a high degree of reproducibility. The linearized

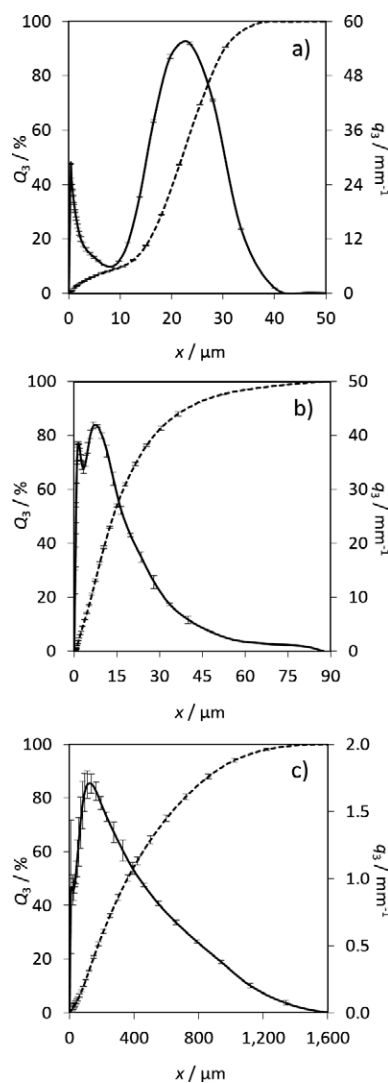


Figure 4. Results of PSD analyses of (a) CP, (b) AC, (c) HO. Q_3 (dashed line), q_3 (solid line).

Table 2. PSD properties of the model systems.

System	CP	AC	HO
$x_{50,3}$ [μm]	22	14	360
Biggest modal value [μm]	22	7.5	135
S [-]	0.9	2.5	2.25

data were utilized to determine the coefficients of the linear functions. The numerical results of this study were derived from the coefficients of the linear functions.

Fig. 5 exhibits the different filtration runs with CP. A steeper slope of the curve indicates a greater mass flow and a shorter filtration. For reference (Fig. 5, solid black line), a filter cake composed of only suspension solids was used.

The solid and dashed gray curves in Fig. 5 correspond to filtrations through the Raflux structure and Ralu rings, respec-

1) List of symbols at the end of the paper.

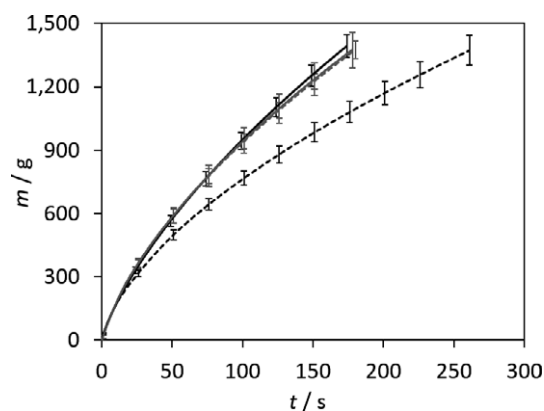


Figure 5. The filtrate mass over time for CP: reference (solid black), Raflux (solid gray), Ralu (dashed gray), and Raschig (dashed black).

tively. They are very similar to that of the reference curve, which indicates that these packings have neither a positive nor negative effect on the experimental duration. Contrastingly, the Raschig rings packing had a negative effect on filtration; considering that the accumulated mass was 1350 g, the experiment was observed to last 53 % longer than that the other runs.

Based on these results, void volume is the packing property that majorly influences the filtration of CP. A void volume greater than 90 % had no effect; however, a value lower than 60 % considerably decelerated the process (Tab. 1). The relatively small inner spaces of the rings are also more susceptible to clogging, which increases the overall flow resistance of the filter cake. It is likely that the relatively small ring-to-housing diameter ratio considerably increases the tortuosity of the flow's path through the cake and, consequently, the time required to permeate. The calculated cake properties are presented in Tab. 3.

Table 3. Medium resistance and relative cake resistances from the linearized data of CP.

Packed bed	R^2 [-]	R_M [m^{-1}]	α_K [m^{-2}]
-	0.9996	4.690×10^{10}	7.803×10^{12}
Raflux	0.9997	4.184×10^{10}	9.354×10^{12}
Raschig	0.9996	4.304×10^{10}	1.684×10^{13}
Ralu	0.9995	4.131×10^{10}	9.640×10^{12}

The coefficients of determination confirm the validity of all linear regressions. The filter medium resistance, R_M , was two orders of magnitude lower than the relative cake resistance. The standard deviation of R_M represents 5 % of its mean value; thus, its determination by using this method is considered to be adequate. Following the VDI's classification for flow resistances [34], all systems, except the combination with Raschig rings, can be considered as easily separable (below $1.0 \times 10^{13} \text{ m}^{-2}$). The Raschig system is moderately separable, with a 116 % increase in α_K . It is clear that this spatially averaged approach does not allow for an in-depth analysis in the

present case. The purpose here is merely to quantify the differences between the filtrate mass curves for further comparison. As reported by Tiller et al. [35], relatively simple models based on averages of the properties of the cakes, although approximate, can be used to compare experiments with different solids.

Although there are no statistically significant differences between the reference and curves with Raflux and Ralu packings (Fig. 5), the relative resistance estimation does show a 20 % increase for the latter. The results prove that, thus far, these packings do not positively influence the flow resistance, while filtering substances with properties similar to those of CP.

Fig. 6 exhibits the different filtration runs with AC. Those corresponding to Raflux and Ralu (gray solid and dashed lines) behave differently than those with CP; they are identical to each other and slower than the reference, which indicates that the packed beds have a negative effect on the flow rate. Furthermore, the packing of Raschig rings decelerates filtration more than the other packings, which is analogous to the previous series. This effect is more pronounced than that on CP, and the longest run lasted 91 % longer than the reference.

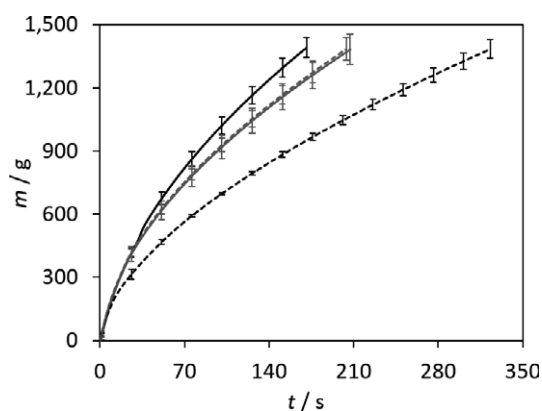


Figure 6. The filtrate mass over time for AC: reference (solid black), Raflux (solid gray), Ralu (dashed gray), Raschig (dashed black).

The void volume of the packed bed continues to be a decisive factor; however, different factors can also be considered, e.g., the manner in which the suspended solid interacts with the packing. If the characteristics of the solid particles further deviate from monodispersity and incompressibility, it will be more difficult to predict their behavior inside the packed bed. Because the suspended cellulose fibers are oriented in different directions, in contrast to spherical particles, they can be easily arranged or rearranged in a manner that aggravates the clogging of the packing, which, in turn, affects the filtrate flow. The numerical results are presented in Tab. 4.

R_M was three orders of magnitude lower than the relative cake resistance and was different from that of CP (Tab. 3); this demonstrated that R_M depended not only on the medium, but also on its interaction with the suspension. The Raschig rings series deviates slightly from the rest, if the values of R^2 and R_M are compared. This can be attributed to the intrinsic properties

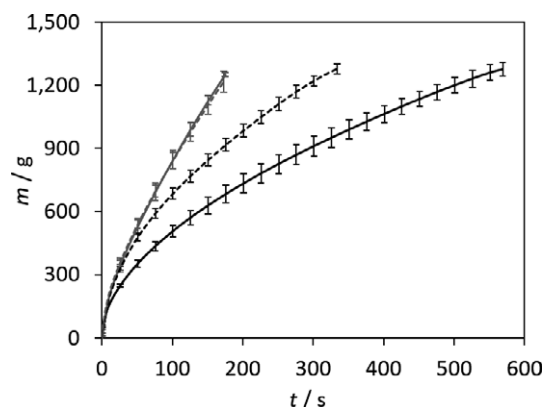
Table 4. Medium resistance and relative cake resistances from the linearized data of AC.

Packed bed	R^2 [-]	R_M [m^{-1}]	α_K [m^{-2}]
–	1.0000	2.378×10^{10}	1.135×10^{13}
Raflux	0.9999	2.188×10^{10}	1.516×10^{13}
Raschig	0.9982	3.269×10^{10}	2.474×10^{13}
Ralu	0.9997	2.119×10^{10}	1.497×10^{13}

of AC, which allow small variations in the filter-cake structure during the process. Regardless, the regression is considered to be valid for this purpose, and the real R_M value is more likely to be closer to the other results.

All systems can be graded as moderately separable if all α_K values are greater than $1.0 \times 10^{13} m^{-2}$. Moreover, according to the results in Tab. 4, the relative resistance increases occasioned by Raflux and Ralu packings were approximately 33 %, whereas it was approximately 118 % for the Raschig rings. Therefore, the packings that were evaluated did not positively influence the flow resistance, while filtering substances with properties similar to those of AC. According to the results, this separation method is not considered to be favorable for approximately incompressible solids, such as CP and AC, under the investigated conditions, even though the PSD and compressibility of the solid vary slightly. More complex and compressible materials, however, seem to behave in a very different manner.

Fig. 7 exhibits different filtration runs with the suspension of HO. Similar to the previous systems, the Raflux and Ralu (gray solid and dashed lines) curves overlap, whereas that corresponding to the Raschig packing (dashed black line) describes a slower separation. In contrast with the previous series, the durations of the experiments remain sorted by the void volume of the packings, but the reference filtration takes considerably longer than the rest. All packed beds have a positive effect on separation, which results in a noticeable acceleration of the process. As observed in Fig. 7, while filtering 1200 mL of suspension, the packings cause time savings of approximately


Figure 7. The filtrate mass over time for HO: reference (solid black), Raflux (solid gray), Ralu (dashed gray), Raschig (dashed black).

42 % with the Raschig rings and approximately 66 % with the Raflux and Ralu packings.

Despite the relatively low void volume of the Raschig rings, the packed bed was beneficial for this system. Furthermore, it is also important to consider the interactions between the packing and solid particles. The PSD span of this suspension is comparable to that of AC (Tab. 2). However, the characteristic values of HO (e.g., $x_{50,3}$) are much larger, which influences the process, as do the intrinsic properties of the solid particles, such as shape. The corresponding numerical results are presented in Tab. 5.

Table 5. Medium resistance and relative cake resistances from the linearized data of HO.

Packed bed	R^2 [-]	R_M [m^{-1}]	α_K [m^{-2}]
–	0.9997	3.259×10^9	2.968×10^{12}
Raflux	0.9950	7.138×10^9	5.102×10^{11}
Raschig	0.9992	2.207×10^9	1.674×10^{12}
Ralu	0.9943	5.357×10^9	7.117×10^{11}

R_M was at least two orders of magnitude lower than the relative cake resistance and was remarkably different from that of the previous series (Tabs. 3 and 4) because of the coarser mesh size of the filter medium. Notably, all R_M values differ from each other. These variations seem to be related to the void volume; a smaller void volume of the packing results in a smaller R_M value.

Suspensions without a packed bed and with the Raschig rings can be graded as easily separable, with α_K values lower than $1.0 \times 10^{13} m^{-2}$. For the other two systems, the α_K values are lower than $1.0 \times 10^{12} m^{-2}$; thus, they can be graded to be very easily separable. The relative resistance decreases caused by the Raschig, Ralu, and structured Raflux packings were approximately 44, 76, and 83 %, respectively. This is the first report of relative cake resistance reduction by using packed beds, and it indicates that they may be beneficial for separating complex, compactible materials because the process is considerably accelerated. The following hypotheses intend to elucidate this phenomenon.

The increase in filtration velocity depends on the composition of the suspension and the manner in which its particles interact with each other and with the packing. Surface effects are also involved, which include not only electrokinetic interactions, but also adhesion effects between, e.g., the resin-covered HO particles. The filter cake structure also depends on the size and shape distributions of the particles and, as depicted above, systems such as HO present rather irregular ones. It is, therefore, likely that the packings act as some kind of macroscopic filter aid, building a more permeable, and more porous, structure than that comprised of only the suspension solid.

The packings can also be considered as a vertical extension of the filter medium, which acts as a depth prefilter that retains part of the solids, while the rest continue their way to the sieve and build the cake. This effect enhances the porosity and depends on a given structure of the packed bed that remains constant over time; therefore, it can be referred to as a stationary effect of the bed.

A transient effect of the bed can also be considered. If the suspension solid is compressible, the first solid layer at the filter medium becomes susceptible to undergo the “skin effect” [36], which is a time function that depends on the drag pressure in the cake. Providing internal wall support, in addition to the housing, through the packed bed can help to counteract compression of the solid, also as a function of time. The support prevents the cake from varying considerably with pressure, and from reducing its porosity and permeability.

Thus, the effect of packings on the dead-end filtration of materials such as HO is twofold and seems to be remarkably positive with respect to process duration.

3.3 Filtrate Transmission

To ensure that the packings do not negatively affect the filtrate quality, samples were analyzed after each filtration. The transmission value of distilled water was measured as a reference (95.39 ± 0.08 %). Fig. 8 depicts the results corresponding to the CP series.

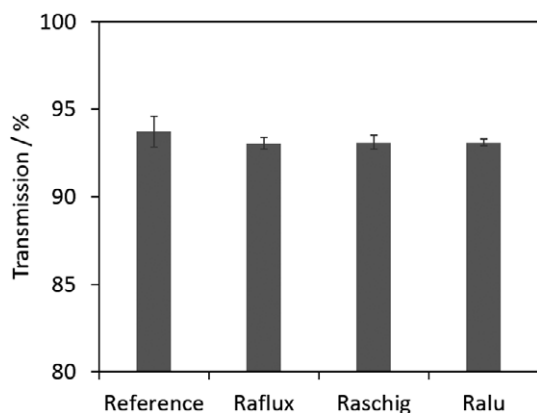


Figure 8. Filtrate transmissions for CP.

A clear filtrate was obtained, regardless of the presence of the packings; all values were similar to that of pure water. The filtrates collected from the packed beds were not statistically different from that filtered without packing. Therefore, the use of packings was not advantageous in this aspect.

Fig. 9 presents the transmissions of the filtrates collected from AC. A positive effect on the turbidity of the filter cannot be observed here either. The transmission values of the samples separated with the packings were smaller than that of the reference experiment; furthermore, because the error bars do not overlap, it can be concluded that the method is not only counterproductive for process duration, but also for the quality of the product.

Fig. 10 depicts results corresponding to the experimental series with HO. The transmission values are considerably smaller than the values for the other systems; however, this was expected because the oil-containing HO particles dye the liquid they are suspended in. Regardless, the trend is opposite to those previously observed. There were no statistical differences between the results corresponding to the reference and to the

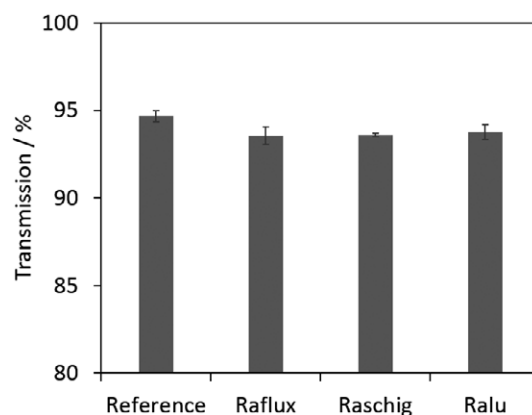


Figure 9. Filtrate transmissions for AC.

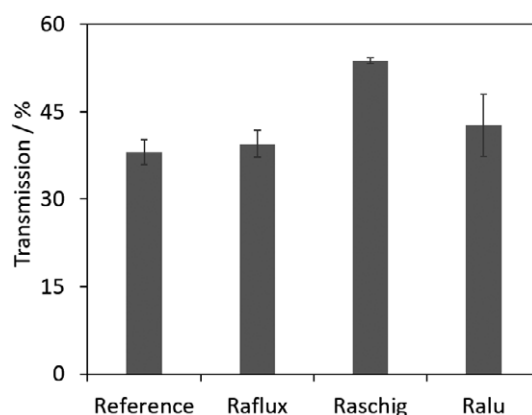


Figure 10. Filtrate transmissions for HO.

Raflux and Ralu packings. The Raschig rings bed, however, remarkably improved the resultant transmission. The measured values were at least 25 % higher than the reference values, which indicated that there were less suspended solids in the liquid. This may be attributed to the higher flow resistance at the filter medium and the reduced porosity of the cake, compared with the other packings.

Hence, the use of packed beds during cake filtration of a biogenic suspension may be beneficial not only because it considerably accelerates the process, but also because it maintains the turbidity, or even improves it noticeably. This strategy shows considerable potential to enhance the efficiency of the industrial separation of complex organic substances. The effects described herein will be further investigated to develop more advanced strategies for this and other similar processes.

4 Conclusions

Because the separation of cake-forming biogenic suspensions can be significantly energy- and time consuming, a new process strategy was proposed. Packed beds were used unconventionally in a dead-end filtration chamber to assess whether they could be beneficial in this context. Three model systems were selected and combined with three different packings. The solids

were analyzed and filtered with and without the packing structures. For each case, the filtrate mass over time and filtrate turbidity were evaluated.

The use of packings for the separation of the two approximately incompressible solids was not beneficial because they increased the flow resistance through the filter cake and, thus, the duration of the process. This was more noticeable for the relatively compressible solid, which indicated that the particle-packing interactions should also be considered. It was also observed that the Raschig rings packing, which had a smaller void volume, yielded slower curves. Although clear filtrates were obtained, the use of packings did not improve the turbidity either.

The more compressible material exhibited the opposite behavior. All packed beds had a positive effect on separation, considerably decreasing the flow resistance and accelerating the process. Thus, it was assumed that the structure of the bed presented a porosity-enhancing effect by loosening the suspended particles in the cake. Additionally, the packings also maintained the quality of the filtrate. Because this simple strategy has shown considerable potential to increase the efficiency of the separation of complex organic substances, further exploration should be performed.

Future work involves experiments on additional biological systems. Furthermore, it becomes clear that separating the filtered solids from the packing would be crucial for industrial application. Different options would have to be investigated, such as the use of disposable packing materials or designing packed beds, which can be easily cleaned and separated, e.g., magnetically. Another potential obstacle for economic viability could be retrieving the remaining filtrate at the end of the process. Typically, pressing of the filter cake is performed. This is not possible in the case of common random packings. However, washing or leaching of the cake could be an option.

Interactions between the packings and suspended solids are also worth investigating. The presence of certain functional groups or charged particles would result in additional effects on the separation process. According to Theliander and Fathi-Najafi [37], localized pressure measurements at the filter cake could help to detect changes over time. Moreover, it was possible to assess only the impact of the packed bed on cake permeability and not on compressibility. This should be focus of future work as well. Correlations between operating pressure, compression factor, and benefits of the packings could be found. This would allow greater understanding of the transient effect of the packing.

Acknowledgment

The authors would like to thank the staff of Banke Process Solutions and J. Rettenmaier & Söhne, who supplied materials for the experiments. The help provided by Christoph Metzger with the microscope and by the workshop staff with the hardware is greatly appreciated.

The authors have declared no conflict of interest.

Symbols used

A	[m ²]	filter area
k	[-]	concentration constant
m	[g]	filtrate mass
p	[Pa]	pressure
Q	[%]	cumulative distribution
q	[mm ⁻¹]	normalized differential distribution
R_M	[m ⁻¹]	medium resistance
R^2	[-]	coefficient of determination
S	[-]	particle size distribution span
t	[s]	filtration time
V	[m ³]	filtrate volume
x	[μm]	particle size

Greek letters

α_K	[m ⁻²]	relative cake resistance
η	[Pa s]	fluid viscosity
λ	[nm]	wavelength

Sub/superscripts

10	10 % accumulation
3	volumetric size distribution
50	50 % accumulation
90	90 % accumulation

Abbreviations

AC	Arbocel [®] UFC 100
CP	Crosspure [®] XF
HO	hop pellets
PSD	particle size distribution
VDI	Verein Deutscher Ingenieure (Association of German Engineers)

References

- [1] K.-J. Hwang, S.-Y. Lyu, F.-F. Chen, *Powder Technol.* **2006**, *161* (1), 41–47. DOI: <https://doi.org/10.1016/j.powtec.2005.07.006>
- [2] K.-J. Hwang, P.-Y. Su, E. Iritani, N. Katagiri, *Sep. Sci. Technol.* **2016**, *51* (11), 1947–1953. DOI: <https://doi.org/10.1080/01496395.2016.1187629>
- [3] D. J. Lee, C. H. Wang, *Water Res.* **2000**, *34* (1), 1–20. DOI: [https://doi.org/10.1016/S0043-1354\(99\)00096-2](https://doi.org/10.1016/S0043-1354(99)00096-2)
- [4] T. Mattsson, M. Sedin, H. Theliander, *Sep. Purif. Technol.* **2012**, *96*, 139–146. DOI: <https://doi.org/10.1016/j.seppur.2012.05.029>
- [5] D. Bourcier, J. P. Féraud, D. Colson, K. Mandrick, D. Ode, E. Brackx, F. Puel, *Chem. Eng. Sci.* **2016**, *144*, 176–187. DOI: <https://doi.org/10.1016/j.ces.2016.01.023>
- [6] R. Wakeman, *Sep. Purif. Technol.* **2007**, *58* (2), 234–241. DOI: <https://doi.org/10.1016/j.seppur.2007.03.018>
- [7] F. M. Mahdi, R. G. Holdich, *Chem. Eng. Res. Des.* **2013**, *91* (6), 1145–1154. DOI: <https://doi.org/10.1016/j.cherd.2012.11.012>

- [8] E. Iritani, N. Katagiri, S. Kanetake, *Sep. Purif. Technol.* **2012**, *92*, 143–151. DOI: <https://doi.org/10.1016/j.seppur.2011.05.011>
- [9] E. Vorobiev, *Chem. Eng. Sci.* **2006**, *61* (11), 3686–3697. DOI: <https://doi.org/10.1016/j.ces.2006.01.010>
- [10] C. M. Alles, *Ph.D. Thesis*, Universität Fridericiana Karlsruhe **2000**.
- [11] C. Selomulya, X. Jia, R. A. Williams, *Chem. Eng. Res. Des.* **2005**, *83* (7), 844–852. DOI: <https://doi.org/10.1205/cherd.04330>
- [12] P.-K. Park, C.-H. Lee, S. Lee, *Environ. Sci. Technol.* **2006**, *40* (8), 2699–2705. DOI: <https://doi.org/10.1021/es0515304>
- [13] T. Hunt, in *Encyclopedia of Bioprocess Technology* (Eds: M. C. Flickinger, S. W. Drew), John Wiley & Sons, Hoboken, NJ **2002**.
- [14] M. Kuhn, H. Briesen, *Chem. Eng. Technol.* **2016**, *39* (3), 425–434. DOI: <https://doi.org/10.1002/ceat.201500347>
- [15] L. Eshed, S. Yaron, C. G. Dosoretz, *Appl. Environ. Microbiol.* **2008**, *74* (23), 7338–7347. DOI: <https://doi.org/10.1128/aem.00631-08>
- [16] M. Kuhn, W. Pietsch, H. Briesen, *Chem. Ing. Tech.* **2017**, *89* (9), 1126–1132. DOI: <https://doi.org/10.1002/cite.201700025>
- [17] C. Fee, S. Nawada, S. Dimartino, *J. Chromatogr. A* **2014**, *1333*, 18–24. DOI: <https://doi.org/10.1016/j.chroma.2014.01.043>
- [18] S. Nawada, S. Dimartino, C. Fee, *Chem. Eng. Sci.* **2017**, *164*, 90–98. DOI: <https://doi.org/10.1016/j.ces.2017.02.012>
- [19] Z.-X. Low, Y. T. Chua, B. M. Ray, D. Mattia, I. S. Metcalfe, D. A. Patterson, *J. Membr. Sci.* **2017**, *523*, 596–613. DOI: <https://doi.org/10.1016/j.memsci.2016.10.006>
- [20] Z. Liu, W. Wang, R. Xie, X.-J. Ju, L.-Y. Chu, *Chem. Soc. Rev.* **2016**, *45* (3), 460–475. DOI: <https://doi.org/10.1039/c5cs00692a>
- [21] M. Fourati, V. Roig, L. Raynal, *Chem. Eng. Sci.* **2012**, *80*, 1–15. DOI: <https://doi.org/10.1016/j.ces.2012.05.031>
- [22] Z. Wang, A. Afacan, K. Nandakumar, K. T. Chuang, *Chem. Eng. Process.* **2001**, *40* (3), 209–219. DOI: [https://doi.org/10.1016/S0255-2701\(00\)00108-2](https://doi.org/10.1016/S0255-2701(00)00108-2)
- [23] G. Q. Wang, X. G. Yuan, K. T. Yu, *Ind. Eng. Chem. Res.* **2005**, *44* (23), 8715–8729. DOI: <https://doi.org/10.1021/ie050017w>
- [24] Q. Qian, H. Wang, P. Bai, G. Yuan, *Chem. Eng. Res. Des.* **2011**, *89* (12), 2560–2565. DOI: <https://doi.org/10.1016/j.cherd.2011.06.004>
- [25] K. G. Allen, T. W. von Backström, D. G. Kröger, *Powder Technol.* **2013**, *246*, 590–600. DOI: <https://doi.org/10.1016/j.powtec.2013.06.022>
- [26] E. Erdim, Ö. Akgiray, İ. Demir, *Powder Technol.* **2015**, *283*, 488–504. DOI: <https://doi.org/10.1016/j.powtec.2015.06.017>
- [27] X. Zhang, L. Yao, L. Qiu, X. Zhang, *Chin. J. Chem. Eng.* **2013**, *21* (9), 959–966. DOI: [https://doi.org/10.1016/S1004-9541\(13\)60576-5](https://doi.org/10.1016/S1004-9541(13)60576-5)
- [28] P. Niegodajew, D. Asendrych, M. Marek, S. Drobniak, *J. Phys. Conf. Ser.* **2014**, *530*, 12053. DOI: <https://doi.org/10.1088/1742-6596/530/1/012053>
- [29] G. E. Mueller, *Powder Technol.* **2005**, *159* (2), 105–110. DOI: <https://doi.org/10.1016/j.powtec.2005.06.002>
- [30] P. Niegodajew, M. Marek, *Powder Technol.* **2016**, *297*, 193–201. DOI: <https://doi.org/10.1016/j.powtec.2016.04.024>
- [31] P. Niegodajew, D. Asendrych, S. Drobniak, *Arch. Thermodyn.* **2013**, *34* (4). DOI: <https://doi.org/10.2478/aoter-2013-0033>
- [32] S. Pardo-Alonso, J. Vicente, E. Solórzano, M. Á. Rodríguez-Perez, D. Lehmhus, *Procedia Mater. Sci.* **2014**, *4*, 145–150. DOI: <https://doi.org/10.1016/j.mspro.2014.07.553>
- [33] R. Di Felice, L. G. Gibilaro, *Chem. Eng. Sci.* **2004**, *59* (14), 3037–3040. DOI: <https://doi.org/10.1016/j.ces.2004.03.030>
- [34] VDI 2762 Blatt 2, *Mechanical Solid-Liquid Separation by Cake Filtration. Determination of Filter Cake Resistance*, Beuth Verlag GmbH, Berlin **2010**.
- [35] F. M. Tiller, R. Lu, J. H. Kwon, D. J. Lee, *Water Res.* **1999**, *33* (1), 15–22. DOI: [https://doi.org/10.1016/S0043-1354\(98\)00192-4](https://doi.org/10.1016/S0043-1354(98)00192-4)
- [36] F. M. Tiller, T. C. Green, *AIChE J.* **1973**, *19* (6), 1266–1269. DOI: <https://doi.org/10.1002/aic.690190633>
- [37] H. Theliander, M. Fathi-Najafi, *Filtr. Sep.* **1996**, *33* (5), 417–421. DOI: [https://doi.org/10.1016/S0015-1882\(97\)84302-9](https://doi.org/10.1016/S0015-1882(97)84302-9)

4.2 Paper II: Investigating the Effect of Packed Structures on Filter Cake Compressibility

The second paper is a direct continuation of the previous investigation. It complements the first experimental methods and gathered data. As such, the author contributions to this systematic approach were analogous to the ones previously described.

The background of this paper is also set in the context of laboratory-scale cake filtration, highlighting its relevance for the industry. Considering some examples and properties of highly compressible substances, the phenomenon of cake compression is regarded as fundamental in solid–liquid separation research. Consequently, conventional filtration theory and compressional rheology are introduced as two frameworks for the description of suspension dewatering, from which this paper benefits. After citing a broad spectrum of strategies, which have been tailored to fit various applications, the approach explored in the first paper is explained: purposefully using packed beds to incorporate more wall support in a filter and counteract compression. However, it is remarked that the first experiments addressed filter cake permeability rather than compressibility. Hence, this study aims to close the gap and investigates the effects of packings on filter cake compressibility, proposing to find a correlation between operating pressure, cake compression factor, and packing influence.

To test the hypothesis, the same combinations of suspended solids (Crosspure, Arbocel, and hops) and packed beds (Raschig, Ralu, and Raflux rings) as before are analyzed to identify key factors that make the use of packings advantageous. In addition to previous characterization methods, the systems are separated in a newly upgraded dead-end filtration chamber at various differential pressures. Filtrate mass is recorded over time. In another set of experiments, the suspensions are separated and subsequently compressed with a tailored piston in a universal testing machine (without and with packings), measuring height at various given compression forces in stepped pressure tests.

The discussion first focuses on suspension characterization regarding particle size distribution and filter cake resistance and global compressibility according to conventional filtration theory. The experiments show significant qualitative differences among the systems' compressibilities due to particle morphology and nature; it is clear that Arbocel is much more compressible than Crosspure, and hops are much more compressible than Arbocel. The systems are easily separable at almost all pressures according to the VDI method.

The results of the experiments according to compressional rheology without packings agree with the tendency observed in the former experiments. With packings, all combinations dramatically increase the systems' resistance to compressive stress because the beds provide structural support and absorb friction forces. The greater the applied pressure or the material compressibility, the more pronounced is the measured effect. The fixed packing proves to be more beneficial than the random packings once more. Nevertheless, it is observed that reducing compressibility does not automatically mean improving permeability. It is necessary to maintain the structure of the porous network to have an improved filtration process; in other words, to find a compromise between the presented transient and non-transient effects of the packings.

For this reason, future work should involve finding a correlation between particle size distribution and packing influence. After that, the packings could be even purposefully designed for particular systems and scenarios of interest. Hence, knowing more about the effect of packings on cake filtration, a new approach is proposed next.

Peter Michael Bandelt Riess
Michael Kuhn
Petra Först
Heiko Briesen*

Investigating the Effect of Packed Structures on Filter Cake Compressibility

Packed beds used in absorption columns have shown to increase filter cake permeability during specific filtration processes. Their effect on filter cake compressibility is evaluated. Different model systems are characterized using dead-end filtration equipment and a modified universal testing machine. Compression experiments are conducted with different packings to assess the systems' response to compressive stress. The structural support of the packings reduces filter cake compressibility for the tested configurations. The extent of this effect depends on packing type, applied pressure, and material compressibility. These results help to understand the advantages of using packed beds as aids for filtration processes and represent a step further in designing tailored packings.

Keywords: Cake filtration, Compressibility, Packed beds, Process strategy

Received: October 02, 2020; *revised:* January 21, 2021; *accepted:* January 25, 2021

DOI: 10.1002/ceat.202000451



This is an open access article under the terms of the Creative Commons Attribution-NonCommercial License, which permits use, distribution and reproduction in any medium, provided the original work is properly cited and is not used for commercial purposes.



Supporting Information
available online

1 Introduction

Laboratory-scale cake filtration studies gather relevant data, which are then used in the design of industrial rotary filters, filter presses, or centrifuges, among others, for countless applications [1]. Several variables and correlations should be considered. For example, treated suspensions are very rarely ideal (monodisperse, incompressible spheres). Filter cake porosity is reduced in the direction of the filter medium in real, compressible systems, where the weight of all solid layers is supported and hydrodynamics are most affected [2]. Suspensions can show slightly to extremely high degrees of compressibility. Some examples of highly compressible substances are microcrystalline cellulose [3], wastewater sludge [4], alginate beads [5], and chromatography gels [6]. Such systems tend to form a nearly impenetrable skin at the filter medium, thus stopping the process [2]. Hence, filter cake compression is one of the fundamental phenomena and, therefore, an intensively studied subject in solid-liquid separation research.

Comparisons between two frameworks describing the dewatering of compressible suspensions have been made in recent investigations [7]. They are known as conventional filtration theory, attributed to Ruth, Tiller, and Shirato [8], and compressional rheology, developed by Buscall, White, and Landman [9]. While the former mostly uses space-averaging approaches to quantify separation descriptors empirically, the latter yields local information from a phenomenological point of view. Nevertheless, the two theories have been proven to be interchangeable and able to complement each other [7]. Hence, this study benefits from both frameworks to evaluate process strategies based on dealing with filter cake compressibility.

Several investigators, such as Alles [10], have analyzed filter cake compression in detail and derived general guidelines to handle the type of suspension accordingly. To date, numerous

strategies have been published to improve various processes one way or another. The spectrum of complexity has become very broad since the method must always be tailored to the application at hand. For example, the flow rate can be increased by using continuous [11] or discrete [12] mechanical vibrations during cake filtration. If the suspension contains paramagnetic solids, or if said solids are purposefully added to it, a magnetic field can also render more permeable filter cakes [13]. In the case of dewatering, the superposition of shear forces to increase efficiency is an ongoing subject of investigation [14]. The classic method of coagulation of water contaminants can be combined with ozone oxidation to reduce membrane fouling [15]. Antifouling behavior has also been achieved by changing the properties of the membrane, either chemically through functional groups [16] or physically through printed textures [17].

The latter makes use of a wavy structure at the filter medium to provide increased support, which alters the local hydrodynamics. Similar results were obtained for thin-film microfiltration of algae by incorporating rigid particles into the suspension [18] to reduce compression and increase porosity and flux. Coincidentally, it is known in the field of thermal separation processes that beds packed inside absorption columns can exhibit analogous channeling and preferential flow caused by wall effects [19]. Considering this, it is plausible that packed beds can be purposefully applied to filtration processes as an

Peter Michael Bandelt Riess, Dr.-Ing. Michael Kuhn, Prof. Dr.-Ing. Petra Först, Prof. Dr.-Ing. Heiko Briesen
briesen@wzw.tum.de

Technical University of Munich, TUM School of Life Sciences Weihenstephan, Chair of Process Systems Engineering, Gregor-Mendel-Strasse 4, 85354 Freising, Germany.

alternative method for incorporating wall support and counter-acting compression.

This strategy was already put to the test by Bandelt Riess et al. [20]. Random and structured packings were assessed using averaging approaches within the context of cake-forming filtration for three model systems. In the case of two nearly incompressible model systems, the packings exhibited a negative effect, adding resistance to the cake and prolonging separation time. However, a very positive effect on the filtration of a highly compressible biological suspension was identified and separation time was strikingly shortened.

These observations may be related to those made in the field of high-performance liquid chromatography by Lan et al. [21] and Lan [22]. They implemented a systematic enhancement of cylindrical wall support in a chromatography column packed with compressible resins. By doing so, the same level of resin compression was achieved at a much higher critical flow velocity. They demonstrated that the results were, among others, dependent on the material properties of the resins, e.g., Young's modulus. For this reason, it would be interesting to consider this correlation when studying solid-liquid separations as well.

Bandelt Riess et al. [20] initially proposed that packings caused two types of effects when used for cake filtration: a so-called steady-state effect, which is based on filter cake permeability, and a transient-state effect, which is based on filter cake compressibility. In the first case, more porous and permeable structures could be formed when incorporating the packed beds into the filter, and therefore specific flow resistance was reduced for a fixed operating pressure. The second case considers forces that interact within the cake itself during separation. As the structure collapses under stress, additional wall support can oppose this effect through friction. However, a more detailed characterization of the systems regarding their compressibility associated with packed beds has not yet been reported.

This study aims to close the gap and investigates the effects of packings on filter cake compressibility. Finding a correlation between operating pressure, cake compression factor, and packing influence is proposed, which would clarify the aforementioned transient effects of this strategy. Once this is understood, the packing can be adapted to the particularities of a suspension of interest. To test this hypothesis, various combinations of suspended solids and packed beds are analyzed to identify the key factors that make the use of packings advantageous.

2 Materials and Methods

2.1 Model Systems

The first suspended solid is the virtually incompressible Crosspure[®] XF (CP; BASF SE). CP is a mixed extrudate made up of 70 % polystyrene and 30 % polyvinylpyrrolidone which is used in beer filtration as a filter aid. It was

selected because of its simplicity; in addition to its relative rigidity, the particles have a rather spherical shape.

The second substance, Arbocel[®] UFC 100 (AC; J. Rettenmaier & Söhne GmbH & Co. KG), is another type of filter aid made of 99.5 % cellulose fibers. The average particle size is between 6 and 12 μm . Particles can reorganize during filtration because the particle structure of AC has more degrees of freedom than CP; thus, the material should be slightly more compressible.

Hop pellets (HO; Simon H. Steiner, Hopfen, GmbH) are a good example of a complex biogenic solid. They are comprised of dried, ground hops. Once the pellets are dispersed, the system becomes noticeably polydisperse. The pellets used were of the Cascade hops variety. This variety contains 16.5 % resins, which greatly contributes to its compressibility. Fig. 1 depicts the materials.

2.2 Packed Beds

The first packing used was a random one made of Raschig rings (1400/6, Glaswarenfabrik Karl Hecht GmbH & Co. KG). Ralu rings (Raschig GmbH) were employed in a second random packing. Finally, a rather structured packing was fabricated using three standing, adjacent 25-4 Raflux rings (RVT process equipment GmbH). The packings are presented in Fig. 2, and their properties are summarized in Tab. 1.

The number of rings that were placed into the filter was determined by the number required to cover the filter area and

Table 1. Properties of the packings used in this study for one filter cake.

Type	Raschig	Ralu	Raflux
Material	Glass	Plastic	Steel
Diameter [mm]	6	15	25
Length [mm]	6	15	25
Wall thickness [mm]	1	1	0.5
Surface [m^2m^{-3}]	940	320	215
Void volume [%]	58	94	95
Ring quantity [-]	96	10	3

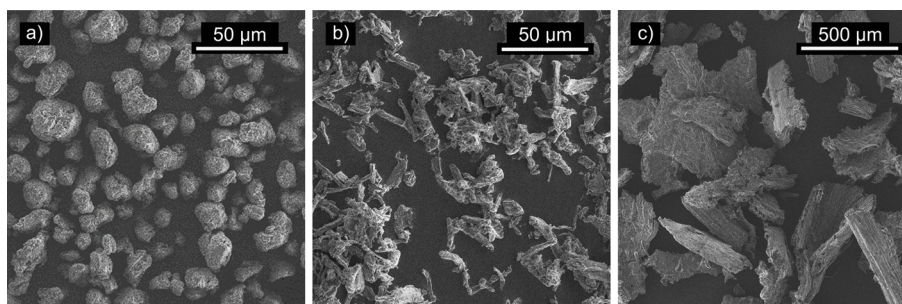


Figure 1. Scanning electron microscope images of (a) CP, (b) AC, (c) HO.

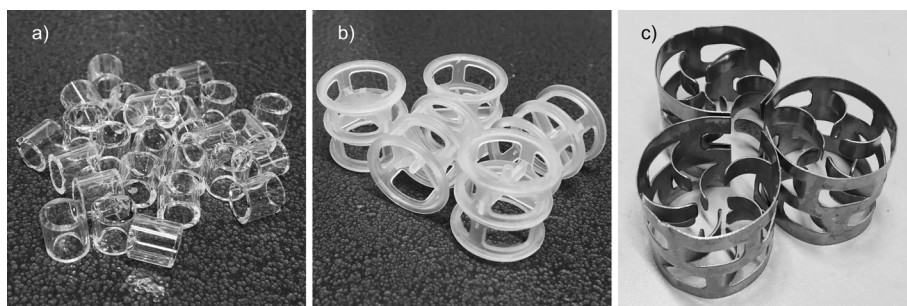


Figure 2. Photographs of (a) Raschig, (b) Ralu, (c) Raflux rings.

form a single layer of packed rings on top of the filter medium. Hence, the height of each packing was the corresponding ring length given in Tab. 1.

2.3 Particle Size Distribution Analysis

The particle size distributions (PSDs) of the model systems were analyzed in normalized differential and cumulative forms using the laser diffraction setup HELOS/KR (Sympatec GmbH) and WINDOX 5.7.0.0 software. The samples were suspended in water and uniformly dispersed in the setup using its QUIXEL dispersion unit. The lens module R2 or R7T was used depending on the particle size range.

2.4 Filtration Equipment

The filtration experiments were conducted using an experimental stand designed and built according to Association of German Engineers standards (VDI guideline 2762 Part 2). The equipment included two separate housings to disperse and then filter the suspensions under pressure. The first housing was equipped with a stirrer and had an internal diameter of 120 mm and a volume capacity of 1.7 L, whereas the second housing had an internal diameter of 100 mm, equivalent to a filtration area of 78.54 cm². DP 1575 090 filter paper (Hahnemühle FineArt GmbH) with 2 μm retention capacity was used as the filter medium. The permeate mass was measured using an automated Kern & Sohn GmbH KB 10000-1N precision scale. The data were processed using MATLAB (The MathWorks, Inc.) code. A schematic of the equipment is illustrated in Fig. 3.

2.5 Compression Equipment

The first stage of the compression experiments was conducted using a small filtration chamber, also built according to Association of German Engineers standards (VDI guideline 2762 Part 2), equipped with a detachable Plexiglas ring for filter cake accumulation. The housing had an internal diameter of 66.5 mm (filtration area of 34.68 cm²) and a volume capacity of 0.85 L. The filter medium was the above-mentioned type of filter paper. In the second stage, the same Plexiglas ring was set for piston-driven compression experiments in a universal testing machine (model zwickiLine; ZwickRoell GmbH & Co. KG).

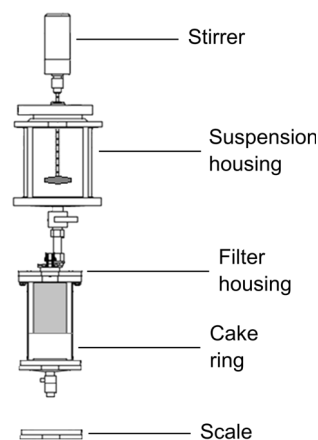


Figure 3. Experimental filtration equipment.

A base for the filter cake ring and a sealed, rigid piston with bleed line were adapted for these tests, allowing for complementary experiments and precise force and height measurements. The movement of the piston was controlled and recorded with testXpert II software (version 3.4), and the data were processed using further MATLAB (The MathWorks, Inc.) code. A schematic of the equipment is illustrated in Fig. 4. Coupling filtration with material testing represents a fast and uncomplicated method for performing this kind of experiment.

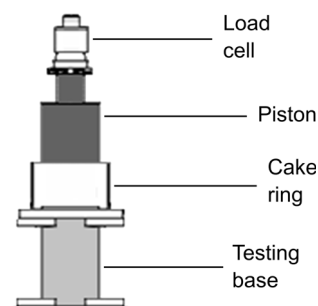


Figure 4. Experimental compression equipment.

2.6 Experimental Procedures

A series of experiments without packings was first performed for reference and characterization of the model systems and, thus, standard filtration and compression curves were obtained for each suspension and each equipment. All experiments were

performed in triplicate, and the results were expressed as the arithmetic mean value. The error bars indicate standard deviations.

Regarding the filtrations, the suspensions were separated under pressures between 0.5 and 2.0 bar to detect changes in filtrate flow caused by compression. The dead-end filtrations were conducted according to VDI guideline 2762, Part 2 [23]. Each suspension was prepared using distilled water at a final volume of 1.5 L. The CP and AC samples were weighed and presuspended in the distilled water before being homogenized in an ultrasonic tub. To disperse the HO particles, the pellets had to be submerged in water overnight before preparing the suspension. The sample quantity was determined based on a cake height of 1.1 cm for CP and AC (40 and 30 g, respectively) and 2.3 cm for HO (30 g). The latter was designed to be higher to achieve comparable filtration times for all systems.

The sample was transferred to the suspension housing after configuring its stirrer to maintain homogeneity. Subsequently, the valve leading to the filter housing was opened, the system was pressurized, and filtration and data recording were initiated.

According to the standardized norm [23], filtration data (accumulated filtrate mass over time) are to be plotted in the form of time/accumulated filtrate volume over the same volume to obtain the flow resistance of the filter medium, $R_M^{(1)}$, and relative filter cake resistance, α_K , following Eq. (1):

$$\frac{t}{V} = \frac{k\eta\alpha_K}{2A^2\Delta p} V + \frac{R_M\eta}{A\Delta p} \quad (1)$$

where t denotes the filtration time, V the filtrate volume, k a concentration constant calculated from the cake thickness, η the fluid viscosity, A the filter area, and Δp the differential pressure.

However, recent research conducted by Kuhn et al. [24] effectively showed that fitting the filtration curve nonlinearly to a root function is more precise both in terms of execution and results. Thus, the change in filtrate volume over time is described as:

$$V = \sqrt{\frac{2\Delta p A^2}{\eta\alpha_K k} t} + \left(\frac{R_M A}{\alpha_K k}\right)^2 - \frac{R_M A}{\alpha_K k} \quad (2)$$

The parameters of interest were estimated by finding the deviation minimum with the usual least-squares method after choosing this fitting strategy. The procedure was repeated for every operating pressure and for each system to draw conclusions about their compressibility. This last parameter is often determined by fitting power functions, such as Eq. (3) [25, 26], to the changes in flow resistance due to increases in differential pressure.

$$\alpha_K = K_\alpha \Delta p^{N_\alpha} \quad (3)$$

Here, N_α represents global compressibility and its value can be used as a point of reference for comparison of compressible

network behavior. The coefficient K_α does not necessarily have a physical meaning but it is often associated with filter cake resistance at a low differential pressure.

For the reference filter cake compressions in the testing machine, the systems first had to be separated in the small filtration chamber under 1.0 bar, analogous to the previous method. Each suspension was prepared using distilled water at a final volume of 0.5 L. The samples were weighed, suspended, and homogenized in the ultrasonic tub as before. The quantities were again determined based on a cake height of 1.1 cm for CP and AC (15 and 10 g, respectively) and 2.3 cm for HO (10 g). The suspension was transferred directly into the filter housing, the system was closed and pressurized, and the filtrate was then purged until the wet filter cake formed in the Plexiglas ring (2 mm of liquid remained above the solid network).

Subsequently, the ring containing the filter cake was detached from the housing to be fixated and aligned below the piston of the testing machine. The starting point of the measurement was the initial filter cake height, which had been determined upon first contact with the piston. Subsequently, the piston was lowered automatically at a rate of 1 mm min^{-1} until predetermined pressures were reached, while continuously recording both force and distance to obtain characteristic compression curves for the systems. These stepped pressure tests (analogous to Usher et al. [27]) were performed seamlessly between 20 and 500 kPa, allowing the system to reach mechanical equilibrium for 20 s. The equilibrium pressure in the solid network is known as compressive yield stress p_y . The evolution of this value according to the relative variation in filter cake volume V_K was used to complement the global compressibility results of the previous method.

Furthermore, filter cake compressions were conducted with the different packings in Tab.1 to detect variations in the compression behaviors of the systems. The procedures were repeated as explained, this time after additionally placing the predetermined quantity of packed elements into the small filter chamber before transferring the suspensions. This way, the solids accumulated around and above the packings during the separation, forming layered structures. The sample quantities were previously adjusted to guarantee that the filter cake height above the packing was at least as tall as the corresponding reference filter cake. This was done to keep the piston from coming into direct contact with the packed rings during the compression experiments. The formed filter cakes were subsequently fixated and compressed in the testing machine.

Fig. 5 illustrates the example of an AC filter cake (with height (b) 1.1 cm) with Raschig rings (packing height (c) 0.6 cm). The initial combined cake height (a) of 1.7 cm was compressed to

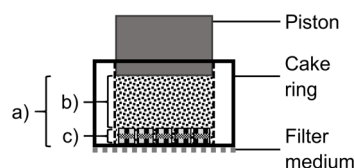


Figure 5. Schematic of a filter cake compression with packing; (a), (b), and (c) are the heights of the combined filter cake, suspended solids cake, and packing, respectively.

1) List of symbols at the end of the paper.

an end height of 1.0 cm. All compressions were performed within the extension of (b).

3 Results and Discussion

3.1 Particle Size Distribution

The results of the volumetric PSD tests are presented as characteristic values in Tab. 2. The representative variables are particle sizes $x_{10,3}$, $x_{50,3}$, and $x_{90,3}$, modal value x_h , relative span S , and specific surface S_V . The normalized differential (q_3) and accumulated forms (Q_3) of the PSDs are given in the Supporting Information.

Table 2. PSD characteristic values of the model systems.

System	CP	AC	HO
$x_{10,3}$ [μm]	10.5	2.9	58.9
$x_{50,3}$ [μm]	21.9	11.3	238.3
$x_{90,3}$ [μm]	30.3	24.9	423.4
x_h [μm]	23.0	7.2	280
S [-]	0.90	1.95	1.53
S_V [m^2cm^{-3}]	0.61	1.00	0.08

All values were estimated using laser diffraction software except for the relative PSD span S , which was determined using Eq. (4):

$$S = \frac{x_{90,3} - x_{10,3}}{x_{50,3}} \quad (4)$$

The CP sample shows a modal value that is similar to its $x_{50,3}$ value. Its PSD is rather normally distributed and relatively narrow. The AC distribution exhibits smaller characteristic values in general but a much broader relative span than that of CP. Although the AC sizes are not as evenly distributed, they are of similar orders of magnitude as the CP results and are contained within the same spectrum. HO is a more complex system where the solids consist of different substances, and it shows a distinct PSD with generally much larger values and a broad absolute span. Its S value is comparable to that of AC, also exhibiting some asymmetry in the characteristic properties of Tab. 2.

3.2 Relative Flow Resistance

During each experiment, the accumulated filtrate mass was recorded as a function of time. Furthermore, the compression behavior of the systems during filtration was assessed graphically by expressing the filtration curves according to Eq. (1) and then normalizing for differential pressure. This yields a representation for each experiment, where the gradient only depends on relative filter cake resistance. An incompressible system can be represented with a single master curve, regard-

less of the pressure [1]. An example of this method for HO is displayed in Fig. 6.

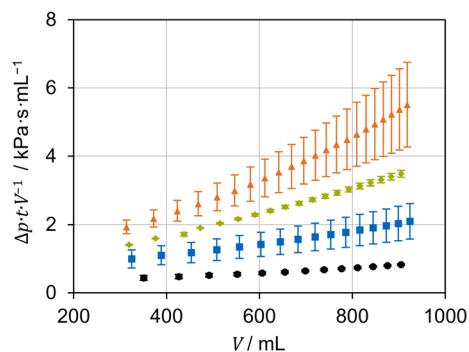


Figure 6. Pressure-normalized representation of the HO filtration curves at differential pressures of 0.5 bar (black circles), 1.0 bar (blue squares), 1.5 bar (green rhombuses), 2.0 bar (orange triangles).

The filtration runs with HO at different differential pressures are indicated and compared. It can be concluded that the system is compressed further each time, making the filter cake resistance greater since the function values grow notably when pressure is increased. This is reflected in the exponent of Eq. (3) (see Tab. 3). The same representation for all systems can be found in the Supporting Information.

Eq. (2) was employed to fit the raw filtration data to a root function by means of a least-squares method. The obtained function parameters were used to solve for the space-averaged relative flow resistance of the filter cakes. The numerical results of this study are presented in Tab. 3 for all systems.

Table 3. Relative cake resistances and global compressibilities of all systems based on filtration data.

Parameter	Δp [bar]	CP	AC	HO
α_K [10^{12}m^{-2}]	0.5	7.16 ± 1.60	6.24 ± 1.39	1.04 ± 0.11
	1.0	8.53 ± 1.16	8.08 ± 0.66	4.08 ± 0.62
	1.5	7.86 ± 1.42	9.75 ± 0.52	4.57 ± 0.45
	2.0	9.35 ± 2.85	12.36 ± 0.61	7.55 ± 1.57
N_α [-]	-	0.14 ± 0.06	0.49 ± 0.15	1.36 ± 0.02

The relative flow resistances of CP do not yield a very clear dependence on differential pressure under the given experimental conditions, as expected, since the solid is relatively incompressible. Fitting to a power function resulted in a relatively small exponent. The flow resistances of both AC and HO exhibit a considerable increase as the pressure rises, which is characteristic of plant-based suspended particles (see Fig. 1). While the former system is made up of deformable cellulose fibers, the latter resembles platelets, which can collapse under pressure. After quadrupling Δp , the flow resistance of AC doubled and that of HO increased more than sevenfold. Fitting α_K over Δp to power functions resulted in the exponents 0.49 and 1.36, respectively, making AC much more compress-

ible than CP, and, in turn, HO much more compressible than AC in this framework.

According to the VDI classification for flow resistances [23], all determined values, except AC at 2.0 bar, can be roughly considered easily separable (below $1.0 \times 10^{13} \text{ m}^{-2}$). The presented global compressibilities provide a rather qualitative overview of the compression behavior of the analyzed systems. The following results section aims at quantifying this property more accurately and introducing variations into the process.

3.3 Compression Behavior

The applied force was recorded simultaneously with the filter cake height for all compressions in the testing machine. Of the gathered data, pressures at mechanical equilibrium (compressive yield stresses) are the most relevant. For all systems and combinations, the measured values are plotted against the relative volume decrements in the network, similarly to Höfgen et al. [7].

Fig. 7 presents the different compression runs with all reference systems. A steeper slope of the curve indicates greater resistance to compressive stress. Another important property of the compression run is the abscissa of the initial value at the lowest pressure. It indicates cake height displacement between no force (at the origin) and the first compressive yield stress.

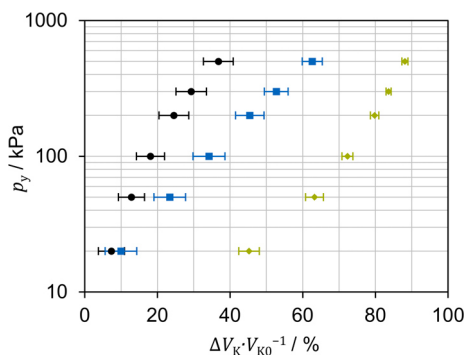


Figure 7. Compressive yield stress over relative volume change for all reference systems: CP (black circles), AC (blue squares), HO (green rhombuses).

In this regard, CP, AC, and HO exhibit respective volume reductions at the first compression of 7, 10, and 45 %. This allows for a first comparison of the systems' resistance to compressive stress, which is similar to the one in Tab. 3. With these results, however, the way networks react to a specific amount of force can be directly seen. Some differences are also observable after the first stage. The CP and AC curves start at similar values, after which the different slopes become visible. The CP slope is steeper and evidences the relative stiffness of the material again.

Since this method allows for higher pressures, it becomes possible to affect not just the particle arrangement but also the material integrity of the solids. The AC slope is smaller, spanning over a broader compression and ending at a much higher volume variation than that of CP. As expected, the HO curve exhibits the characteristic compression. It takes the lowest pres-

sure to reduce the cake height to almost half of its initial value. After this point, the curve rises similarly to CP. Compressing the already densified HO cake grows increasingly difficult since its last equilibrium is almost only 10 % of the original volume.

Thus, the differences and similarities between the materials as disperse systems and porous filter cakes have been established through standard filtration and compression experiments. The latter method is also applied to evaluate the effects of the packings used on the above-mentioned properties.

Fig. 8 shows the different compression runs with CP. For the reference (black), the filter cake is composed only of suspension solids. The colored curves correspond to the cakes including a packed bed at the bottom. Regarding the first compression step, it is not possible to identify an effect of the packings. For the tested configurations, it is necessary to overcome the pressure required to force the solid network into the packing. When the applied pressure grows, however, additional friction forces come into play and, if wall support is provided to absorb part of these forces, the resistance to stress is increased. A clear difference between the reference and all packing curves becomes visible at 300 kPa. In the end, three separate trends are identifiable, and the last reference equilibrium is at least 10 % away from the others. The Raschig and Ralu packings manage to counteract compression in a similar way, attributed to the fact that both are random and can rearrange during the experiment, and the Raflux structure has the most considerable effect.

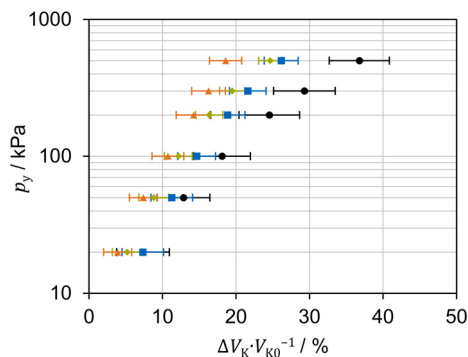


Figure 8. Compressive yield stress over relative volume change for CP: reference (black circles), Raschig rings (blue squares), Ralu rings (green rhombuses), Raflux structure (orange triangles).

In past filtration experiments [20], packings were used with CP, AC, and HO to assess changes in cake permeability. Although Fig. 7 proves that they counteracted compression in a CP cake, Ralu and Raflux rings had no influence on its permeability and the Raschig packing even reduced it. Since those effects were observed in filtrations at 1.5 bar, it is arguable that the effect of the packings was not relevant enough at such low pressures, which should be considered for future experiments. Additionally, it was discussed that the small rings exhibited a void volume lower than 60 % and therefore relatively small inner spaces, susceptible to clogging and lower permeability. Both groups of experiments lead to the conclusion that counteracting compressibility and improving permeability with packings are not necessarily coupled effects, and that further considerations must be made, such as material properties, to find a compromise.

Fig. 9 demonstrates the different runs with the more compressible AC. Regarding the compression step at 50 kPa, it is already possible to identify the influence of the packings, as opposed to CP. All three combinations noticeably decrease the volume reduction in a similar manner. As compression progresses, greater distances are put between the curves until the last reference equilibrium and its nearest one are at least 20 % away, which is a greater effect than before. The runs with Raschig and Ralu rings are practically identical up to the last point, where the latter counteracts compression more. The run with the Raflux structure represents the most stable filter cake from the start. At the end of this run, the network is even less compressed than CP. As stated before, the void space in the packing structure seems to be beneficial.

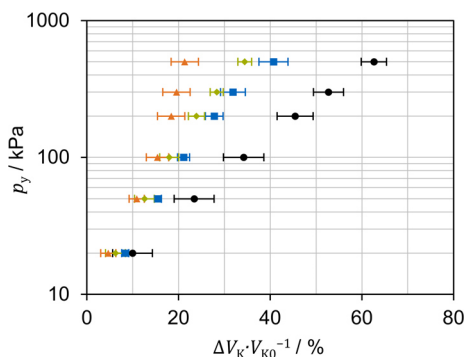


Figure 9. Compressive yield stress over relative volume change for AC: reference (black circles), Raschig rings (blue squares), Ralu rings (green rhombuses), Raflux structure (orange triangles).

Even though the packings increased resistance to compression here, they could not improve the filter cake permeability in previous investigations. It is proposed that the same forces that held the solid particles together during these experiments, opposing compressive stress and making them less compressible, are the same ones, which formed denser, less permeable cakes during the filtration experiments. Again, avoiding compression could become beneficial at higher pressures than 1.5 bar. Thus, it is possible to influence the compressibility of systems like AC favorably, while simultaneously yielding less porous networks.

Fig. 10 displays the different runs with HO. Significant differences are observed at the lowest compression step. All combinations inhibit volume reduction much better than in the previous cases, due to the compressibility of the solid network. Upon starting the experiment, the difference between the reference and its nearest curve was already approximately 6 %. As the compression progresses, greater distances appear between the reference and the Raschig and Raflux curves, respectively, while the difference to the Ralu curve remains rather constant. At the last equilibrium, four clear trends are observable in the order of the corresponding void volume. The Raflux structure stabilizes the filter cake to the point of becoming practically incompressible after the first step.

In previous filtration experiments [20], HO was the only case that exhibited permeability improvement when combined with each packing. It was proposed that the effects were caused by

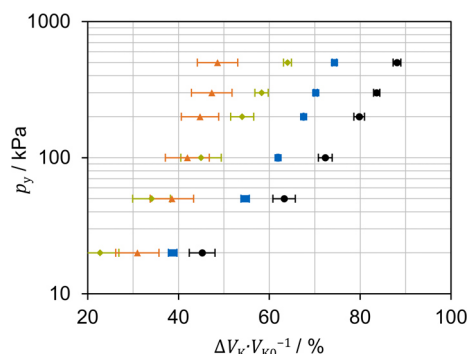


Figure 10. Compressive yield stress over relative volume change for HO: reference (black circles), Raschig rings (blue squares), Ralu rings (green rhombuses), Raflux structure (orange triangles).

the material's compressibility as well. The curves in Fig. 10 are further evidence that the greater the network compressibility, the greater the packings' effects on it. Thus, with systems like HO, it is possible to influence both the compressibility and the permeability of the solid network favorably. It is hypothesized that, due to the particle size distribution of this system and to its ratio in respect of the packing elements, forming and clogging a denser filter cake is not as plausible as with the other solids. This way, the solids form a rather porous network, which is stabilized by the packing and is compressed much less during filtration, remaining relatively porous. Hence, both compression and filtration tests were positive.

According to the results of this study, it becomes clear that filter cake compressibility has a strong influence on filtration performance, and that it can be dramatically reduced by using packings during the process. It must be stressed that the exhibited analyses are dependent on the chosen array, and it is especially challenging to quantify the influence of packings on compressibility experimentally. Therefore, different methods may complement this study in the future.

Nonetheless, the way solid particles accumulate within the filter (with or without a packed bed) has an equally considerable influence, if not more. Even if the filter cake has become less compressible, permeability can still be compromised and filtration is noticeably prolonged. A compromise between the two effects must be found for each system of interest. Thus far, the tests have been successful for HO, but testing for CP, AC, and further systems should be the aim of future investigation.

4 Conclusions and Outlook

The use of packed beds has been applied as an unconventional strategy to accelerate the separation processes of challenging biological suspensions. To evaluate the observed effects, previous studies focused on filter cake permeability and specific flow resistance without analyzing system compressibility.

Different model systems were characterized using classic filtration equipment as well as coupled filtration-compression experiments with a universal testing machine. The filter cakes were classified corresponding to their compressibility accord-

ing to both methods, showing agreement. Further compressions were conducted combining the suspended solids with defined packed configurations to analyze the effect of compressive stress on the systems. All packings provided structural support, which absorbed friction and increased compression resistance, for all systems. The greater the applied pressure or the material compressibility, the more pronounced was the effect. The fixed packing proved to be more beneficial than the random packings.

It was observed that improving compressibility is not associated with enhancing permeability. It is necessary to maintain the structure of the porous network in the process, in other words, to find a compromise. Future work should involve finding a correlation between particle size distribution and packing influence. The mentioned transient effect of this strategy may now be somewhat better understood, but the static impact is just as relevant. After that, packings can be purposefully designed for particular systems of interest.

Supporting Information

Supporting Information for this article can be found under DOI: <https://doi.org/10.1002/ceat.202000451>.

Acknowledgment

The authors would like to thank the Chair of Process Systems Engineering's workshop for their help with the hardware, and Philip Pergam for his MATLAB consultation. The practical work performed by Elena Wingerath and Maximilian Vorwerk is greatly appreciated. Open access funding enabled and organized by Projekt DEAL.

The authors have declared no conflict of interest.

Symbols used

A	$[\text{m}^2]$	filter area
K	$[\text{m}^{-2}\text{Pa}^{-N}]$	coefficient of power function
k	$[-]$	concentration constant
N	$[-]$	global compressibility
p	$[\text{bar}, \text{kPa}]$	pressure, compressive stress
Q	$[\%]$	cumulative distribution
q	$[\text{mm}^{-1}]$	normalized differential distribution
R	$[\text{m}^{-1}]$	absolute flow resistance
S	$[\text{m}^2\text{cm}^{-3}, -]$	specific surface, particle size distribution span
t	$[\text{s}]$	filtration time
V	$[\text{mL}]$	volume
x	$[\mu\text{m}]$	particle size

Greek letters

α	$[\text{m}^{-2}]$	relative flow resistance
η	$[\text{Pa s}]$	fluid viscosity

Subscripts

K	relative to filter cake
M	relative to filter medium
V	volumetric
y	vertical orientation
α	respect of relative flow resistance
0	initial condition
10	10 % accumulation
3	volumetric size distribution
50	50 % accumulation
90	90 % accumulation

Abbreviations

AC	Arbocel [®] UFC 100
CP	Crosspure [®] XF
HO	hops pellets
PSD	particle size distribution

Data Availability Statement

The data that support the findings of this study are available from the corresponding author upon reasonable request.

References

- [1] H. Anlauf, *Wet Cake Filtration: Fundamentals, Equipment, Strategies*, Wiley-VCH, Weinheim 2020.
- [2] F. M. Tiller, T. C. Green, *AIChE J.* **1973**, *19* (6), 1266–1269. DOI: <https://doi.org/10.1002/aic.690190633>
- [3] T. Mattsson, M. Sedin, H. Theliander, *Sep. Purif. Technol.* **2012**, *96*, 139–146. DOI: <https://doi.org/10.1016/j.seppur.2012.05.029>
- [4] S. J. Skinner, L. J. Studer, D. R. Dixon, P. Hillis, C. A. Rees, R. C. Wall, R. G. Cavalida, S. P. Usher, A. D. Stickland, P. J. Scales, *Water Res.* **2015**, *82*, 2–13. DOI: <https://doi.org/10.1016/j.watres.2015.04.045>
- [5] K.-J. Hwang, P.-Y. Su, E. Iritani, N. Katagiri, *Sep. Sci. Technol.* **2016**, *51* (11), 1947–1953. DOI: <https://doi.org/10.1080/01496395.2016.1187629>
- [6] D. Y. Kong, S. Gerontas, R. A. McCluckie, M. Mewies, D. Gruber, N. J. Titchener-Hooker, *J. Chem. Technol. Biotechnol.* **2018**, *93* (7), 1959–1965. DOI: <https://doi.org/10.1002/jctb.5411>
- [7] E. Höfgen, S. Kühne, U. A. Peuker, A. D. Stickland, *Powder Technol.* **2019**, *346*, 49–56. DOI: <https://doi.org/10.1016/j.powtec.2019.01.056>
- [8] F. M. Tiller, C. S. Yeh, W. F. Leu, *Sep. Sci. Technol.* **1987**, *22* (2–3), 1037–1063. DOI: <https://doi.org/10.1080/01496398708068998>
- [9] R. Buscall, L. R. White, *J. Chem. Soc., Faraday Trans. 1* **1987**, *83* (3), 873. DOI: <https://doi.org/10.1039/F19878300873>
- [10] C. M. Alles, *Prozeßstrategien für die Filtration mit kompressiblen Kuchen*, Ph.D. Thesis, Universität Karlsruhe (TH) **2000**.
- [11] R. J. Wakeman, P. Wu, *KONA* **2002**, *20*, 115–124. DOI: <https://doi.org/10.14356/kona.2002014>

- [12] O. Shevchenko, S. Tynyna, *Chem. Ing. Tech.* **2017**, *89* (6), 823–830. DOI: <https://doi.org/10.1002/cite.201600019>
- [13] C. Eichholz, M. Stolarski, V. Goertz, H. Nirschl, *Chem. Eng. Sci.* **2008**, *63* (12), 3193–3200. DOI: <https://doi.org/10.1016/j.ces.2008.03.034>
- [14] E. Höfgen, D. Collini, R. J. Batterham, P. J. Scales, A. D. Stickland, *Chem. Eng. Sci.* **2019**, *205*, 106–120. DOI: <https://doi.org/10.1016/j.ces.2019.03.080>
- [15] W. Yu, N. J. D. Graham, G. D. Fowler, *Water Res.* **2016**, *95*, 1–10. DOI: <https://doi.org/10.1016/j.watres.2016.02.063>
- [16] Z.-X. Low, J. Ji, D. Blumenstock, Y.-M. Chew, D. Wolverson, D. Mattia, *J. Membr. Sci.* **2018**, *563*, 949–956. DOI: <https://doi.org/10.1016/j.memsci.2018.07.003>
- [17] A. Al-Shimmery, S. Mazinani, J. Ji, Y. J. Chew, D. Mattia, *J. Membr. Sci.* **2019**, *574*, 76–85. DOI: <https://doi.org/10.1016/j.memsci.2018.12.058>
- [18] M. T. Hung, J. C. Liu, *Sep. Purif. Technol.* **2018**, *198*, 10–15. DOI: <https://doi.org/10.1016/j.seppur.2016.10.063>
- [19] C. Fee, S. Nawada, S. Dimartino, *J. Chromatogr. A* **2014**, *1333*, 18–24. DOI: <https://doi.org/10.1016/j.chroma.2014.01.043>
- [20] P. M. Bandelt Riess, J. Engstle, M. Kuhn, H. Briesen, P. Först, *Chem. Eng. Technol.* **2018**, *41* (10), 1956–1964. DOI: <https://doi.org/10.1002/ceat.201800254>
- [21] T. Lan, S. Gerontas, G. R. Smith, J. Langdon, J. M. Ward, N. J. Titchener-Hooker, *Biotechnol. Prog.* **2012**, *28* (5), 1285–1291. DOI: <https://doi.org/10.1002/btpr.1597>
- [22] T. Lan, *An Experimental and Simulation Study of the Influence Made by Inserts on Chromatographic Packed Bed Hydrodynamics*, Ph.D. Thesis, University College London **2013**.
- [23] VDI 2762 Part 2, *Mechanical Solid-Liquid Separation by Cake Filtration. Determination of Filter Cake Resistance*, VDI guideline, Verein Deutscher Ingenieure, Düsseldorf **2010**.
- [24] M. Kuhn, P. Pergam, H. Briesen, *Chem. Eng. Technol.* **2020**, *43* (3), 493–501. DOI: <https://doi.org/10.1002/ceat.201900511>
- [25] P. Kovalsky, M. Gedrat, G. Bushell, T. D. Waite, *AIChE J.* **2007**, *53* (6), 1483–1495. DOI: <https://doi.org/10.1002/aic.11193>
- [26] W. Chen, *Drying Technol.* **2006**, *24* (10), 1251–1256. DOI: <https://doi.org/10.1080/07373930600840401>
- [27] S. P. Usher, R. G. de Kretser, P. J. Scales, *AIChE J.* **2001**, *47* (7), 1561–1570. DOI: <https://doi.org/10.1002/aic.690470709>

4.3 Paper III: Assessing the Wall Effects of Packed Concentric Cylinders and Angular Walls on Granular Bed Porosity

This third and last paper is a case study based on validated discrete element method (DEM) simulations. The concept was inspired by the knowledge gained in the previous papers, and the collective author contributions remained unchanged. The simulation programming and validation were performed by the last author, and the background research and writing lie with the first and last authors.

Filtration is a mechanical solid–liquid separation process where porosity has a decisive role. Compressible solids form filter cakes which exhibit a porosity gradient between the cake surface and the filter medium, where its value is at its lowest. In opposition, it is known that the porosity of a particle bed is at its maximum at the container wall. Considering both effects, it is plausible that incorporating more walls to the said container would increase the particle bed's porosity, eventually aiding filtration processes. This train of thought is used in this work to introduce relevant studies in matter of bulk and radial porosity changes in cylindrical beds of randomly packed spheres. Even though the topic is well known and has been successfully modeled by several authors, the strategy of altering wall quantity and orientation is not found often. After exposing the advancements and benefits of DEM simulations, it is proposed that they be used to explore the influence of wall support on bed porosity and manipulate the former to increase the latter's value. This would shed more light on the findings of the previous papers.

To perform the case study, numerical DEM simulations with LIGGGHTS software are set up according to published literature data (experimental and correlation results), and determined parameters are calibrated until the obtained values can be validated. The porosities are determined using a Monte Carlo integration scheme. One of the calibrated models (3 mm monodisperse glass spheres in a 120 mm-diameter cylinder) is subsequently used to simulate sphere deposition into the container with three newly defined wall arrangements: one to seven inner concentric cylinders, four to sixteen vertical angular walls, and combinations of these two cases.

After comparing the simulated results with those reported in the literature through experiments and correlations, very good agreement is observed amongst all cases. The porosity values strongly depend on the ratio between container and sphere diameters; the results grow with decreasing ratio. Having validated the method, the system variations are simulated, and the results are compared to a base case.

First, the number of inner concentric cylinders is incremented, choosing the diameters so there is a constant distance between adjacent walls. When using six cylinders, the bulk porosity is greatly increased by 17%, and this is fitted to an equation to model the results. It is noted that the bulk porosity is not increased homogeneously in each generated annulus, with the maximal value always being at the arrangement center. Porosity is then analyzed as a function of distance from the outer cylinder wall for each case, displaying the expected classical sinusoidal behavior. It becomes clear that adding walls generates more peaks to the profile, increasing overall porosity: the more walls, the greater the effect. For this reason, the highest value is achieved with six cylinders and sixteen angular walls (26% increase).

Since such porosity increases could contribute to flow velocity in separation processes, there is application potential in this strategy. Thanks to this study, it becomes clearer how packed particles interact with walls and the observed effects in this and previous papers can be better understood. Future research can benefit from the obtained results.



Assessing the wall effects of packed concentric cylinders and angular walls on granular bed porosity

Peter Michael Bandelt Riess¹ · Heiko Briesen¹ · Daniel Schiochet Nasato¹

Received: 26 August 2021 / Accepted: 2 December 2021
© The Author(s) 2021

Abstract

The effect of added wall support on granular bed porosity is systematically studied to elucidate performance enhancements in filtration processes achieved by using inserts, as demonstrated experimentally (Bandelt Riess et al. in Chem Eng Technol 2018, 2021). Packed beds of spheres are simulated through discrete element method in cylinders with different internal wall configurations. Three containing systems are generated: concentric cylinders, angular walls, and a combination of both. Variations of particle size and wall friction and thickness are also considered, and the resulting granular bed porosities are analyzed. The porosity increase is proportional to the incorporated wall support; the combination of cylindrical and angular inserts displays the greatest effect (up to 26% increase). The sinusoidal porosity values near the walls are exhibited to clarify the effects. The presented method can change and evaluate granular bed porosity increments, which could lead to filtration process improvements, and the obtained behaviors and profiles can be used to explore additional effects and further systems.

Keywords Porosity · Wall support · Filter cake · Packed bed · DEM

List of symbols

Roman symbols

a	Empirical coefficient (–)
c	Viscous term (Ns m^{-1})
d	Sphere diameter (m)
D	Container diameter (m)
e	Coefficient of restitution (–)
F	Force (N)
g	Pair correlation function (–)
G	Shear modulus (Pa)
k	Elastic term (N m^{-1})
m	Particle mass (kg)
n	Particle number in a defined volume (–)
r	Particle position (m)
R	Particle radius (m)
Y	Young's modulus (Pa)

Greek letters

β	Dissipative term (–)
Δ	Difference (–)

ε	Porosity (–)
μ_s	Coefficient of friction (–)
ν	Poisson's ratio (–)
ξ	Particle overlap (m)
ρ	Particle number density (m^{-3})

Subscripts

b	Bulk property
i	Particle name
j	Particle name
n	In normal direction
t	In tangential direction
∞	Located at the container center

Superscripts

\wedge	Modifies e to unit vector
$*$	Equivalent property
$'$	Modifies D to distance between adjacent walls

Abbreviations

DEM	Discrete element method
RDF	Radial distribution function

✉ Daniel Schiochet Nasato
daniel.nasato@tum.de

¹ Chair of Process Systems Engineering, Technical University of Munich, TUM School of Life Sciences Weihenstephan, Gregor-Mendel-Str. 4, 85354 Freising, Germany

1 Introduction

Mechanical solid–liquid separation processes rely on physical principles to achieve their goal. The cake filtration process offers the advantage of allowing multiple applications, where the collected solids can be directly post-treated. During cake filtration, solid particles form porous, permeable layers with millimeters up to decimeters of thickness [1]. Porosity has a key role in filtration; hence, it has been thoroughly described by Tiller and co-workers in their notable works [2–4]. If solids are compressible, filter cake porosity is reduced in the direction of the filter medium, where the weight of all layers is supported, often leading to complications during equipment operation. Conversely, friction at the filter walls is known to consume part of the applied load, which should counteract compression. These two phenomena occur simultaneously during the process and can, therefore, be fruitfully set against each other [5]. Thus, adding more wall support through some random or structured packing should reduce filter cake compressibility, increasing porosity and throughput.

The common use of such packings is in absorption and rectification columns to increase the contact surface between phases as much as possible. Heat and mass transfers are enhanced, and equipment performs more effectively as a result. At the same time, they pose the benefit of exhibiting relatively low hydraulic pressure drops through the apparatus [6]. For these reasons, packings are a current topic in many investigations [7–10]. Furthermore, the effects of column walls on packed bed porosity are mentioned in various experimental and numerical works [11–15], allowing for an evident parallel to cake filtration.

The azimuthally averaged porosity of a granular medium (e.g., filter cake) contained in a cylinder changes with the radial position. If the solid particles are considered as randomly packed, uniform spheres, considerable amounts of data gathered in well-known works, such as those by Sonntag [16] and Jeschar [17], become available. Bulk porosity ε_b correlations are found in the following form:

$$\varepsilon_b = \varepsilon_\infty + a \frac{d}{D}, \quad (1)$$

where ε_∞ is the center porosity (no wall influence); a is an empirical coefficient; d is the sphere diameter; D is the container diameter. For monodisperse spheres poured into the column, Jeschar [17] reported bulk porosities between 0.375 and 0.391. Later, Desmond and Weeks [18] realized the importance of studying polydisperse packings because of the tendency of monodisperse ones to crystallize near flat walls.

More recently, Mueller [19] compiled the abovementioned works and several others as bases to improve existing models for predicting bulk and even local, radial porosities in a cylindrical bed of spheres, where the highest possible value (1) is always found at the container wall. However, studies regarding the strategic incorporation of more wall support and applications thereof are still scarce. This is understandable in the case of fixed beds for absorption and rectification, where wall effects are disadvantageous, causing channeling and reducing liquid residence time.

Nevertheless, using packed beds to incorporate more wall effects into separation processes involving solids retention has yielded promising results. This was approached in the case of high-performance liquid chromatography in Lan et al. [20] and Lan [21]. They investigated the enhancement of wall support inside a chromatography column packed with compressible materials by using different cylindrical insert configurations. Consequently, the compressible resins could endure a significantly higher throughput velocity at the onset compression. The results were a function of insert position, number, and dimensions, mechanical properties of the resins, and wall roughness.

In the field of cake filtration, Bandelt Riess et al. [5, 22] investigated similar phenomena using random and structured packings. Their effect was proposed as twofold: (1) a stationary effect, which, like a filter aid, provides a permeable structure with high porosity for the cake to accumulate; and (2) a transient effect, with which the packing's internal wall support counteracts the developing filter cake compression. Even though the transient effect was recently addressed in more detail [5], mechanistic explanations for the stationary one are still missing, which is the motivation of this study. To this end, numerical simulations based on discrete element method (DEM) have been identified as a useful tool for taking this systematic approach.

Modeling granular assemblies numerically employing discrete elements has been around for some time [23]. Nowadays, it can be applied to much more complex problems, such as studying the rearrangements of non-spherical particles through vibrations [24]. The investigation of porous media has benefited from the DEM simulations of, for example, Reboul et al. [25], who focused on the void size distribution of a packed bed, and Dong et al. [26], who focused on the influence of different forces on particles while sedimenting and forming filter cakes. More recently, Zhang and McCarthy [27] proposed a modified modeling approach for cake filtration by implementing a DEM-coupled method and comparing it with the classic Kozeny–Carman model [28]. The modified model more accurately predicted the flow rates in the case of polydisperse systems. McCarthy et al. [29] and Lovregio et al.

[30] showed that porosity values of spheres confined in annular and cylindrical cells, respectively, obtained through DEM and experimental methods can agree well quantitatively. Meanwhile, Gerontas et al. [31] successfully developed a structural mechanics model of resin compression in a liquid chromatography column, which used the finite element method to simulate the effect of wall support inside the column on the process in agreement with the experimental data of Lan et al. [20]. This consequently allowed the model to predict previously untested scenarios, thereby providing a convenient case study method.

This work aims at elucidating how wall support manipulation increases granular bed porosity in different scenarios. Different insert configurations are simulated to modify the porosity of cylindrical beds of uniform spheres. It is proposed that an insert geometry can be found, which provides significant porosity and permeability enhancements. This would support previous experimental results [22] and could lead to improvements in industrial filtration processes.

2 Methodology

2.1 Simulation method

LIGGGHTS software (Version 3.8.0; DCS Computing GmbH) was used to perform the numerical DEM simulations, while OVITO software (Version 3.0; OVITO GmbH) was utilized to visualize and calculate the radial distribution function (RDF). The RDF [also called pair correlation function $g(r)$] measures the probability of finding a particle at a distance r away from an arbitrary reference particle. It gives insight into the structure of the granular packing and is essentially a histogram of inter-particle distances. The RDF is given by [32]:

$$g(r) = \frac{n(r)}{4\pi r^2 \Delta r \rho^2}, \tag{2}$$

where $n(r)$ is the number of particles inside a spherical shell located between the radial distances r and $r + \Delta r$ from the center of the specified particle, and ρ is the number density of particles, that is, the total number of particles divided by the simulation cell volume [33]. The averaging is done over all particles in the system.

In the DEM, Newton’s equations of motion are solved for the translational and rotational movements of all particles in the system. Particles do not deform during collisions but are allowed to overlap slightly instead. This overlap is given in normal direction as follows:

$$\xi_n = (R_i + R_j - |\vec{r}_i - \vec{r}_j|) \hat{e}_n, \tag{3}$$

where $R_i, R_j, \vec{r}_i,$ and \vec{r}_j are the radii and positions of particles i and j , respectively. The unit vector \hat{e}_n is obtained from:

$$\hat{e}_n = \frac{\vec{r}_i - \vec{r}_j}{|\vec{r}_i - \vec{r}_j|}. \tag{4}$$

The contact force \vec{F} between colliding particles is obtained from the Hertz [34] contact law in the normal direction and the model proposed by Mindlin and Deresiewicz [35] in the tangential direction. This contact force can be divided into a normal and a tangential component as:

$$\vec{F} = \vec{F}_n + \vec{F}_t \tag{5}$$

$$\vec{F}_n = (\vec{F} \cdot \hat{e}_n) \hat{e}_n = k_n \xi_n + c_n \dot{\xi}_n \tag{6}$$

$$\vec{F}_t = \vec{F} - \vec{F}_n = k_t \xi_t + c_t \dot{\xi}_t, \tag{7}$$

where k_n and k_t are the normal and tangential elastic terms, respectively, and c_n and c_t are the normal and tangential viscous terms, respectively. The equivalent mass m^* is calculated from the masses of particles i and j , denoted by m_i and m_j , respectively, following the rule below:

$$\frac{1}{m^*} = \frac{1}{m_i} + \frac{1}{m_j} \tag{8}$$

The elastic and viscous terms are given as follows, respectively:

$$k_n = \frac{4}{3} Y^* \sqrt{R^* \xi_n} \tag{9}$$

$$c_n = -\beta \sqrt{5m^* k_n} \geq 0 \tag{10}$$

$$k_t = 8G^* \sqrt{R^* \xi_n} \tag{11}$$

$$c_t = -\beta \sqrt{\frac{10}{3} m^* k_t} \geq 0, \tag{12}$$

where R^* is the equivalent radius calculated analog to Eq. (8). The parameter β is obtained from:

$$\beta = \frac{\ln(e)}{\sqrt{\ln^2(e) + \pi^2}}, \tag{13}$$

where e is the coefficient of restitution; Y^* is the equivalent Young’s modulus obtained from Eq. (14); and G^* is the equivalent shear modulus obtained from Eq. (15).

$$\frac{1}{Y^*} = \frac{1 - v_i^2}{Y_i} + \frac{1 - v_j^2}{Y_j} \quad (14)$$

$$\frac{1}{G^*} = \frac{1 - v_i^2}{G_i} + \frac{1 - v_j^2}{G_j} \quad (15)$$

The coefficient of friction μ_s is defined as the upper limit of the tangential force through the Coulomb criterion:

$$F_t = \mu_s F_n. \quad (16)$$

The tangential damping contribution is only added in time steps without slip (i.e., the Coulomb criterion is not met). Please refer to Di Renzo and Di Maio [36] and Antypov [37] for a more detailed description.

The porosities were calculated using a Monte Carlo integration scheme (see Fig. 1), where 10^7 points were randomly seeded in the region of interest (annular region in this case). Increasing the number of points would have only yielded variations in the fourth decimal. For every generated point, it was checked if that point was inside of any of the spheres confined in the simulation's domain. The solid fraction in the region of interest was obtained from the ratio between the number of points inside spheres to the total number of randomly generated points. Accordingly, the void fraction was calculated as 1 minus the solid fraction. To avoid distortions in the results, the top layer of the particles was leveled according to the height of the lowest annular region. Particles above the aforementioned level were excluded from porosity calculations.

2.2 Simulation procedure

To validate the numerical simulations, the results were compared with the experimental data of Lovregio et al. [30] and Sederman et al. [38], as well as with the correlations of Sonntag [16], Jeschar [17], and De Klerk [39].

The procedure consisted of pouring monodisperse spheres inside a fixed-diameter cylinder and then calculating the bulk porosity. The coefficient of friction for the DEM simulations was initially calibrated until the simulation results matched one experimental point. Subsequently, further experimental and correlation data were simulated using the same coefficient of friction obtained from the calibration.

A cylinder with 22 mm diameter and monodisperse polypropylene spheres with 2.1, 3, 4, 5, and 6 mm diameters were used for the comparison with Lovregio et al. [30]. A cylinder with 45 mm diameter and monodisperse glass spheres of 3.2, 5, 7.5, 11.25, 15, and 22.5 mm diameters were used for the comparison with Sederman et al. [38].

The DEM model validated through Sederman et al. [38] was chosen to simulate the deposition of 3 mm diameter monodisperse spheres in newly defined systems. Additionally, slightly polydisperse particles with sizes ranging from 2.5 to 3.5 mm (3 mm average diameter) were used in further cases. Their size distribution was generated as follows: 10% of the bed mass consisted of particles with 2.5 cm diameter, 20% with 2.75 cm, 40% with 3.0 cm, 20% with 3.25 cm, and 10% with 3.5 cm. Using polydisperse particles allowed to avoid ordered arrangements as opposed to monodisperse ones. Seven systems were simulated:

- Concentric cylinders inserted into the 120 mm-diameter main cylinder: one to seven cylinders were inserted sequentially into the main cylinder, keeping a constant distance between adjacent cylinder walls. Figure 2 (top) depicts the cases with three and six internal cylinders. The walls were defined without thickness here to reduce variables and simplify the comparisons to the base case.
- Same setup as in (a) but using polydisperse particles.
- Same setup as in (b) but using a higher particle–wall coefficient of friction.

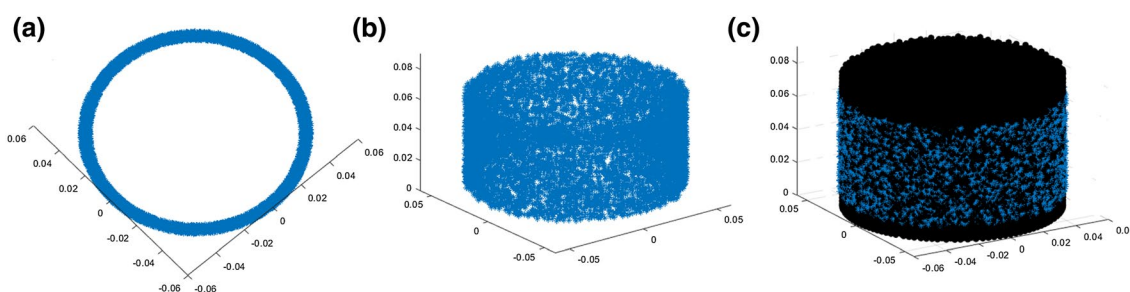


Fig. 1 Schematic of the Monte Carlo scheme implemented to calculate the void fraction. Points are randomly generated in the annular region of interest. **a** Is a top view and **b** is a side view of the generated points. The location of every point is checked against the posi-

tion of all spheres in the simulation, as shown in **c**. The fraction of points inside spheres to the total number of points results in the solid fraction of the region of interest. The void fraction is obtained directly from the calculated solid fraction

- (d) Same setup as in (a) but using 1 mm thick walls. Figure 2 (bottom) depicts the cases with three and six internal cylinders.
- (e) Same setup as in (b) but using 1 mm thick walls.
- (f) Angular walls inserted into the main cylinder: for this system, 4, 8, and 16 walls were used, keeping a constant angular distance between the walls. Polydisperse particles were used.
- (g) Combination of systems (b) and (f): both concentric cylinders and angular walls were inserted into the main cylinder. Polydisperse particles were used. Figure 3 illustrates examples of systems (f) and (g).

The number of particles generated in each simulation varied depending on the particle size distribution, as well as on the number and thickness of the walls. The number of particles ranged from 37,404 to 43,500 in the different systems.

3 Results and discussion

3.1 Numerical validation

The parameter values used in the simulations for validation with the results of Lovregio et al. [30] and Sederman et al. [38] are shown in Table 1. The Poisson's ratio and coefficient of restitution for the comparison with Lovregio et al. [30] were the ones provided in the same study. The coefficient of friction was calibrated as described in the simulation procedure. For the comparison with Sederman et al. [38], the Poisson's ratio and coefficient of restitution were respectively obtained from Gu and Yang [40] and Tang et al. [41].

The walls were made of the same material as the particles, so the values in Table 1 were valid for the walls as well.

The obtained numerical results are compared with the experimental results of Lovregio et al. [30] and the correlations of De Klerk [39], Jeschar [17], and Sonntag [16] at defined D/d ratios in Table 2. A very good agreement is shown among the simulation, experimental, and correlation results for all the evaluated ratios. The largest discrepancy with the experimental results is 3.8%. The expected tendency of the porosity values to grow with decreasing D/d ratios is clear.

Table 3 shows the validation results against the experimental data of Sederman et al. [38]. A very good agreement is found between the simulations and the correlations for almost every investigated D/d ratio, except for the ratio of 3. This is attributed to the spheres forming an ordered arrangement in the simulation, as shown by evaluating its radial distribution function (Fig. 4).

The ordered arrangement formed by the spheres in Fig. 4a is characterized by the well-defined, isolated peaks of the RDF. Such regular arrangements produce denser sphere packings compared to irregular, amorphous ones [42]. As presented by Desmond and Weeks [18], monodisperse systems are susceptible to wall-induced crystallization, which modifies the structure of the granular bed near the walls, and this is confirmed here, justifying the need for further simulations with polydisperse particles. A continuous RDF without isolated peaks is shown for the amorphous structure is shown in Fig. 4b.

Having validated the simulation parameters and results, new systems and variations are introduced as noted in Sect. 2.2.

Fig. 2 Top: simulation setups of system (a) using three and seven inserts. Bottom: setups of system (d) using three and seven inserts

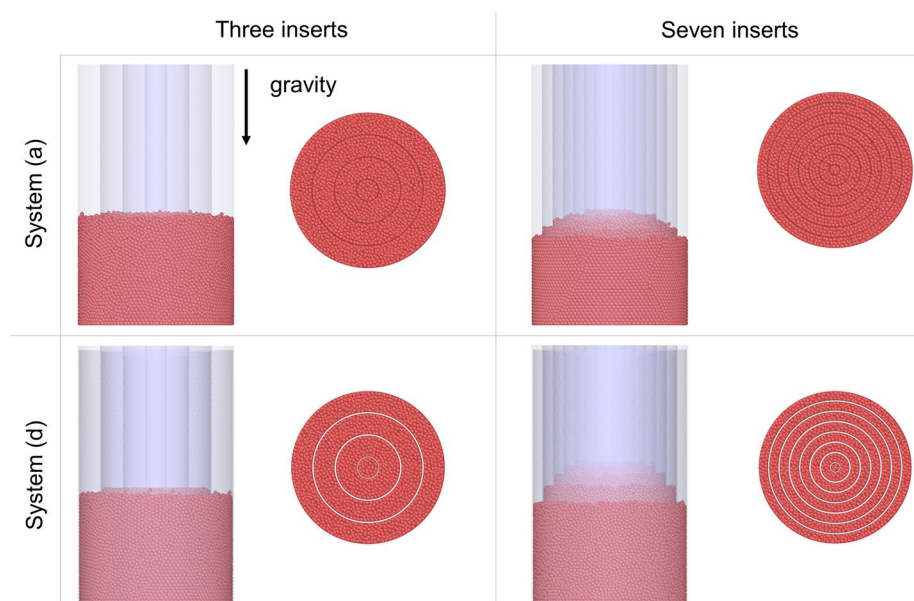


Fig. 3 Simulation setups of system (f) using 16 angular walls (left) and system (g) combining six inner cylinders with 16 angular walls (right)

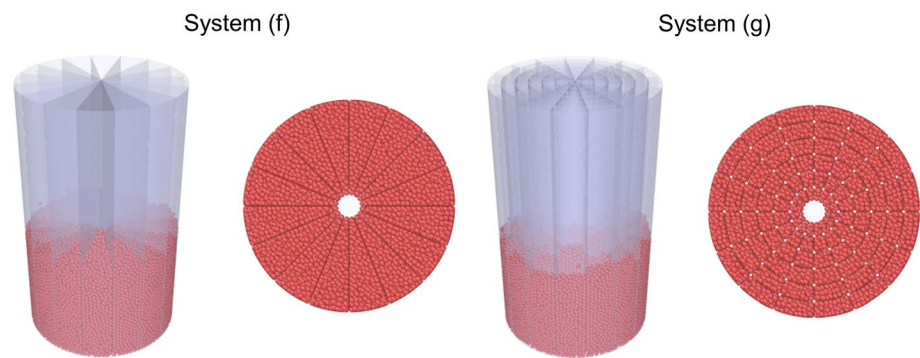


Table 1 Parameter values used in the validations of the numerical simulations

Parameter	Validation with Lovregio et al. [30]	Validation with Sederman et al. [38]
Young's modulus	1×10^8 Pa	1×10^8 Pa
Poisson's ratio	0.42	0.23
Coefficient of friction	0.36	0.19
Coefficient of restitution	0.66	0.93

Table 2 Bulk porosity validation using the experimental data of Lovregio and the correlations of De Klerk, Jeschar, and Sonntag

D/d	10.5	7	5.25	4.2	3.5
Simulation	0.403	0.423	0.443	0.452	0.491
Lovregio (exp.)	–	0.410	0.440	0.470	–
De Klerk ($\epsilon_\infty = 0.391$)	0.397	0.414	0.436	0.459	0.480
Jeschar ($\epsilon_\infty = 0.375$)	0.407	0.424	0.439	0.456	0.472
Sonntag ($\epsilon_\infty = 0.375$)	0.406	0.422	0.437	0.453	0.469

The ϵ_∞ values used for the correlations are also indicated

3.2 Numerical experiments

Systems (a)–(c) are discussed first. Table 4 shows the bulk porosities calculated in the main cylinder without inserts as a reference. The D/d ratio is maximal here and equal to 40.

Table 3 Bulk porosity validation using the experimental data of Sederman and the correlations of De Klerk, Jeschar, and Sonntag

D/d	14	9	6	4	3	2
Simulation	0.384	0.400	0.415	0.432	0.431	0.531
Sederman (exp.)	0.385	0.400	–	–	–	–
De Klerk ($\epsilon_\infty = 0.391$)	0.392	0.401	0.425	0.465	0.500	0.551
Jeschar ($\epsilon_\infty = 0.375$)	0.399	0.413	0.432	0.460	0.488	0.545
Sonntag ($\epsilon_\infty = 0.375$)	0.398	0.412	0.430	0.457	0.485	0.540
Sonntag ($\epsilon_\infty = 0.359$)	0.383	0.396	0.415	0.443	0.471	0.527

The ϵ_∞ values used for the correlations are also indicated

The mean porosity values were obtained from five measurements in different positions of the bed. The control region for porosity calculations was a cylinder with the diameter of the outer cylinder and a height of 30 mm. The respective standard deviations were also calculated. The number of inner cylinders was then incremented to up to seven inserts, where the D'/d ratio was equal to 2.67 in each annulus (D' being the shortest distance between adjacent walls). The insert diameters were previously selected such that all walls would be equidistant.

For system (a) containing monodisperse particles, the bulk porosity does not exhibit a very clear trend. An overall increase with insert number is observed. However, inserting four, five, and seven cylinders caused porosity decrements. This is due to the ordered arrangement of monodisperse particles, which is seen in Fig. 5. The structural arrangements in Fig. 5a, b are in sharp contrast. It is remarked that monodispersity is an idealization.

In opposition, the polydisperse systems (closer to reality) follow a clear trend. As shown in Fig. 5c, d such particles did not form ordered arrangements. The most noticeable porosity increase is by 15.5% (compared to the reference) from five to six inserts. These results do not correspond with the correlations for cylindrically packed beds, which predict porosity increases of over 20% for a D/d of 4 and over 30% for a D/d of 3. Nevertheless, a direct transference cannot be made here because additional effects appear in these systems due to the internal

Fig. 4 Radial distribution function calculated for the D/d ratios **a** 3 and **b** 6

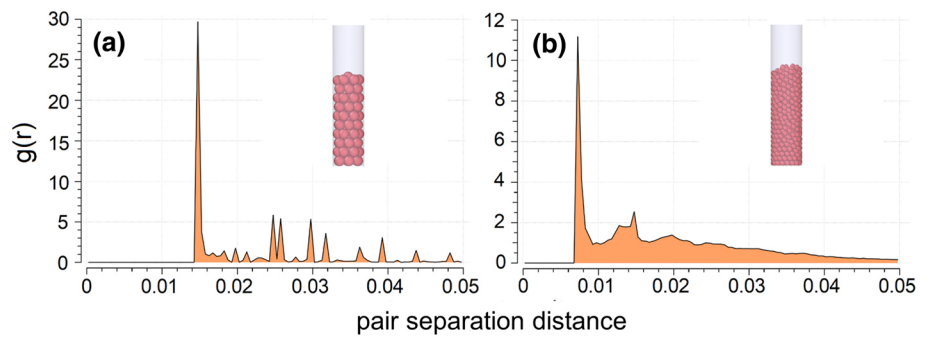


Table 4 ϵ_b Values for different numbers of volume-less cylindrical inserts

Insert number	D/d	ϵ_b (a)	ϵ_b (b)	ϵ_b (c)
0	40	0.367 ± 0.008	0.367 ± 0.007	0.367 ± 0.007
1	13.33	0.372 ± 0.004	0.371 ± 0.003	0.372 ± 0.002
2	8	0.380 ± 0.002	0.379 ± 0.001	0.381 ± 0.001
3	5.71	0.391 ± 0.004	0.389 ± 0.001	0.390 ± 0.000
4	4.44	0.380 ± 0.002	0.395 ± 0.001	0.398 ± 0.001
5	3.64	0.376 ± 0.002	0.403 ± 0.001	0.406 ± 0.000
6	3.08	0.428 ± 0.001	0.423 ± 0.001	0.425 ± 0.001
7	2.67	0.409 ± 0.009	0.422 ± 0.003	0.425 ± 0.001

walls (it is not a reduction but a division). To the best of the authors' knowledge, these correlations have not yet been investigated. However, they show potential considering that merely the right number of inserts can cause the observed effects, which would considerably increase a packed bed's permeability.

Table 4 also shows that a seventh insert did not affect the bulk porosities. Effects similar to the one for the mono-disperse case may have taken place. However, ordered arrangements could not be identified (see Fig. 5d).

When the friction between particles and walls was increased from 0.19 to 0.9 [system (c)], there were no changes in bulk porosity in comparison with system (b). This indicates that the frictional forces at the walls are dissipated in the granular material, probably due to the large granular arrangement in the azimuthal direction between the cylinders. Therefore, very specific wall material properties would not be necessary to obtain such porosity

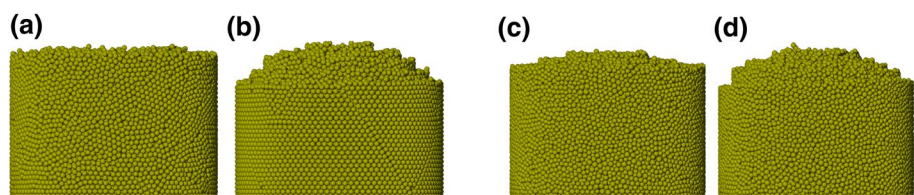
increases in a rigid granular bed. Nevertheless, this would likely play a role in a highly compressible one, as seen in Bandelt Riess et al. [5].

Systems (d) and (e) evaluate the insertion of cylinders with 1 mm thickness and the results are shown in Table 5. Note that the D/d ratios are different from those in the previous cases. The porosities of system (d) follow a clearer trend than that of system (a), and porosity was greatly increased by 26% with the seventh insert. System (e) exhibits a very similar trend, and the obtained values are comparable to those of system (b). This would mean that the porosity increases are mainly a function of D/d with wall thickness becoming a rather secondary variable. Both systems (d) and (e) show noticeable deviations from the observed tendencies when using six inserts, which can again be attributed to ordered arrangements.

The results of systems (b) and (e) were modeled by fitting an equation in the form of the correlation of De Klerk [39] for the region of interest. Figure 6 depicts the fitted curve and the equation parameters. D/d values up to 8 were used to fit the curve since larger values caused only small porosity increments. Results altered by ordered arrangements were not considered for the fitting. The coefficient of determination (R^2) for the fitted curve is 0.97.

Note that only bulk porosities of entire systems have been discussed so far. Despite all adjacent cylinder walls being equidistant, the porosity is mostly increased in the central cylinder. This is due to the differences in geometry and wall distribution between the inner cylindrical region and outer annular regions. Figure 7 shows the porosity values inside each annulus for system (b) using different numbers of inserts. The porosity in the innermost region, which is purely cylindrical, follows the correlations of De Klerk or

Fig. 5 Monodisperse particles with **a** three and **b** seven inserts. Polydisperse particles with **c** three and **d** seven inserts



Jeschar. This result is thus attributed to a higher amount of particle–wall contact points and points towards equipment designs maximizing it. However, the annular regions of the system exhibit a lower porosity than predicted, which behaves as a constant. In a separation process, this could ensure a homogeneous porosity distribution in the filter cake and become a great advantage.

The porosity results are also analyzed as a function of distance from the outer cylinder wall. The obtained values display the classical sinusoidal behavior in all cases. Near the walls, the particles inefficiently pack into layers (particle density heterogeneity) and cause the observed porosity oscillations and packing behavior changes [18]. The peak porosity values (nearly 1) mark the particle–wall contact region where the inner cylinders were inserted, thereby contributing positively to the bulk porosity. In the reference case, the layering influence covers about two particle diameters and decays into the bulk for ten diameters. Figure 8 shows the results for the reference, three, and six inner cylinders.

Angular walls were inserted to change the bulk porosity in system (f). In addition to angular walls, three and six inner cylinders were again inserted into system (g). Table 6 presents the obtained results. For some geometries, the innermost region had to be removed from the calculations because they became too small for the spheres to enter. Nevertheless, the bulk porosities increase remarkably compared to system (b). This happens not only for a constant number of cylinders and a growing angular wall number but also for a constant angular wall number and a growing cylinder number. That is, the more walls there are, the greater is the effect, leading to up to a 26% porosity increase, which would cause a corresponding permeability enhancement. Figure 9 illustrates the porosity profile of system (f).

The sinusoidal profile is well captured near the wall (at $D/d = 40$) and similar for all studied cases. At this point, the angular walls are furthest away from each other and do not affect the porosity significantly. In contrast, their wall effects become clear near the center region of the system. In particular, for the 8 and 16 inserts, the porosity is increased

Table 5 ϵ_b Values for different numbers of 1 mm thick cylindrical inserts

Insert number	D'/d	ϵ_b (d)	ϵ_b (e)
0	39.33	0.368 ± 0.009	0.368 ± 0.008
1	13	0.373 ± 0.005	0.372 ± 0.002
2	7.67	0.381 ± 0.002	0.381 ± 0.001
3	5.38	0.386 ± 0.002	0.390 ± 0.000
4	4.11	0.406 ± 0.000	0.402 ± 0.000
5	3.30	0.419 ± 0.000	0.415 ± 0.001
6	2.74	0.380 ± 0.003	0.415 ± 0.001
7	2.33	0.464 ± 0.000	0.454 ± 0.001

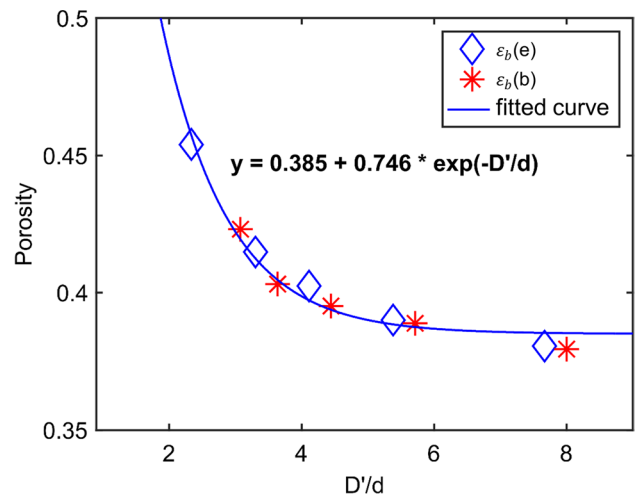


Fig. 6 Equation fitted to the numerical bulk porosity results of systems (b) and (e)

to 1 before reaching the middle, revealing the region where the spheres do not fit anymore.

Figures 10 and 11 show the obtained porosity profiles for system (g), which contained three and six inner cylinders in addition to the 4, 8, and 16 angular walls, respectively. The sinusoidal profile is again well captured near the wall and similar for all studied cases, regardless of the cylinder number. Another property of these cases is the symmetrical evolution of the porosity value between the walls. The porosity again increases to 1 near the center because no particles could be deposited in that region. The interference of the angular walls is noticeable upon reaching that point, further increasing the overall porosity (Table 6).

Considering the presented cases, it becomes clearer how particles interact with different packed wall configurations, increasing bed porosity and therefore permeability as well.

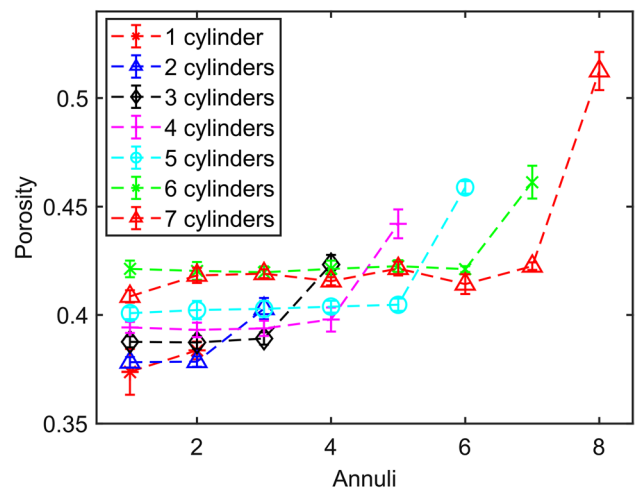


Fig. 7 Porosity calculated in the different annuli of system (b)

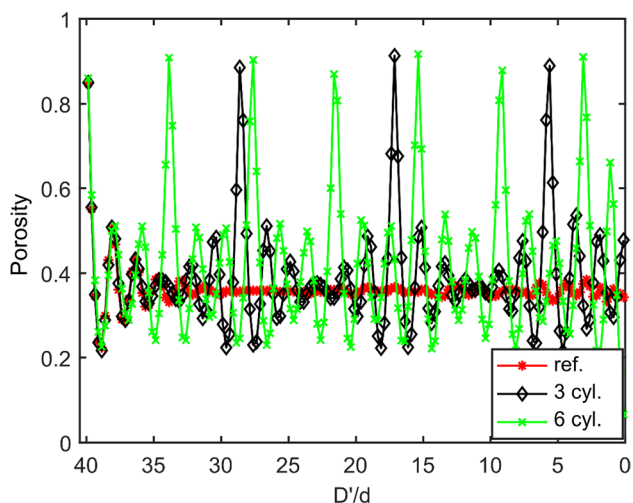


Fig. 8 Porosity of system (b) as a function of distance from the outer wall for the reference and with three and six inner cylinders

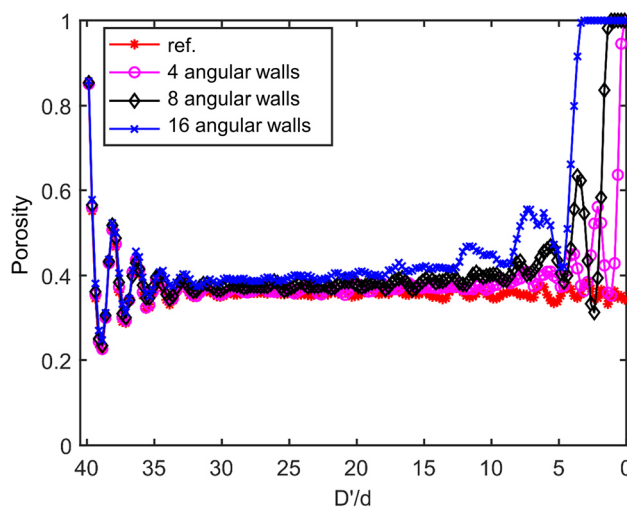


Fig. 9 Porosity of system (f) as a function of the distance from the outer wall for the insertion of 0, 4, 8, and 16 angular walls

This would contribute to the flow velocity in a solid–liquid separation through a structured packing and explain part of the effects observed by Bandelt Riess et al. [22]. Moreover, the obtained behaviors and profiles can be used to explore further systems and additional effects.

4 Conclusions and outlook

This investigation demonstrated how using different packed wall configurations affects the porosity of a granular bed. The DEM simulations were set up and validated with literature data. Ordered arrangements were observed in the monodisperse systems (as was expected, considering the literature), which cannot be predicted with the correlations of Sonntag [16], Jeschar [17], and De Klerk [39] (Table 3).

Adding inner concentric cylinders, angular inserts, or a combination of both generally increased the bulk porosity due to the wall effects. They favorably reproduced the known sinusoidal porosity profile, which is commonly observed only in the near-wall region of the outer cylinder. Since the comparison to usual porosity correlations for granular beds confined in cylindrical containers was limited by the newly evaluated geometries, a new specific correlation was defined.

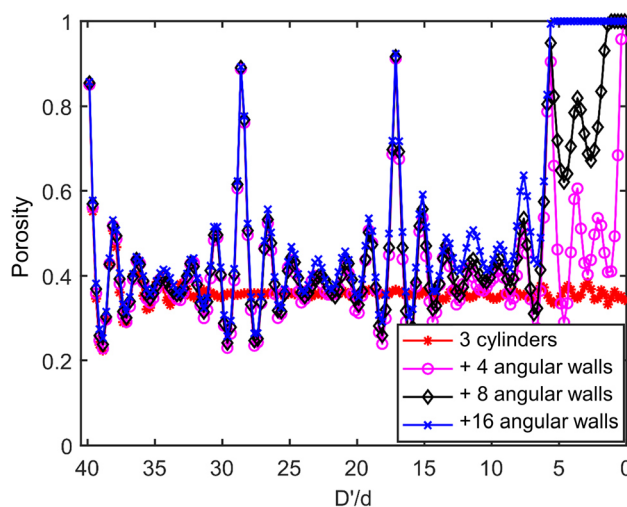


Fig. 10 Porosity of system (g) as a function of the distance from the outer wall for the insertion of 3 cylinders and 0, 4, 8, and 16 angular walls

A distance between adjacent walls was found at six cylindrical inserts for system (b), which caused a significant porosity enhancement. This elucidates the geometric interactions needed to improve throughput in a filter cake.

Table 6 ϵ_b Values for the systems containing 0, 4, 8, and 16 angular walls combined with 0, 3, and 6 cylindrical inserts

Cylinder no	0 ($D'/d = 40$)				3 ($D'/d = 5.71$)				6 ($D'/d = 3.08$)			
	0	4	8	16	0	4	8	16	0	4	8	16
ϵ_b	0.367	0.378	0.389	0.410	0.389	0.400	0.413	0.429	0.423	0.435	0.444	0.462
Std. Dev	0.007	0.008	0.007	0.008	0.001	0.008	0.007	0.007	0.001	0.007	0.007	0.007

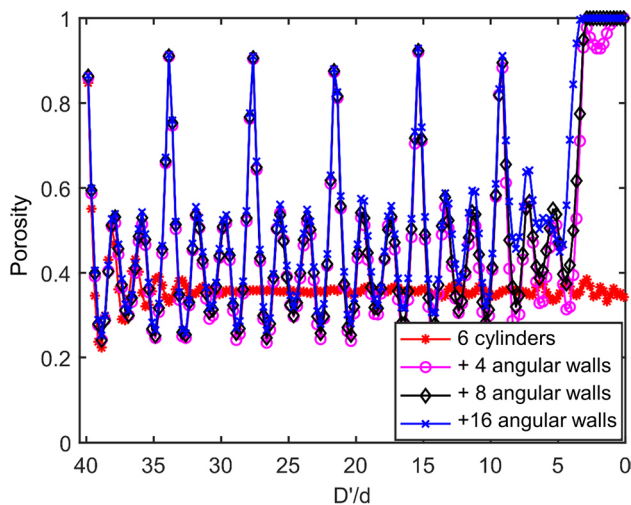


Fig. 11 Porosity of system (g) as a function of the distance from the outer wall for the insertion of 6 cylinders and 0, 4, 8, and 16 angular walls

Furthermore, a homogeneous porosity distribution was observed in the annular spaces of this system, showing potential for applications demanding porosity control, such as the freeze-drying of bulky solids [43] and heat transfer in a fixed-bed reactor [44].

Additionally, variations of the coefficient of friction and insert thickness were considered but did not show significant effects. Future work should involve applying the variations to highly compressible particles. Other studies could assume the task of rigorously optimizing insert number and placement for a given system and experimentally validating the predictions. Additional control variables of interest could be the pressure at the walls and the contact forces between particles.

Using angular walls [system (f)] had a mild effect on the granular bed. However, in combination with the inner cylinders [system (g)], the increase in the bulk porosity was remarkable (up to 26%), which could lead to significant improvements in solid–liquid separation processes. In these cases, the increasing size of the center region, where no particle can be inserted, must be considered.

System (g) can be roughly compared to the structures of a Raflux or Pall ring, which have already been experimentally tested [5, 22]. Future investigations should benefit from this research to find further numerical and practical correlations.

Authors' contributions Conceptualization: all authors; Data curation: Schiochet Nasato; Formal analysis: Bandelt Riess, Schiochet Nasato; Funding acquisition: Briesen; Investigation: Bandelt Riess, Schiochet Nasato; Methodology: Bandelt Riess, Schiochet Nasato; Project administration: all authors; Resources: Briesen; Software: Schiochet Nasato; Supervision: Briesen; Validation: Schiochet Nasato; Visualization:

Bandelt Riess, Schiochet Nasato; Writing—original draft: Bandelt Riess, Schiochet Nasato; Writing—review & editing: all authors.

Funding Open Access funding enabled and organized by Projekt DEAL. This work was supported by the Research Association of the German Food Industry (FEI) via AiF (19359 N) within the program for promoting the Industrial Collective Research (IGF) of the German Ministry of Economic Affairs and Energy (BMWi).

Availability of data and material The datasets generated and analysed during the current study are available from the corresponding author on reasonable request.

Declarations

Conflicts of interest The authors have no relevant financial or non-financial interests to disclose.

Open Access This article is licensed under a Creative Commons Attribution 4.0 International License, which permits use, sharing, adaptation, distribution and reproduction in any medium or format, as long as you give appropriate credit to the original author(s) and the source, provide a link to the Creative Commons licence, and indicate if changes were made. The images or other third party material in this article are included in the article's Creative Commons licence, unless indicated otherwise in a credit line to the material. If material is not included in the article's Creative Commons licence and your intended use is not permitted by statutory regulation or exceeds the permitted use, you will need to obtain permission directly from the copyright holder. To view a copy of this licence, visit <http://creativecommons.org/licenses/by/4.0/>.

References

1. Anlauf H (2020) Wet cake filtration. Fundamentals, equipment, strategies. WILEY VCH, Weinheim (2020)
2. Tiller, F.M., Haynes, S., Lu, W.-M.: The role of porosity in filtration VII effect of side-wall friction in compression-permeability cells. *AIChE J.* (1972). <https://doi.org/10.1002/aic.690180104>
3. Tiller, F.M., Green, T.C.: Role of porosity in filtration IX skin effect with highly compressible materials. *AIChE J.* (1973). <https://doi.org/10.1002/aic.690190633>
4. Tiller, F.M., Kwon, J.H.: Role of porosity in filtration: XIII. Behavior of highly compactible cakes. *AIChE J.* (1998). <https://doi.org/10.1002/aic.690441005>
5. Bandelt Riess, P.M., Kuhn, M., Först, P., Briesen, H.: Investigating the effect of packed structures on filter cake compressibility. *Chem. Eng. Technol.* (2021). <https://doi.org/10.1002/ceat.20200451>
6. Maćkowiak, J.: *Fluidynamik von Füllkörpern und Packungen*. Springer, Berlin (2003)
7. Fee, C., Nawada, S., Dimartino, S.: 3D printed porous media columns with fine control of column packing morphology. *J. Chromatogr. A* (2014). <https://doi.org/10.1016/j.chroma.2014.01.043>
8. Nawada, S., Dimartino, S., Fee, C.: Dispersion behavior of 3D-printed columns with homogeneous microstructures comprising differing element shapes. *Chem. Eng. Sci.* (2017). <https://doi.org/10.1016/j.ces.2017.02.012>
9. Neukäufer, J., Hanusch, F., Kutscherauer, M., Rehfeldt, S., Klein, H., Grützner, T.: Methodik zur Entwicklung additiv gefertigter Packungsstrukturen im Bereich der thermischen Trenntechnik. *Chem. Ing. Tech.* (2019). <https://doi.org/10.1002/cite.201800171>

10. Marek, M., Niegodajew, P.: A new experimental approach to examination of orientation distribution of cylindrical particles in random packed beds. *Powder Technol.* (2020). <https://doi.org/10.1016/j.powtec.2019.10.077>
11. Cohen, Y., Metzner, A.B.: Wall effects in laminar flow of fluids through packed beds. *AIChE J.* (1981). <https://doi.org/10.1002/aic.690270502>
12. Bey, O., Eigenberger, G.: Fluid flow through catalyst filled tubes. *Chem. Eng. Sci.* (1997). [https://doi.org/10.1016/S0009-2509\(96\)00509-X](https://doi.org/10.1016/S0009-2509(96)00509-X)
13. Wang, Z., Afacan, A., Nandakumar, K., Chuang, K.T.: Porosity distribution in random packed columns by gamma ray tomography. *Chem. Eng. Process. Process Intensif.* (2001). [https://doi.org/10.1016/S0255-2701\(00\)00108-2](https://doi.org/10.1016/S0255-2701(00)00108-2)
14. Di Felice, R., Gibilaro, L.G.: Wall effects for the pressure drop in fixed beds. *Chem. Eng. Sci.* (2004). <https://doi.org/10.1016/j.ces.2004.03.030>
15. Allen, K.G., von Backström, T.W., Kröger, D.G.: Packed bed pressure drop dependence on particle shape, size distribution, packing arrangement and roughness. *Powder Technol.* (2013). <https://doi.org/10.1016/j.powtec.2013.06.022>
16. Sonntag, G.: Einfluß des Lückenvolumens auf den Druckverlust in gasdurchströmten Füllkörpersäulen. *Chem. Ing. Tech.* (1960). <https://doi.org/10.1002/cite.330320502>
17. Jeschar, R.: Druckverlust in Mehrkornschüttungen aus Kugeln. *Arch. Eisenhüttenwes.* (1964). <https://doi.org/10.1002/srin.196402300>
18. Desmond, K.W., Weeks, E.R.: Random close packing of disks and spheres in confined geometries. *Phys. Rev. E Stat. Nonlinear Soft Matter Phys.* (2009). <https://doi.org/10.1103/PhysRevE.80.051305>
19. Mueller, G.E.: A modified packed bed radial porosity correlation. *Powder Technol.* (2019). <https://doi.org/10.1016/j.powtec.2018.10.030>
20. Lan, T., Gerontas, S., Smith, G.R., Langdon, J., Ward, J.M., Titchener-Hooker, N.J.: Investigating the use of column inserts to achieve better chromatographic bed support. *Biotechnol. Progr.* (2012). <https://doi.org/10.1002/btpr.1597>
21. Lan, T.: An experimental and simulation study of the influence made by inserts on chromatographic packed bed hydrodynamics. Doctoral dissertation, London (2013)
22. Bandelt Riess, P.M., Engstle, J., Kuhn, M., Briesen, H., Först, P.: Decreasing filter cake resistance by using packing structures. *Chem. Eng. Technol.* (2018). <https://doi.org/10.1002/ceat.201800254>
23. Cundall, P.A., Strack, O.D.L.: A discrete numerical model for granular assemblies. *Géotechnique* (1979). <https://doi.org/10.1680/geot.1979.29.1.47>
24. Wu, Y., An, X., Yu, A.B.: DEM simulation of cubical particle packing under mechanical vibration. *Powder Technol.* (2017). <https://doi.org/10.1016/j.powtec.2016.09.029>
25. Reboul, N., Vincens, E., Cambou, B.: A statistical analysis of void size distribution in a simulated narrowly graded packing of spheres. *Granul. Matter* (2008). <https://doi.org/10.1007/s10035-008-0111-5>
26. Dong, K.J., Zou, R.P., Yang, R.Y., Yu, A.B., Roach, G.: DEM simulation of cake formation in sedimentation and filtration. *Miner. Eng.* (2009). <https://doi.org/10.1016/j.mineng.2009.03.018>
27. Zhang, S., McCarthy, J.J.: Modeling of the pressure drop across polydisperse packed beds in cake filtration. *AIChE J.* (2019). <https://doi.org/10.1002/aic.16557>
28. Bear, J.: Modeling phenomena of flow and transport in porous media. Theory and applications of transport in porous media, vol. 31. Springer, Cham (2018)
29. McCarthy, J.J., Jasti, V., Marinack, M., Higgs, C.F.: Quantitative validation of the discrete element method using an annular shear cell. *Powder Technol.* (2010). <https://doi.org/10.1016/j.powtec.2010.04.011>
30. Lovreglio, P., Das, S., Buist, K.A., Peters, E.A.J.F., Pel, L., Kuipers, J.A.M.: Experimental and numerical investigation of structure and hydrodynamics in packed beds of spherical particles. *AIChE J.* (2018). <https://doi.org/10.1002/aic.16127>
31. Gerontas, S., Lan, T., Micheletti, M., Titchener-Hooker, N.J.: Evaluation of a structural mechanics model to predict the effect of inserts in the bed support of chromatographic columns. *Chem. Eng. Sci.* (2015). <https://doi.org/10.1016/j.ces.2015.02.010>
32. Parafiniuk, P., Molenda, M., Horabik, J.: Influence of particle shape and sample width on uniaxial compression of assembly of prolate spheroids examined by discrete element method. *Phys. A Stat. Mech. Appl.* (2014). <https://doi.org/10.1016/j.physa.2014.08.063>
33. Stukowski, A.: Visualization and analysis of atomistic simulation data with OVITO—the Open Visualization Tool. *Model. Simul. Mater. Sci. Eng.* (2010). <https://doi.org/10.1088/0965-0393/18/1/015012>
34. Hertz, H.: Über die Berührung fester elastischer Körper. *J. Reine. Angew. Math.* **92**, 156–171 (1881)
35. Mindlin, R.D., Deresiewicz, H.: Elastic spheres in contact under varying oblique force. *Trans. ASME J. Appl. Mech.* **20**, 327–344 (1953)
36. Di Renzo, A., Di Maio, F.P.: Comparison of contact-force models for the simulation of collisions in DEM-based granular flow codes. *Chem. Eng. Sci.* (2004). <https://doi.org/10.1016/j.ces.2003.09.037>
37. Antypov, D., Elliott, J.A.: On an analytical solution for the damped Hertzian spring. *EPL* (2011). <https://doi.org/10.1209/0295-5075/94/50004>
38. Sederman, A.J., Alexander, P., Gladden, L.F.: Structure of packed beds probed by magnetic resonance imaging. *Powder Technol.* (2001). [https://doi.org/10.1016/S0032-5910\(00\)00374-0](https://doi.org/10.1016/S0032-5910(00)00374-0)
39. de Klerk, A.: Voidage variation in packed beds at small column to particle diameter ratio. *AIChE J.* (2003). <https://doi.org/10.1002/aic.690490812>
40. Gu, X.Q., Yang, J.: A discrete element analysis of elastic properties of granular materials. *Granul. Matter* (2013). <https://doi.org/10.1007/s10035-013-0390-3>
41. Tang, H., Song, R., Dong, Y., Song, X.: Measurement of restitution and friction coefficients for granular particles and discrete element simulation for the tests of glass beads. *Materials* (Basel, Switzerland) (2019). <https://doi.org/10.3390/ma12193170>
42. Hales, T.C.: Historical overview of the Kepler conjecture. *Discret. Comput. Geom.* (2006). <https://doi.org/10.1007/s00454-005-1210-2>
43. Foerst, P., Gruber, S., Schulz, M., Vorhauer, N., Tsotsas, E.: Characterization of Lyophilization of Frozen Bulky solids. *Chem. Eng. Technol.* (2020). <https://doi.org/10.1002/ceat.201900500>
44. Eppinger, T., Jurtz, N., Kraume, M.: Influence of macroscopic wall structures on the fluid flow and heat transfer in fixed bed reactors with small tube to particle diameter ratio. *Processes* (2021). <https://doi.org/10.3390/pr9040689>

Publisher's Note Springer Nature remains neutral with regard to jurisdictional claims in published maps and institutional affiliations.

Chapter 5: General Conclusions and Future Work

This last chapter wraps up the discoveries made throughout the presented investigations and proposes how the development of this process strategy could be taken even further.

On paper, it makes perfect sense to take advantage of more wall support in a vessel to optimize the pressure drop of a liquid flowing through a compressible porous medium. Aimed micromanipulations thereof should stabilize the solid network where it is most needed. However, those theories had not yet been systematically turned to practice before this thesis. Since so many industrial applications benefit from cake filtration processes, this was the chosen context to put the new optimization strategy to the test. To simplify the first approach, the macroscopic method of using standard packed bed components was selected, transferring a concept from one of the fundamental unit operations in chemical engineering to another one. Thus, the thesis goal of observing and understanding the interplays between the chosen systems was established and divided into three hypotheses, which were correspondingly addressed in three research papers.

Initially, it was postulated that, since packed beds are so beneficial for thermal separation processes, they could also pose advantages for mechanical ones, especially cake filtration, by reducing flow resistance. Even though the whole theoretical base exhibited above was already behind the claim, the main objective of Paper I was merely to observe and record the appearing effects. The investigation was based on permeability changes caused by determined packings when filtering three different model systems. The used packings indeed had a remarkable effect on the separation, decreasing flow resistance and considerably accelerating the whole process without losing filtrate quality. This was a hint at the packings effectively increasing filter cake porosity and counteracting compression. Nevertheless, this only applied to the system with the highest compressibility and biggest particles; the packing's benefits were not omnipresent. Using the packings for the separations of the other two systems, which were approximately incompressible, caused the opposing effect, increasing flow resistance and process duration. This correlation between cake compressibility and packing support was not considered in detail during the first investigation but was the main motivator of the second one.

Under the premise that using the walls of packings to provide more structural support counteracts the compression of a solid network, Paper II aimed to find correlations between the key process parameters operating pressure, filter cake compression factor, and packing type. To prove this, the same previously studied systems and combinations were analyzed in further developed filtration and compression experiments to directly quantify the observed effects using the compressive yield stress. The compressibility results obtained through the new method were validated by showing good agreement with the predictions of the standardized method. As expected, the additional packing support did significantly increase the compression resistance of all systems. Moreover, the greater the applied pressure or the material compressibility, the more pronounced was the effect. However, considering these first two investigations, it became evident that reducing compressibility did not necessarily mean improving overall permeability as well. Most likely, the compression-counteracting effect of the packings was indeed present during the first filtrations, but their porosity-enhancing effect was

not. This was attributed to the dimensions of packings and solids not being compatible for exhibiting the expected behavior. Consequently, the need of performing case studies to find the sweet spot between particle size distribution and wall support amount arose, becoming the objective of Paper III.

The third and final hypothesis formulated that, if appropriately manipulated, the wall support inside a vessel will greatly increase the bulk porosity of the contained particulate network. To be able to test several different wall arrangements and closely study their effects, the method of using discrete element method simulations to generate cylindrical beds of monodisperse spheres was chosen. This also allowed to better understand the particle–particle and particle–wall interactions due to the set parameters derived from mechanical laws, which were validated with well-known literature data. Thus, the investigation showed how the granular bed porosity evolved when progressively adding more wall support in the form of concentric cylinders, angular inserts, and combinations thereof. The general effect was a bulk porosity rise with each additional wall, making the most intricate geometry the most effective one. It was also shown that the greatest changes appear when a specific dimensional ratio is reached, which was probably not the case in Paper I, causing the observed negative effects. Nonetheless, the combined discoveries of the three research articles make clear that this process strategy is one with considerable application potential due to its simplicity and versatility and should therefore be explored further.

As mentioned before, the investigations helped to corroborate the hypotheses and answered some questions but also originated other follow-up ones. Many of them concern the future applicability of the strategy in industrially scaled processes. What happens with the packing during and after its use? However, it should not be long until that goal is achieved. As a matter of fact, the first systematic studies regarding the development of a support structure to enhance the wort lautering process in the beer industry have already been performed, yielding very promising results (Bandelt Riess et al. 2019). This should be one case of many since the ultimate objective of this research would be to eventually enable the manufacture of tailored packings which have been adapted to a specific system, making its mechanical separation much more efficient.

To achieve this, many more scenarios would have to be tested and understood; the interactions between further materials and packings with different properties should be studied. This thesis showed that the technology to design, manipulate, and manufacture porous media is already available. Even a functionalization of the packed bed components, analog to the smart gating membranes, is thinkable. Hence, this research has begun to fill the needed know-how gap to take advantage of the discussed effects and techniques and transfer them to various cake filtration processes. However, there is still much to be done as the strategy has to be validated with each system of interest.

Regarding the presented methodology, the available equipment could be enhanced with further automation and additional sensors. For instance, in situ measurements of localized liquid pressure and porosity inside the filter cake during the process would help to detect transient structural network changes and packing effects, accelerating the gathering of more crucial data. The conceptual work to achieve this has already been started. Besides validating the previously performed DEM simulations with real-life experiments, further case studies should assume the task of systematically optimizing the amount and form of wall support in a vessel for any given granular system. Some observed geometric effects still need to be cleared. Moreover, additional physical parameters of interest, such as the pressure at the walls and the contact forces between particles, could be analyzed.

Future investigation projects should benefit from this research and carry on with the topic to find further practical and numerical correlations between packed beds and mechanical separations. After that, the purposeful design of support structures for the optimization of many applications should become a reality. Only then will the potential of this process strategy be completely... unpacked.

References

- Allen, K. G.; Backström, T. W. von; Kröger, D. G. (2013): Packed bed pressure drop dependence on particle shape, size distribution, packing arrangement and roughness. In *Powder Technology* 246, pp. 590–600. DOI: 10.1016/j.powtec.2013.06.022.
- Alles, C. M. (2000): Prozeßstrategien für die Filtration mit kompressiblen Kuchen. Doctoral dissertation. Karlsruhe.
- Alles, C. M.; Anlauf, H. (2003): Filtration mit kompressiblen Kuchen: Effiziente Konzepte für eine anspruchsvolle Trennaufgabe. In *Chemie Ingenieur Technik* 75 (9), pp. 1221–1230. DOI: 10.1002/cite.200303268.
- Al-Shimmery, A.; Mazinani, S.; Ji, J.; Chew, Y. M. J.; Mattia, D. (2019): 3D printed composite membranes with enhanced anti-fouling behaviour. In *Journal of Membrane Science* 574, pp. 76–85. DOI: 10.1016/j.memsci.2018.12.058.
- Anlauf, H. (1994): Standardfiltertests zur Bestimmung des Kuchen- und Filtermediumwiderstandes bei der Feststoffabtrennung aus Suspensionen. In *Chemie Ingenieur Technik* 66 (8), pp. 1069–1071. DOI: 10.1002/cite.330660812.
- Anlauf, H. (2020): Wet Cake Filtration. Fundamentals, equipment, strategies. Weinheim: WILEY VCH.
- Bandelt Riess, P. M.; Engstle, J.; Först, P. (2018a): Characterizing the Filtration Behavior of Hop Particles for Efficient Dry Hopping Methods. In *BrewingScience* 71 (9/10), pp. 74–80.
- Bandelt Riess, P. M.; Kuhn, M.; Briesen, H.; Först, P. (2018b): Increasing Wort Flow by Flocculation of Fine Particle Fractions. In *BrewingScience* 71 (7/8), pp. 68–72.
- Bandelt Riess, P. M.; Kuhn, M.; Briesen, H.; Först, P. (2019): Evaluation of Process Strategies to Homogenize the Lautering Filter Cake Structure and Enhance Wort Production. In Filtech Exhibitions Germany GmbH & Co. KG (Ed.): FILTECH 2019 - Proceedings. International Conference & Exhibition for Filtration and Separation Technology. FILTECH. Köln, October 22-24. 700th ed. Meerbusch.
- Bear, J. (2018): Modeling Phenomena of Flow and Transport in Porous Media. Cham: Springer International Publishing (Theory and Applications of Transport in Porous Media, 31). Available online at <http://dx.doi.org/10.1007/978-3-319-72826-1>.
- Bellmann, C. (2003): Stabilität von Dispersionen. In *Chemie Ingenieur Technik* 75 (6), pp. 662–668. DOI: 10.1002/cite.200390127.
- Bey, O.; Eigenberger, G. (1997): Fluid flow through catalyst filled tubes. In *Chemical Engineering Science* 52 (8), pp. 1365–1376. DOI: 10.1016/S0009-2509(96)00509-X.
- Borea, L.; Naddeo, V.; Shalaby, M. S.; Zarra, T.; Belgiorno, V.; Abdalla, H.; Shaban, A. M. (2018): Wastewater treatment by membrane ultrafiltration enhanced with ultrasound: Effect of membrane flux and ultrasonic frequency. In *Ultrasonics* 83, pp. 42–47. DOI: 10.1016/j.ultras.2017.06.013.
- Bosma, R.; van Spronsen, W. A.; Tramper, J.; Wijffels, R. H. (2003): Ultrasound, a new separation technique to harvest microalgae. In *Journal of Applied Phycology* 15 (2/3), pp. 143–153. DOI: 10.1023/A:1023807011027.

- Bourcier, D.; Féraud, J. P.; Colson, D.; Mandrick, K.; Ode, D.; Brackx, E.; Puel, F. (2016): Influence of particle size and shape properties on cake resistance and compressibility during pressure filtration. In *Chemical Engineering Science* 144, pp. 176–187. DOI: 10.1016/j.ces.2016.01.023.
- Buscall, R.; White, L. R. (1987): The consolidation of concentrated suspensions. Part 1. — The theory of sedimentation. In *J. Chem. Soc., Faraday Trans. 1* 83 (3), p. 873. DOI: 10.1039/F19878300873.
- Chen, W. (2006): Analyses of Compressible Suspensions for an Effective Filtration and Deliquoring. In *Drying Technology* 24 (10), pp. 1251–1256. DOI: 10.1080/07373930600840401.
- Cohen, Y.; Metzner, A. B. (1981): Wall effects in laminar flow of fluids through packed beds. In *AIChE J.* 27 (5), pp. 705–715. DOI: 10.1002/aic.690270502.
- Darcy, H. P. G. (1856): Les Fontaines publiques de la ville de Dijon. Exposition et application des principes à suivre et des formules à employer dans les questions de distribution d'eau, etc. V. Dalamont.
- David Suits, L.; Sheahan, T. C.; Stickland, A. D.; Scales, P. J.; Styles, J. R. (2005): Comparison of Geotechnical Engineering Consolidation and Physical Science Filtration Testing Techniques for Soils and Suspensions. In *Geotech. Test. J.* 28 (6), p. 11887. DOI: 10.1520/GTJ11887.
- Di Felice, R.; Gibilaro, L. G. (2004): Wall effects for the pressure drop in fixed beds. In *Chemical Engineering Science* 59 (14), pp. 3037–3040. DOI: 10.1016/j.ces.2004.03.030.
- Draws, A.; Prieske, H.; Meyer, E.-L.; Senger, G.; Kraume, M. (2010): Advantageous and detrimental effects of air sparging in membrane filtration: Bubble movement, exerted shear and particle classification. In *Desalination* 250 (3), pp. 1083–1086. DOI: 10.1016/j.desal.2009.09.113.
- Eichholz, C.; Stolarski, M.; Fuchs, B.; Nirschl, H. (2007): Magnetfeldüberlagerte Pressfiltration. In *Chemie Ingenieur Technik* 79 (4), pp. 416–420. DOI: 10.1002/cite.200600134.
- Eichholz, C.; Stolarski, M.; Goertz, V.; Nirschl, H. (2008): Magnetic field enhanced cake filtration of superparamagnetic PVAc-particles. In *Chemical Engineering Science* 63 (12), pp. 3193–3200. DOI: 10.1016/j.ces.2008.03.034.
- Engstle, J.; Briesen, H.; Först, P. (2017): Mash Separation in the Lauter Tun - a Particle Size Dependent Separation Process. In *BrewingScience* 70 (1/2), pp. 26–30.
- Engstle, J.; Reichhardt, N.; Först, P. (2015): Filter Cake Resistance of Horizontal Filter Layers of Lautering Filter Cakes. In *MBAA TQ* 52 (2), pp. 29–35. DOI: 10.1094/TQ-52-2-0405-01.
- Epstein, N. (1989): On tortuosity and the tortuosity factor in flow and diffusion through porous media. In *Chemical Engineering Science* 44 (3), pp. 777–779. DOI: 10.1016/0009-2509(89)85053-5.
- Erdim, E.; Akgiray, Ö.; Demir, İ. (2015): A revisit of pressure drop-flow rate correlations for packed beds of spheres. In *Powder Technology* 283, pp. 488–504. DOI: 10.1016/j.powtec.2015.06.017.
- Eshed, L.; Yaron, S.; Dosoretz, C. G. (2008): Effect of permeate drag force on the development of a biofouling layer in a pressure-driven membrane separation system. In *Applied and environmental microbiology* 74 (23), pp. 7338–7347. DOI: 10.1128/aem.00631-08.

- Fee, C.; Nawada, S.; Dimartino, S. (2014): 3D printed porous media columns with fine control of column packing morphology. In *Journal of chromatography. A* 1333, pp. 18–24. DOI: 10.1016/j.chroma.2014.01.043.
- Fourati, M.; Roig, V.; Raynal, L. (2012): Experimental study of liquid spreading in structured packings. In *Chemical Engineering Science* 80, pp. 1–15. DOI: 10.1016/j.ces.2012.05.031.
- Grossmann, I. E.; Westerberg, A. W. (2000): Research challenges in process systems engineering. In *AIChE J.* 46 (9), pp. 1700–1703. DOI: 10.1002/aic.690460902.
- Hess, W.; Thier, B. (Eds.) (1991): *Maschinen + Apparate zur Fest/Flüssig-Trennung. Grundlagen, Anwendung, Technik.* 1. Ausg. Essen: Vulkan-Verl.
- Hlavacek, M.; Bouchet, F. (1993): Constant flowrate blocking laws and an example of their application to dead-end microfiltration of protein solutions. In *Journal of Membrane Science* 82 (3), pp. 285–295. DOI: 10.1016/0376-7388(93)85193-Z.
- Höfgen, E.; Collini, D.; Batterham, R. J.; Scales, P. J.; Stickland, A. D. (2019a): High pressure dewatering rolls: Comparison of a novel prototype to existing industrial technology. In *Chemical Engineering Science* 205, pp. 106–120. DOI: 10.1016/j.ces.2019.03.080.
- Höfgen, E.; Kühne, S.; Peuker, U. A.; Stickland, A. D. (2019b): A comparison of filtration characterisation devices for compressible suspensions using conventional filtration theory and compressional rheology. In *Powder Technology* 346, pp. 49–56. DOI: 10.1016/j.powtec.2019.01.056.
- Höfgen, E.; Teo, H.-E.; Scales, P. J.; Stickland, A. D. (2020): Vane-in-a-Filter and Vane-under-Compressional-Loading: novel methods for the characterisation of combined shear and compression. In *Rheol Acta* 59 (6), pp. 349–363. DOI: 10.1007/s00397-020-01193-w.
- Hudson, D. R. (1949): Density and Packing in an Aggregate of Mixed Spheres. In *Journal of Applied Physics* 20 (2), pp. 154–162. DOI: 10.1063/1.1698327.
- Hunt, T. (2002): Filter Aids. In Michael C. Flickinger, Stephen W. Drew (Eds.): *Encyclopedia of Bioprocess Technology.* Hoboken, NJ, USA: John Wiley & Sons, Inc, pp. 1190–1197.
- Hwang, K.-J.; Lyu, S.-Y.; Chen, F.-F. (2006): The preparation and filtration characteristics of Dextran–MnO₂ gel particles. In *Powder Technology* 161 (1), pp. 41–47. DOI: 10.1016/j.powtec.2005.07.006.
- Hwang, K.-J.; Su, P.-Y.; Iritani, E.; Katagiri, N. (2016): Compression and filtration characteristics of yeast-immobilized beads prepared using different calcium concentrations. In *Separation Science and Technology* 51 (11), pp. 1947–1953. DOI: 10.1080/01496395.2016.1187629.
- Illies, S.; Anlauf, H.; Nirschl, H. (2017): Vibration-enhanced compaction of filter cakes and its influence on filter cake cracking. In *Separation Science and Technology* 52 (18), pp. 2795–2803. DOI: 10.1080/01496395.2017.1304416.
- Iritani, E.; Katagiri, N.; Kanetake, S. (2012): Determination of cake filtration characteristics of dilute suspension of bentonite from various filtration tests. In *Separation and Purification Technology* 92, pp. 143–151. DOI: 10.1016/j.seppur.2011.05.011.
- Jeschar, R. (1964): Druckverlust in Mehrkornschüttungen aus Kugeln. In *Archiv für das Eisenhüttenwesen* 35 (2), pp. 91–108. DOI: 10.1002/srin.196402300.

- Jiao, R.; Fabris, R.; Chow, C. W. K.; Drikas, M.; van Leeuwen, J.; Wang, D.; Xu, Z. (2017): Influence of coagulation mechanisms and floc formation on filterability. In *Journal of environmental sciences (China)* 57, pp. 338–345. DOI: 10.1016/j.jes.2017.01.006.
- Kim, Y. T.; Park, K. J.; Kim, S.; Kim, S. A.; Lee, S. J.; Kim, D. H. et al. (2018): Portable vibration-assisted filtration device for on-site isolation of blood cells or pathogenic bacteria from whole human blood. In *Talanta* 179, pp. 207–212. DOI: 10.1016/j.talanta.2017.09.075.
- Koch, W.; Höflinger, W.; Pongratz, E.; Oechsle, D. (1999): Continuous Pressure Filter with Rotating Disks and Cake Thickness Limitation by Scrapers. In *Chem. Eng. Technol.* 22 (11), p. 912. DOI: 10.1002/(SICI)1521-4125(199911)22:11<912::AID-CEAT912>3.0.CO;2-E.
- Kong, D. Y. C.; Gerontas, S.; McCluckie, R. A.; Mewies, M.; Gruber, D.; Titchener-Hooker, N. J. (2018): Effects of bed compression on protein separation on gel filtration chromatography at bench and pilot scale. In *Journal of chemical technology and biotechnology (Oxford, Oxfordshire: 1986)* 93 (7), pp. 1959–1965. DOI: 10.1002/jctb.5411.
- Kovalsky, P.; Gedrat, M.; Bushell, G.; Waite, T. D. (2007): Compressible cake characterization from steady-state filtration analysis. In *AIChE J.* 53 (6), pp. 1483–1495. DOI: 10.1002/aic.11193.
- Kuhn, M. (2018): New Paths in Filtration – Optimal Control Approaches Based on Continuum Models. Doctoral dissertation.
- Kuhn, M.; Briesen, H. (2016): Dynamic Modeling of Filter-Aid Filtration Including Surface- and Depth-Filtration Effects. In *Chem. Eng. Technol.* 39 (3), pp. 425–434. DOI: 10.1002/ceat.201500347.
- Kuhn, M.; Briesen, H. (2019): Systemverfahrenstechnik – Eine philosophische Begriffsanalyse. In *Chemie Ingenieur Technik* 91 (9), pp. 1229–1237. DOI: 10.1002/cite.201800220.
- Kuhn, M.; Pergam, P.; Briesen, H. (2020): Parameter Estimation for Incompressible Cake Filtration: Advantages of a Modified Fitting Method. In *Chem. Eng. Technol.* 43 (3), pp. 493–501. DOI: 10.1002/ceat.201900511.
- Kuhn, M.; Pietsch, W.; Briesen, H. (2017): Clarifying Thoughts About the Clarification of Liquids - Filtration and the Philosophy of Science. In *Chemie Ingenieur Technik* 89 (9), pp. 1126–1132. DOI: 10.1002/cite.201700025.
- Kyllönen, H. M.; Pirkonen, P.; Nyström, M. (2005): Membrane filtration enhanced by ultrasound: a review. In *Desalination* 181 (1-3), pp. 319–335. DOI: 10.1016/j.desal.2005.06.003.
- Lan, T. (2013): An experimental and simulation study of the influence made by inserts on chromatographic packed bed hydrodynamics. Doctoral dissertation. London.
- Lan, T.; Gerontas, S.; Smith, G. R.; Langdon, J.; Ward, J. M.; Titchener-Hooker, N. J. (2012): Investigating the use of column inserts to achieve better chromatographic bed support. In *Biotechnology progress* 28 (5), pp. 1285–1291. DOI: 10.1002/btpr.1597.
- Landman, K. A.; White, L. R.; Eberl, M. (1995): Pressure filtration of flocculated suspensions. In *AIChE J.* 41 (7), pp. 1687–1700. DOI: 10.1002/aic.690410709.
- Lee, D. J.; Wang, C. H. (2000): Theories of cake filtration and consolidation and implications to sludge dewatering. In *Water Research* 34 (1), pp. 1–20. DOI: 10.1016/S0043-1354(99)00096-2.

- Liu, Z.; Wang, W.; Xie, R.; Ju, X.-J.; Chu, L.-Y. (2016): Stimuli-responsive smart gating membranes. In *Chemical Society reviews* 45 (3), pp. 460–475. DOI: 10.1039/c5cs00692a.
- Low, Z.-X.; Chua, Y. T.; Ray, B. M.; Mattia, D.; Metcalfe, I. S.; Patterson, D. A. (2017): Perspective on 3D printing of separation membranes and comparison to related unconventional fabrication techniques. In *Journal of Membrane Science* 523, pp. 596–613. DOI: 10.1016/j.memsci.2016.10.006.
- Low, Z.-X.; Ji, J.; Blumenstock, D.; Chew, Y.-M.; Wolverson, D.; Mattia, D. (2018): Fouling resistant 2D boron nitride nanosheet – PES nanofiltration membranes. In *Journal of Membrane Science* 563, pp. 949–956. DOI: 10.1016/j.memsci.2018.07.003.
- Luckert, K. (Ed.) (2004): *Handbuch der mechanischen Fest-Flüssig-Trennung*. Essen: Vulkan-Verl.
- Maćkowiak, J. (2003): *Fluidynamik von Füllkörpern und Packungen*. Berlin, Heidelberg: Springer Berlin Heidelberg.
- Mahdi, F. M.; Holdich, R. G. (2013): Laboratory cake filtration testing using constant rate. In *Chemical Engineering Research and Design* 91 (6), pp. 1145–1154. DOI: 10.1016/j.cherd.2012.11.012.
- Marek, M.; Niegodajew, P. (2020): A new experimental approach to examination of orientation distribution of cylindrical particles in random packed beds. In *Powder Technology* 360, pp. 569–576. DOI: 10.1016/j.powtec.2019.10.077.
- Mattsson, T.; Sedin, M.; Theliander, H. (2012): Filtration properties and skin formation of micro-crystalline cellulose. In *Separation and Purification Technology* 96, pp. 139–146. DOI: 10.1016/j.seppur.2012.05.029.
- Merriam-Webster.com, Dictionary, Merriam-Webster, “Engineering”, <https://www.merriam-webster.com/dictionary/engineering>. Accessed 18 Oct. 2020.
- Michel, K.; Gruber, V. (1971): Erfahrungen mit der kontinuierlichen Druckfiltration in einem neuartigen Scheibenfilter. In *Chemie Ingenieur Technik* 43 (6), pp. 380–386. DOI: 10.1002/cite.330430613.
- Mueller, G. E. (2005): Numerically packing spheres in cylinders. In *Powder Technology* 159 (2), pp. 105–110. DOI: 10.1016/j.powtec.2005.06.002.
- Mueller, G. E. (2019): A modified packed bed radial porosity correlation. In *Powder Technology* 342, pp. 607–612. DOI: 10.1016/j.powtec.2018.10.030.
- Narziß, L.; Back, W. (2009): *Die Bierbrauerei*. Hoboken: Wiley-VCH. Available online at <http://gbv.ebib.com/patron/FullRecord.aspx?p=481555>.
- Nawada, S.; Dimartino, S.; Fee, C. (2017): Dispersion behavior of 3D-printed columns with homogeneous microstructures comprising differing element shapes. In *Chemical Engineering Science* 164, pp. 90–98. DOI: 10.1016/j.ces.2017.02.012.
- Neukäufer, J.; Hanusch, F.; Kutscherauer, M.; Rehfeldt, S.; Klein, H.; Grützner, T. (2019): Methodology for the Development of Additively Manufactured Packings in Thermal Separation Technology. In *Chem. Eng. Technol.* 42 (9), pp. 1970–1977. DOI: 10.1002/ceat.201900220.
- Niegodajew, P.; Asendrych, D.; Marek, M.; Drobniak, S. (2014): Modelling liquid redistribution in a packed bed. In *J. Phys.: Conf. Ser.* 530, p. 12053. DOI: 10.1088/1742-6596/530/1/012053.

- Niegodajew, P.; Marek, M. (2016): Analysis of orientation distribution in numerically generated random packings of Raschig rings in a cylindrical container. In *Powder Technology* 297, pp. 193–201. DOI: 10.1016/j.powtec.2016.04.024.
- Pardo-Alonso, S.; Vicente, J.; Solórzano, E.; Rodríguez-Perez, M. Á.; Lehmhus, D. (2014): Geometrical Tortuosity 3D Calculations in Infiltrated Aluminium Cellular Materials. In *Procedia Materials Science* 4, pp. 145–150. DOI: 10.1016/j.mspro.2014.07.553.
- Park, P.-K.; Lee, C.-H.; Lee, S. (2006): Permeability of Collapsed Cakes Formed by Deposition of Fractal Aggregates upon Membrane Filtration. In *Environ. Sci. Technol.* 40 (8), pp. 2699–2705. DOI: 10.1021/es0515304.
- Peuker, U. A.; Stahl, W. (2000): Dewatering and washing flue gas gypsum with steam. In *Filtration & Separation* 37 (8), pp. 28–30. DOI: 10.1016/S0015-1882(00)80075-0.
- Peuker, U. A.; Stahl, W. (2001): Steam Pressure Filtration: Mechanical-Thermal Dewatering Process. In *Drying Technology* 19 (5), pp. 807–848. DOI: 10.1081/DRT-100103771.
- Qian, Q.; Wang, H.; Bai, P.; Yuan, G. (2011): Effects of water on steam rectification in a packed column. In *Chemical Engineering Research and Design* 89 (12), pp. 2560–2565. DOI: 10.1016/j.cherd.2011.06.004.
- Richardson, J. F.; Zaki, W. N. (1954): The sedimentation of a suspension of uniform spheres under conditions of viscous flow. In *Chemical Engineering Science* 3 (2), pp. 65–73. DOI: 10.1016/0009-2509(54)85015-9.
- Ripperger, S.; Gösele, W.; Alt, C. (2000): Filtration, 1. Fundamentals. In: Ullmann's Encyclopedia of Industrial Chemistry, vol. 43. Weinheim, Germany: Wiley-VCH Verlag GmbH & Co. KGaA, p. 271.
- Ruth, B. F. (1946): Correlating Filtration Theory with Industrial Practice. In *Ind. Eng. Chem.* 38 (6), pp. 564–571. DOI: 10.1021/ie50438a010.
- Schultes, M. (2003): Raschig Super-Ring. In *Chemical Engineering Research and Design* 81 (1), pp. 48–57. DOI: 10.1205/026387603321158186.
- Selomulya, C.; Jia, X.; Williams, R. A. (2005): Direct Prediction of Structure and Permeability of Flocculated Structures and Sediments Using 3D Tomographic Imaging. In *Chemical Engineering Research and Design* 83 (7), pp. 844–852. DOI: 10.1205/cherd.04330.
- Shevchenko, O.; Tynyna, S. (2017): Fest-Flüssig-Trennung von feindispersen Suspensionen durch Pressfiltration bei pulsierendem Überdruck. In *Chemie Ingenieur Technik* 89 (6), pp. 823–830. DOI: 10.1002/cite.201600019.
- Shirato, M.; Aragaki, T.; Mori, R.; Sawamoto, K. (1968): Predictions of constant pressure and constant rate filtrations based upon an approximate correction for side wall friction in compression permeability cell data. In *J. Chem. Eng. Japan* 1 (1), pp. 86–90. DOI: 10.1252/jcej.1.86.
- Skinner, S. J.; Studer, L. J.; Dixon, D. R.; Hillis, P.; Rees, C. A.; Wall, R. C. et al. (2015): Quantification of wastewater sludge dewatering. In *Water Research* 82, pp. 2–13. DOI: 10.1016/j.watres.2015.04.045.
- Sonntag, G. (1960): Einfluß des Lückenvolumens auf den Druckverlust in gasdurchströmten Füllkörpersäulen. In *Chemie Ingenieur Technik* 32 (5), pp. 317–329. DOI: 10.1002/cite.330320502.

- Stickland, A. D. (2015): Compressional rheology: A tool for understanding compressibility effects in sludge dewatering. In *Water Research* 82, pp. 37–46. DOI: 10.1016/j.watres.2015.04.004.
- Stolarski, M.; Fuchs, B.; Bogale Kassa, S.; Eichholz, C.; Nirschl, H. (2006): Magnetic field enhanced press-filtration. In *Chemical Engineering Science* 61 (19), pp. 6395–6403. DOI: 10.1016/j.ces.2006.06.009.
- Svarovsky, L. (2001): Solid-Liquid Separation. 4. Aufl. s.l.: Elsevier professional. Available online at <http://gbv.ebib.com/patron/FullRecord.aspx?p=319151>.
- Tichy, J. W. (2007): Zum Einfluss des Filtermittels und der auftretenden Interferenzen zwischen Filterkuchen und Filtermittel bei der Kuchenfiltration. Zugl.: Kaiserlautern, Techn. Univ., Diss., 2007. Als Ms. gedr. Düsseldorf: VDI-Verl. (Fortschritt-Berichte VDI Reihe 3, Verfahrenstechnik, 877).
- Tiller, F. M. (1953): The role of porosity in filtration: numerical methods for constant rate and constant pressure filtration based on Kozeny's law. In *Chem. Eng. Progr.* 49, pp. 467–479.
- Tiller, F. M. (1958): The role of porosity in filtration part 3: Variable-pressure—variable-rate filtration. In *AIChE J.* 4 (2), pp. 170–174. DOI: 10.1002/aic.690040210.
- Tiller, F. M.; Cooper, H. R. (1960): The role of porosity in filtration: IV. Constant pressure filtration. In *AIChE J.* 6 (4), pp. 595–601. DOI: 10.1002/aic.690060418.
- Tiller, F. M.; Green, T. C. (1973): Role of porosity in filtration IX skin effect with highly compressible materials. In *AIChE J.* 19 (6), pp. 1266–1269. DOI: 10.1002/aic.690190633.
- Tiller, F. M.; Horng, L.-L. (1983): Hydraulic deliquoring of compressible filter cakes. Part 1: Reverse flow in filter presses. In *AIChE J.* 29 (2), pp. 297–305. DOI: 10.1002/aic.690290218.
- Tiller, F. M.; Hsyung, N. B. (1993): Unifying the Theory of Thickening, Filtration, and Centrifugation. In *Water Science and Technology* 28 (1), pp. 1–9. DOI: 10.2166/wst.1993.0004.
- Tiller, F. M.; Kwon, J. H. (1998): Role of porosity in filtration: XIII. Behavior of highly compactible cakes. In *AIChE J.* 44 (10), pp. 2159–2167. DOI: 10.1002/aic.690441005.
- Tiller, F. M.; Li, W. P.; Lee, J. B. (2001): Determination of the critical pressure drop for filtration of super-compactible cakes. In *Water Science and Technology* 44 (10), pp. 171–176. DOI: 10.2166/wst.2001.0611.
- Tiller, F. M.; Yeh, C. S.; Leu, W. F. (1987): Compressibility of Particulate Structures in Relation to Thickening, Filtration, and Expression—A Review. In *Separation Science and Technology* 22 (2-3), pp. 1037–1063. DOI: 10.1080/01496398708068998.
- Tippmann, J.; Scheuren, H.; Voigt, J.; Sommer, K. (2010): Procedural Investigations of the Lautering Process. In *Chem. Eng. Technol.* 33 (8), pp. 1297–1302. DOI: 10.1002/ceat.201000109.
- Trujillo, F. J.; Juliano, P.; Barbosa-Cánovas, G.; Knoerzer, K. (2014): Separation of suspensions and emulsions via ultrasonic standing waves - a review. In *Ultrasonics sonochemistry* 21 (6), pp. 2151–2164. DOI: 10.1016/j.ultsonch.2014.02.016.
- Verein Deutscher Ingenieure e.V. VDI-Norm 2762 Part 2, 2010: Mechanical solid-liquid separation by cake filtration. Determination of filter cake resistance.

- Vorobiev, E. (2006): Derivation of filtration equations incorporating the effect of pressure redistribution on the cake–medium interface. A constant pressure filtration. In *Chemical Engineering Science* 61 (11), pp. 3686–3697. DOI: 10.1016/j.ces.2006.01.010.
- Wakeman, R. (2007): The influence of particle properties on filtration. In *Separation and Purification Technology* 58 (2), pp. 234–241. DOI: 10.1016/j.seppur.2007.03.018.
- Wakeman, R. J.; Tarleton, E. S. (1999): Filtration. Equipment selection modelling and process simulation. 1. ed. Oxford: Elsevier.
- Wakeman, R. J.; Wu, P. (2002): Low-Frequency Vibration Effects on Coarse Particle Filtration. In *KONA* 20 (0), pp. 115–124. DOI: 10.14356/kona.2002014.
- Wang, G. Q.; Yuan, X. G.; Yu, K. T. (2005): Review of Mass-Transfer Correlations for Packed Columns. In *Ind. Eng. Chem. Res.* 44 (23), pp. 8715–8729. DOI: 10.1021/ie050017w.
- Wang, Z.; Afacan, A.; Nandakumar, K.; Chuang, K. T. (2001): Porosity distribution in random packed columns by gamma ray tomography. In *Chemical Engineering and Processing: Process Intensification* 40 (3), pp. 209–219. DOI: 10.1016/S0255-2701(00)00108-2.
- Xu, L. D.; Xu, E. L.; Li, L. (2018): Industry 4.0: state of the art and future trends. In *International Journal of Production Research* 56 (8), pp. 2941–2962. DOI: 10.1080/00207543.2018.1444806.
- Yu, W.; Graham, N. J. D.; Fowler, G. D. (2016): Coagulation and oxidation for controlling ultrafiltration membrane fouling in drinking water treatment: Application of ozone at low dose in submerged membrane tank. In *Water Research* 95, pp. 1–10. DOI: 10.1016/j.watres.2016.02.063.
- Zhang, X.; Yao, L.; Qiu, L.; Zhang, X. (2013): Three-dimensional Computational Fluid Dynamics Modeling of Two-phase Flow in a Structured Packing Column. In *Chinese Journal of Chemical Engineering* 21 (9), pp. 959–966. DOI: 10.1016/S1004-9541(13)60576-5.

List of Publications

Peer-reviewed Research Articles

- Bandelt Riess, P. M.; Engstle, J.; Kuhn, M.; Briesen, H.; Först, P. (2018): Decreasing Filter Cake Resistance Using Packing Structures. In *Chem. Eng. Technol.* 41 (10), pp. 1956–1964.
- Bandelt Riess, P. M.; Kuhn, M.; Briesen, H.; Först, P. (2018): Increasing Wort Flow by Flocculation of Fine Particle Fractions. In *BrewingScience* 71 (7/8), pp. 68–72.
- Bandelt Riess, P. M.; Engstle, J.; Först, P. (2018): Characterizing the Filtration Behavior of Hop Particles for Efficient Dry Hopping Methods. In *BrewingScience* 71 (9/10), pp. 74–80.
- Bandelt Riess, P. M.; Kuhn, M.; Först, P.; Briesen, H. (2021): Investigating the Effect of Packing Structures on Filter Cake Compressibility. In *Chem. Eng. Technol.* 44 (4), pp. 661–669.
- Bandelt Riess, P. M.; Bertazzoni Streit, J. A.; Kuhn, M.; Briesen, H.; Först, P. (2021): Assessing the Effects of Packed Beds on Lautering Performance and Wort Quality. In *BrewingScience* 74 (5/6), pp. 82–87.
- Bandelt Riess, P. M.; Briesen, H.; Schiochet Nasato, D. (2022): Assessing the Wall Effects of Packed Concentric Cylinders and Angular Walls on Granular Bed Porosity. In *Granular Matter* 24 (36).

Conference Papers and Oral Presentations

- Bandelt Riess, P. M.; Engstle, J.; Briesen, H.; Först, P. (2017): Filtration von biologischen Suspensionen durch kompressible Medien – Kalthopfung. In: Jahrestreffen der ProcessNet-Fachgruppe Mechanische Flüssigkeitsabtrennung 2017, Köln, Germany.
- Bandelt Riess, P. M.; Wujanz, J.; Kuhn, M.; Briesen, H.; Först, P. (2018): Unkonventionelle Kuchenfiltration – Verwendung von Füllkörpern zur Reduzierung des Durchflusswiderstands. In: Jahrestreffen der ProcessNet-Fachgruppe Mechanische Flüssigkeitsabtrennung 2018, Merseburg, Germany.
- Bandelt Riess, P. M.; Engstle, J.; Kuhn, M.; Briesen, H.; Först, P. (2019): Unkonventionelle Kuchenfiltration – Verwendung von Füllkörpern zur Reduzierung des Durchflusswiderstands. In: 52. BGT Technologisches Seminar, Freising, Germany.
- Bandelt Riess, P. M.; Kuhn, M.; Briesen, H.; Först, P. (2019): Evaluation of Process Strategies to Homogenize the Lautering Filter Cake Structure and Enhance Wort Production. In: FILTECH 2019 - Proceedings. International Conference & Exhibition for Filtration and Separation Technology. Köln, Germany. 700. Aufl. Meerbusch.
- Bandelt Riess, P. M.; Engstle, J.; Först, P. (2020): Charakterisierung der Hopfenabtrennung zur effizienten Kalthopfung. In: 53. BGT Technologisches Seminar, Freising, Germany.

Poster Presentation

Bandelt Riess, P. M.; Kuhn, M.; Först, P.; Briesen, H. (2020): Kompression und Permeation? – Charakterisierung biologischer Filterkuchen mittels Kompressionsrheologie. In: Jahrestreffen der ProcessNet-Fachgruppe Mechanische Flüssigkeitsabtrennung 2020, Leipzig, Germany. (Presentation canceled due to pandemic.)

Non-peer-reviewed Research Articles

Bandelt Riess, P. M.; Oesinghaus, H.; Först, P. (2018): Eine Bindung vor der Trennung – Möglichkeiten der Feinpartikelflockung zur Beschleunigung des Läuterprozesses. In *Der Weihenstephaner* 86 (4), pp. 156–159.

Bandelt Riess, P. M.; Kuhn, M.; Briesen, H.; Först, P. (2019): Möglichkeiten zur Beschleunigung des Läuterprozesses durch Flockung des Feinpartikelanteils. In *BRAUWELT* 159 (26), pp. 728–732.

Bandelt Riess, P. M.; Engstle, J.; Först, P. (2019): Charakterisierung der Hopfenpartikelabtrennung zur effizienten Kalthopfung. In *BRAUWELT* 159 (28/29), pp. 820–824.

Bandelt Riess, P. M.; Krimmer, J.; Kuhn, M.; Först, P. (2019): Charakterisierung der Hopfenaromaextraktion mittels Trockenrückstand und Brechungsindex – Eine neue Möglichkeit der Prozessüberwachung zur effizienten Kalthopfung. In *Der Weihenstephaner* 87 (3), pp. 126–128.

Bandelt Riess, P. M.; Kuhn, M.; Briesen, H.; Först, P. (2019): Possibilities for accelerating the lautering process by means of flocculation of fine particle fraction. In *BRAUWELT International* 37 (5), pp. 336–339.

Bandelt Riess, P. M.; Engstle, J.; Först, P. (2020): Characterisation of Hop Particle Separation for Efficient Dry Hopping. In *BRAUWELT International* 38 (1), pp. 15–20.

Bandelt Riess, P. M.; Hohmann, M.; Briesen, H.; Först, P. (2020): Filtrieren, Waschen, Extrahieren – Untersuchungen der Extraktgewinnung beim Läutern. In *Der Weihenstephaner* 88 (3), pp. 106–108.

Bandelt Riess, P. M.; Bertazzoni Streit, J. A.; Kuhn, M.; Briesen, H.; Först, P. (2022): Effekte von Füllkörpern auf die Läuterleistung und Würzequalität (Teil 1). In *BRAUWELT* 162 (5), pp. 129–133.

Bandelt Riess, P. M.; Bertazzoni Streit, J. A.; Kuhn, M.; Briesen, H.; Först, P. (2022): Effekte von Füllkörpern auf die Läuterleistung und Würzequalität (Teil 2). In *BRAUWELT* 162 (6/7), pp. 158–160.

Final Reports of Funded Investigation Projects

Bandelt Riess, P. M.; BANKE process solutions GmbH & Co. KG; Becker, T.; Briesen, H.; Cotterchio, C.; Engstle, J.; Först, P.; Gastl, M. (2017): Entwicklung eines verlustarmen Kalthopfungsverfahrens ZF 4025001SK5. Project approved between 2015–2017 by *AiF Projekt GmbH*, Berlin, Germany.

Bandelt Riess, P. M.; Becker, T.; Briesen, H.; Först, P.; Gastl, M.; Hennemann, M. (2020): Entwicklung von Prozessstrategien zur homogenen Schichtung des Treberkuchens beim Läutern AiF 19359 N. Project approved between 2017–2020 by *Forschungskreis der Ernährungsindustrie e. V.*, Bonn, Germany.